

**OFDMA-BASED RESOURCE ALLOCATION FOR
WIRELESS COMMUNICATION SYSTEMS**

BIN DA

NATIONAL UNIVERSITY OF SINGAPORE

2010

©2010

BIN DA

All Rights Reserved

**OFDMA-BASED RESOURCE ALLOCATION FOR
WIRELESS COMMUNICATION SYSTEMS**

BIN DA

(B.Eng, HHU)

A THESIS SUBMITTED

FOR THE DEGREE OF DOCTOR OF PHILOSOPHY

DEPARTMENT OF ELECTRICAL AND COMPUTER ENGINEERING

NATIONAL UNIVERSITY OF SINGAPORE

2010

Acknowledgments

First and foremost, my deepest gratitude goes to my supervisor, Professor Chi Chung Ko, for his enlightening guidance, supports, encouragement and unending patience throughout the entire period of my four-year research and study as well as the write-up of this thesis. His invaluable suggestions and discussions are truly rewarding.

Special thanks to my parents, and my wife, who always encourage, support and care for me throughout my life.

I am also grateful to all the colleagues and students in the Communications Laboratory at the Department of Electrical and Computer Engineering, in particular Le Hung Nguyen, Shengwei Hou, Qi Zhang, Xiaolu Zhang, and Fazle Rabbi Mohammad, for their enjoyable discussions with me on communications concepts and interesting ideas.

Lastly, I greatly appreciate all the supports and helps from the staff in National University of Singapore to completion of this thesis.

Contents

Acknowledgments	i
Summary	v
Nomenclature	viii
List of Figures	xi
List of Tables	xiii
Chapter 1 Introduction	1
1.1 Evolution of wireless communication systems	1
1.2 Basic techniques of radio resource allocation	3
1.3 Fundamental principle of OFDMA	4
1.4 Motivations in OFDMA-based resource allocation	6
1.5 Objectives and significance	10
Chapter 2 Resource allocation for SISO-OFDMA	12
2.1 Typical downlink system model	12
2.2 Partial feedback channel state information	14
2.2.1 Review and motivation	14
2.2.2 Problem formulation and opportunistic feedback example	14

2.2.3	Proposed scheme	18
2.2.4	Simulation results	20
2.3	Adjustable quality-of-service	24
2.3.1	Problem formulation and motivation	24
2.3.2	Proposed scheme	25
2.3.3	Simulation results	26
2.4	Conclusions	29
Chapter 3 Resource allocation for MIMO-OFDMA		31
3.1	Review and motivation	31
3.2	MIMO-OFDMA system model	33
3.3	Utility-based resource allocation	36
3.3.1	Utility-based problem formulation	36
3.3.2	System optimality and bargaining solutions	38
3.3.2.1	Generalized Nash bargaining solution (GNBS)	39
3.3.2.2	Kalai-Smorodinsky bargaining solution (KSBS)	41
3.3.3	Implementations of utility-based allocation	42
3.3.4	Simulation results	46
3.4	Conclusions	52
Chapter 4 OFDMA-based relaying		53
4.1	Review and motivation	53
4.2	System model and problem formulation	55
4.3	System analysis and proposed scheme	58
4.4	Simulation results and conclusion	64
4.5	Conclusions	68
Chapter 5 OFDMA-based cognitive radio		70
5.1	Spectrum sharing in OFDMA-based cognitive radio	70

5.1.1	Review and motivation	71
5.1.2	Dynamic spectrum sharing model	73
5.1.3	System analysis and solutions	77
5.1.4	Simulation results	82
5.2	OCR implementation via accessible interference temperature	86
5.2.1	Accessible interference temperature and proposed implementation	87
5.2.2	Simulation results	91
5.3	Conclusions	92
Chapter 6	Conclusions	94
6.1	Summary of contributions	94
6.2	Future research	96
Bibliography		99
References	99
Appendix A	Optimal power allocation to Problem (2.5)	107
Appendix B	MIMO-OFDMA optimality	109
Appendix C	Proof of achievable capacity in equation (4.5)	111
Appendix D	Lagrangian duality and Karush-Kuhn-Tucker conditions	113
Appendix E	Algorithm in [84]	116
Appendix F	List of publications	118

Summary

Multipath fading, shadowing, path-loss and time-variation are important phenomena in wireless communications. The technique of Orthogonal Frequency Division Multiplexing (OFDM) has been widely used to combat these detrimental effects in the past decades. Orthogonal Frequency Division Multiple Access (OFDMA) is a multiuser version of OFDM digital modulation, which is currently adopted in many international standards and is also a popular candidate for multiple access in future wireless systems. OFDMA is capable of allowing different subcarriers to be individually assigned to different users so as to enable simultaneous low data-rate transmissions and to achieve diverse Quality-of-Service (QoS) requirements. In addition, OFDMA can exploit both frequency domain and multiuser diversities to enhance the attainable system capacity. With dynamic resource allocation designed for OFDMA systems, the spectrum efficiency is expected to be further improved.

The main objective of this thesis is to devise efficient algorithms for OFDMA-based resource allocation in wireless communication systems, with joint consideration of system capacity, user fairness, low complexity and spectrum sharing, while trying to achieve controllable tradeoff among these concerns.

Chapter 1 gives a brief introduction to wireless communication systems and provides the fundamental principle in OFDMA-based Radio Resource Allocation (RRA). In Chapter 2, a typical downlink OFDMA system is presented first. Then, two sub-issues on partial feedback Channel State Information (CSI) and adjustable QoS are discussed via

newly developed methods, which lead to significantly reduced CSI and satisfy diverse QoS requirements, respectively.

In Chapter 3, different utility-based resource allocation schemes are investigated for Multiple Input Multiple Output (MIMO) - OFDMA systems. The optimality of the system is reviewed, and two bargaining solutions are utilized to formulate efficient algorithms for flexibly controlling user fairness.

Chapter 4 jointly considers the direct and relaying paths in a relay-assisted OFDMA cellular system. In this system, a novel implementation adopting full-duplex relaying is proposed for relay-destination selection, subcarrier and power allocation. This implementation has significantly improved spectrum efficiency as compared to conventional half-duplex relaying mode. In addition, it enables effective controllability on the tradeoff between system capacity and user fairness.

In Chapter 5, we study two sub-issues for OFDMA-based Cognitive Radio (OCR) systems. Firstly, a novel spectrum sharing model is proposed for OCR. This model can dynamically allocate radio resources to secondary users with the cooperation of primary users so that the capacity of secondary network is maximized and the co-channel interference is minimized. The effect of Interference Temperature Limit (ITL) on the capacity of secondary network is also investigated, which shows that a properly selected ITL value can balance the performance between the primary and secondary networks. Secondly, with a fairness concern, Accessible Interference Temperature (AIT) is exploited to formulate an effective implementation for a simplified OCR model.

In the last Chapter, the contributions made in this thesis are summarized, and the possible extensions and future research are briefly outlined.

Nomenclature

1G	First Generation
2G	Second Generation
3G	Third Generation
4G	Fourth Generation
AF	Amplify-and-Forward
AIT	Accessible Interference Temperature
AMPS	Advanced Mobile Phone System
AWGN	Additive White Gaussian Noise
BER	Bit Error Rate
BS	Base Station
CDMA	Code Division Multiple Access
CDOS	Conventional Downlink OFDMA System
CIC	Cooperative Interference Control
CR	Cognitive Radio
CRN	Cognitive Radio Networks
CSI	Channel State Information
DF	Decode-and-Forward
DRA	Dynamic Resource Allocation
E-TACS	European Total Access Communication System
EDGE	Enhanced Data rates for GSM Evolution
EP	Equal Power

FDD	Frequency Division Duplex
FDMA	Frequency Division Multiple Access
FFT	Fast Fourier Transform
FM	Frequency Modulation
GNBS	Generalized NBS
GPRS	General Packet Radio Service
GSM	Global System for Mobile
ITL	Interference Temperature Limit
IFFT	Inverse Fast Fourier Transform
JFI	Jain's Fairness Index
KKT	Karush-Kuhn-Tucker
KSBS	Kalai-Smorodinsky Bargaining Solution
LTE	Long Term Evolution
MAC	Media Access Control
MIMO	Multiple Input Multiple Output
MMR	Mobile Multi-hop Relay
MQAM	M-ary Quadrature Amplitude Modulation
NBS	Nash Bargaining Solution
NE	Nash Equilibrium
OCR	OFDMA-based Cognitive Radio
OFDM	Orthogonal Frequency-Division Multiplexing
OFDMA	Orthogonal Frequency Division Multiple Access
OSI	Open Systems Interconnection
QoS	Quality-of-Service
PF	Proportional Fairness
RRA	Radio Resource Allocation
RS	Relay Station
PU	Primary User

SDMA	Space-Division Multiple Access
SINR	Signal-to-Interference-plus-Noise Ratio
SISO	Single Input Single Output
SNR	Signal-to-Noise Ratio
SU	Secondary User
TDD	Time Division Duplex
TDMA	Time Division Multiple Access
TD-SCDMA	Time Division - Synchronous CDMA
WF	Water-Filling
WiMAX	Worldwide Inter-operability for Microwave Access
WLAN	Wireless Local Area Network
WRAN	Wireless Regional Area Network

List of Figures

1.1	Typical OFDMA structure and simplification for resource allocation. . .	5
1.2	Principle of multiuser diversity and OFDMA.	6
2.1	Typical downlink OFDMA system model with K users.	12
2.2	Achieved capacity percentage, and number of null subcarriers.	21
2.3	Fairness comparison.	22
2.4	Normalized data-rate distribution.	23
2.5	System capacity versus number of users.	27
2.6	Fairness comparison.	28
3.1	Typical MIMO-OFDMA system model.	34
3.2	System capacity versus average SNR.	47
3.3	System capacity versus number of users.	48
3.4	Data-rate distribution for 8 users.	50
3.5	Effect of bargaining power for two-user case.	51
4.1	Basic transmission paths in a relay-assisted OFDMA cellular system. . .	55
4.2	Example for illustrating geo-locations of the BS, 6 RSs, and 20 users. . .	65
4.3	Iterative power refinement for improving system capacity.	66
4.4	System capacity versus number of users.	67
4.5	Fairness comparison.	68

5.1	System model for two PUs and two SUs.	73
5.2	Geo-location snapshot of the system.	83
5.3	Total capacity of secondary users.	84
5.4	Effect of interference temperature limit.	85
5.5	Subcarrier sharing index.	86
5.6	System model with two PUs and two SUs.	87
5.7	Performance of secondary network.	91

List of Tables

2.1	Example for the feasibility of partial feedback CSI	17
2.2	Implementation of subcarrier allocation	19
2.3	Proposed algorithm for subcarrier allocation	26
3.1	GNBS/KSBS implementation of resource allocation	44
4.1	Implementation of subcarrier allocation	63
4.2	Basic system settings	64
5.1	AIT values	90
E.1	Sequential price-based iterative water-filling algorithm in [84]	117

Chapter 1

Introduction

In this chapter, a brief description of wireless communication systems and traditional Radio Resource Allocation (RRA) techniques is first given, which is followed by the fundamental principle of Orthogonal Frequency Division Multiple Access (OFDMA) and the motivations of the studies in this thesis for OFDMA-based RRA.

1.1 Evolution of wireless communication systems

Due to the fast development of digital signal processing and very large scale integrated circuits, wireless communication systems have been experiencing an explosive growth in the past decades. Cellular systems and Wireless Local Area Network (WLAN) are the most successful wireless applications nowadays, which are also important elements for globally ubiquitous wireless connections.

The birth of the cellular concept was conceived in the 1970s at Bell laboratories. The First Generation (1G) cellular system, known as Advanced Mobile Phone System (AMPS), was deployed in the United States in the 1980s, adopting Frequency Modulation (FM) technology with Frequency Division Multiple Access (FDMA). Following the success of AMPS, the European Total Access Communication System (E-TACS) was

then deployed in Europe. However, due to the capacity limitation of 1G cellular systems, they were phased out by the Second Generation (2G) cellular systems in the early 1990s. There exist three major 2G standards, Interim Standard (IS)-95, IS-136 in the United States, and Global System for Mobile (GSM) in Europe. These standards are still widely used nowadays to provide basic voice services. The enhanced versions of 2G standards with higher data-rate are known as IS-95 High Data Rate for IS-95, IS-136 High Speed for IS-136, and General Packet Radio Service (GPRS) and Enhanced Data rates for GSM Evolution (EDGE) for GSM. These improved 2G cellular systems are usually referred to as 2.5G systems [1].

In recent years, the Third Generation (3G) cellular systems have been deployed globally, while beyond-3G systems adopting Multiple Input Multiple Output (MIMO) - OFDMA physical layer are under development. Similar to 2G systems, 3G systems consist of three global standards, which are Wideband Code Division Multiple Access (WCDMA), CDMA2000, and Time Division - Synchronous CDMA (TD-SCDMA) [1]. Specifically, WCDMA Frequency Division Duplex (FDD) and Time Division Duplex (TDD) standards have been adopted in Europe and China, respectively, while CDMA2000 has been deployed in Korean and America. Since 2009, TD-SCDMA system has been launched in China, while its deployment in some European countries are being carried out.

Another well-known wireless system follows the IEEE 802.11 standard for wireless local area networks, which was originally designed for 1-2 Mbps traffic in the 1990s, and now has evolved to support 600 Mbps in 802.11n and is being considered as a high-throughput (up to 1 Gbps) wireless interface for the nomadic scenarios in the next generation of wireless systems [2]. In general, WLAN has experienced four generations. The first WLAN architecture adopts stand-alone access, where some access points are used to deliver wireless signals between mobile devices and a wired network. The second generation WLAN has a centralized architecture with the consideration of network scal-

ability. Then, an optimized WLAN architecture is formulated to significantly increase the physical transmission data-rate in 802.11n standard, which defines the third generation WLAN architecture. Since the wired and wireless networks are managed separately in all the previous generations, a unified WLAN architecture is thus being developed to truly merge both wired and wireless LANs together to formulate the fourth generation WLAN systems.

Furthermore, the Long Term Evolution (LTE) towards the Fourth Generation (4G) cellular systems is now under development globally. Also, exploiting advanced MIMO-OFDMA techniques, Worldwide Inter-operability for Microwave Access (WiMAX) [3] systems have been used in many countries to form metropolitan-wide broadband access. In recent years, a new paradigm for universal spectrum sharing is established based on using Cognitive Radio (CR) techniques. One current CR application is the Wireless Regional Area Network (WRAN), which corresponds to the IEEE 802.22 standard [4].

1.2 Basic techniques of radio resource allocation

Many conventional techniques have been exploited to achieve Radio Resource Allocation (RRA) in wireless communication systems. These techniques involve strategies and algorithms for controlling transmit power, channel allocation, modulation scheme, and error coding. The main objective is to make the best use of the limited radio resources to increase spectrum efficiency as much as possible [5].

Multiple access method is one essential element in the implementation of RRA schemes, which can be classified into several categories. Time Division Multiple Access (TDMA) is a conventional technique that allows several users to share the same frequency band via transmitting the signals over different time slots. Specifically, different users can transmit in succession, one after the other, with each user using his own time slots. Frequency Division Multiple Access (FDMA) is another fundamental multiple ac-

cess technique via using channelization. In particular, FDMA assigns each user one or several frequency bands or sub-channels for signal transmission [6].

Apart from TDMA and FDMA, Code Division Multiple Access (CDMA) enables several transmitters to send information simultaneously over a single communication channel. To properly multiplex different users, CDMA employs the spread-spectrum technology and pseudo-random codes [5]. By exploiting multiple antennas, Space Division Multiple Access (SDMA) is able to offer significant performance improvement as compared with single-antenna systems [6]. Meanwhile, SDMA can create parallel spatial channels to improve system capacity via spatial multiplexing or diversity.

RRA can also be classified into static or dynamic allocation schemes [6]. To be specific, static RRA such as FDMA and TDMA are fixed allocation schemes, which are widely used in many traditional systems such as 1G or 2G cellular systems. On the other hand, the dynamic RRA schemes can adaptively adjust system parameters, according to the traffic load, user positions, and Quality-of-Service (QoS), so as to achieve better spectrum utilization as compared with fixed allocation schemes.

It is also known that some RRA schemes are centralized, where the Base Stations (BSs) and users are managed by a central controller. Meanwhile, some schemes are formulated as distributed implementations, where autonomous algorithms are used in mobile users and BSs with coordinated information exchange [7].

1.3 Fundamental principle of OFDMA

In typical OFDMA systems, different numbers of subcarriers can be assigned to different users so as to achieve diverse QoS, which is equivalent to serving each user with the requested radio resources [6]. This fundamental principle of OFDMA is illustrated in Fig.1.1. Generally, as studied in [8], OFDMA can exploit both frequency-domain diversity and multiuser diversity to improve the attainable system throughput and spectrum

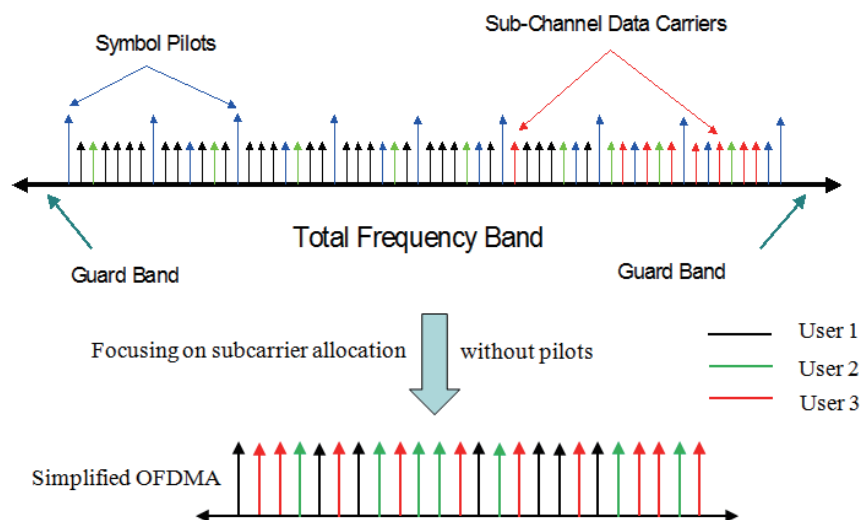


Fig. 1.1: Typical OFDMA structure and simplification for resource allocation.

efficiency.

In this thesis, the subcarriers used as pilots, as shown in the upper part of Fig.1.1, are not considered for simplicity. This means that the RRA schemes proposed in this thesis are only applied to the effective subcarriers that practically carry data, which is illustrated by the lower part of Fig.1.1 for an interleaved OFDMA without pilots. With this simplification, dynamic user-to-subcarrier assignment can enable better spectrum utilization than fixed assignment, based on the feedback Channel State Information (CSI). Note that, in our studies, the CSI means the set of channel gains of the transmission links in a system.

As shown in Fig.1.2¹, multiuser diversity is the reason for the popularity of exploiting OFDMA resource allocation in wireless systems. To be specific, multiuser diversity allows the overall system throughput to be optimized via allocating radio resources to the users that can make the best use of these resources [6]. As demonstrated in Fig.1.2, different users may have mutually independent channel attenuations over different sub-

¹Note that this figure is cited from [7] (Fig.3 in this reference).

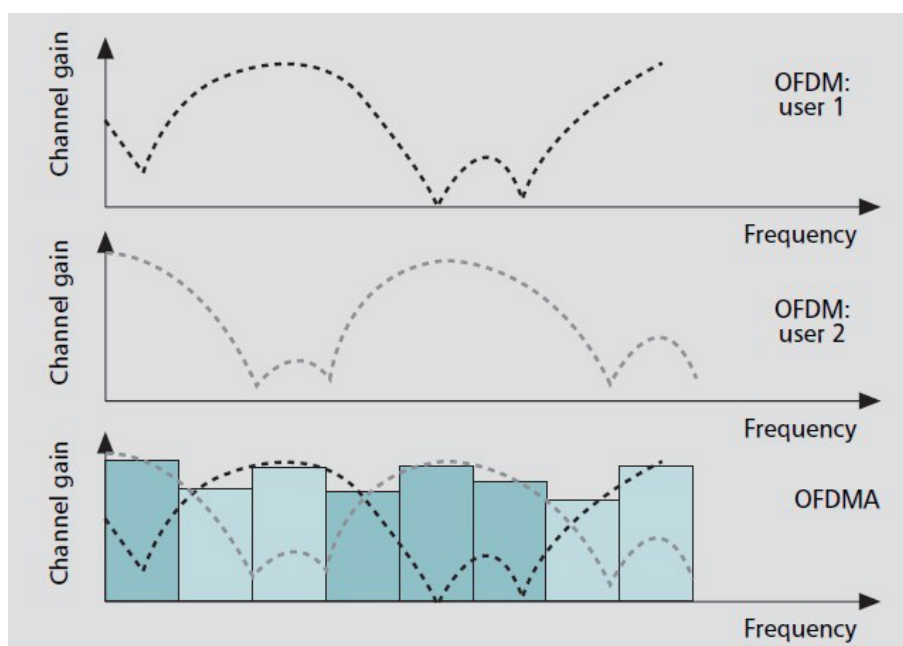


Fig. 1.2: Principle of multiuser diversity and OFDMA.

carriers. For example, the dark and light dashed curves denote the channel gains of users 1 and 2, respectively. A deep fade may affect several subcarriers of one particular user. However, it is quite unlikely for one subcarrier to be in a deep fade for all users. As a result, OFDMA can avoid the subcarrier in a deep fade to be allocated to one user, which can be easily observed from the bottom diagram in Fig.1.2 with interleaved subcarrier allocation for the two users.

1.4 Motivations in OFDMA-based resource allocation

The main allocation issue in OFDMA-based resource allocation is to jointly optimize subcarrier scheduling, power allocation over each subcarrier, user fairness², and other system design metrics such as Bit Error Rate (BER), minimum requested data-rate of each user, and implementation complexity. This joint optimization can be either for

²This metric is usually expressed by a data-rate distribution of all users, which generally indicates the user fairness in terms of data-rates of users in a system.

downlink or uplink signal transmission in wireless networks, and the aforementioned system design metrics are sometime conflicting in nature. In traditional OFDMA-based resource allocation schemes, only one design metric, saying, system capacity or user fairness, is emphasized without considering the other metrics at the same time. This observation motivates the studies in this thesis for various OFDMA-based wireless systems with a more balanced performance over system capacity, user fairness, implementation complexity as well as spectrum sharing. In the rest of this section, more specific motivations of our studies in this thesis are described with brief reviews of related works.

For Single Input Single Output (SISO) - OFDMA resource allocation, a large number of schemes have been proposed in the past decade. The authors in [8] presented a joint subcarrier, bit, and power allocation algorithm with the objective to minimize the total transmit power at the BS subject to BER and data-rate constraints. This was initially discussed as a problem of dynamic OFDMA resource allocation in the downlink. However, this pioneering study has one crucial limitation, that of heavy computational complexity, which makes it not applicable to real-time implementations. Thus, in recent years, many algorithms have been investigated to reduce the implementation complexity [9], [10]. On the other hand, the problem of maximizing total system capacity with a proportional fairness³ constraint was firstly studied in [11], which was later extended in [9], [12]. A low complexity algorithm based on [11] has been proposed to obtain higher spectrum efficiency in [13], where the relaxed fairness constraint is shown to be more feasible than the algorithm in [11]. As further investigated in [9], a priority-based sequential scheduling criteria was demonstrated to obtain even higher system capacity than those achieved in [11], [13] at the cost of severely losing proportional fairness among users. Nevertheless, all these traditional algorithms for downlink resource allocation either adhere to enhance user fairness or to enhance system capacity. In many applications, fairness and capacity should be considered simultaneously. Hence, it may be possible to

³This proportional fairness allows each user to obtain a fraction of the overall system capacity, and its definition is described in Page 40 in Chapter 3.

formulate some algorithms to trade off between these two metrics for SISO-OFDMA systems, which is also the motivation behind the studies in Chapter 2 [14], [15], [16].

Multiple Input Multiple Output (MIMO) techniques enable improvement in physical layer performance of modern wireless communication systems as compared with single-antenna systems [17]. In MIMO systems, multiple antennas are used at both the transmitter and receiver to utilize space diversity for enhanced spectrum efficiency. Combined with OFDMA, MIMO-OFDMA has been demonstrated as the most promising approach for high data-rate wireless networks and has been considered in many international standards for broadband communications, including 802.16e [3] and 802.22 [4]. Although many dynamic resource allocation algorithms [7], [18] have been proposed to adaptively allocate radio resources to users in MIMO-OFDMA systems, these algorithms seldom consider user fairness or do not have a flexible control on the data-rate distribution. As a result, we are motivated to formulate some low-complexity implementations for MIMO-OFDMA resource allocation in Chapter 3, with a balance between user fairness and system capacity [19].

Recently, fixed or mobile relays are exploited in cellular systems to assist signal transmission [20]. The signals are usually transmitted over multiple Relay Stations (RSs) from the source node to the destination node, resulting in the so-called Mobile Multi-hop Relay (MMR). This MMR technique can be used to extend network coverage and improve system capacity at the same time [21]. The multi-hop feature of MMR enables each destination node to combine the signals received from all the previous nodes to improve system performance [22]. In conventional multi-hop relaying systems, the direct path is usually ignored since it is assumed that the destination node is far away from the source node [23]. However, in a cellular system with some RSs deployed, users may not be always far from the BS, and the direct path may be strong enough to carry some data. Therefore, the direct path should not be simply ignored in cellular systems. With independent sub-channels over individual hops, the conventional relaying mode enables each

RS to transmit signals in a full-duplex manner. The authors in [24] initially investigated a joint direct and relaying path scenario for uplink OFDMA systems. Subsequently, many studies for relay-assisted OFDMA systems have been presented [25]. For simplicity of system implementation, each RS normally adopts a half-duplex transmission protocol to avoid interference since the same subcarrier is used in two successive hops of the relaying path [24]. A novel implementation is proposed in [26] to make the user node communicate with the BS either through direct path or half-duplex relaying path intelligently. With these in mind, it might be worthwhile to formulate new system models that jointly consider direct and relaying paths through using full-duplex RSs and dynamic channel switching mechanisms. This is the motivation behind Chapter 4 [27], [28].

Spectrum sharing methods can be applied to significantly improve spectrum efficiency in wireless systems, and stimulate a new system design paradigm via using Cognitive Ratio (CR) techniques for the next generation of wireless networks. Spectrum underlay and overlay techniques are two basic forms of Cognitive Radio Networks (CRNs) [29]. In a typical CRN, Primary Users (PUs, or called licensed users) should be protected when Secondary Users (SUs, or called unlicensed users) access the spectrum. Specifically, in spectrum underlay, the Interference Temperature Limit (ITL) is used to constrain the received interference level at PUs as well as the transmitting power at SUs. On the other hand, spectrum overlay allows SUs to opportunistically access the radio resources owned by PUs if the corresponding frequency band is not being used. The transmission opportunities are usually detected by spectrum sensing techniques [30], [31]. Recently, Niyato presents a series of pioneering studies on market-equilibrium-based approaches for understanding the economic behavior of users in CR systems [32], [33], [34]. However, dynamic spectrum sharing model with interference control has not been well studied in the literature. In addition, the practical application of applying ITL into CR-based cellular systems still remains open. Thus, the practical implementations of OFDMA-based Cognitive Radio (OCR) will be discussed in Chapter 5, where we are motivated to

propose schemes for efficient OCR interference control with low complexity.

1.5 Objectives and significance

With the motivations given by the previous section, the main objective of this thesis can be summarized as devising efficient algorithms for Orthogonal Frequency Division Multiple Access (OFDMA) - based resource allocation in wireless communication systems, with joint consideration of system capacity, user fairness, low complexity and spectrum sharing, while trying to achieve controllable tradeoff among these concerns.

The results that will be presented in this thesis may contribute to design efficient algorithms for OFDMA-based resource allocation in systems such as Single Input Single Output (SISO) - OFDMA, Multiple Input Multiple Output (MIMO) - OFDMA, OFDMA relaying and OFDMA-based Cognitive Radio (OCR). To be specific, the significance of this thesis is briefly described as follows:

- Propose a partial feedback Channel State Information (CSI) mechanism and present a method to achieve adjustable Quality-of-Service (QoS) for SISO-OFDMA systems.
- Extend the SISO-OFDMA resource allocation to MIMO-OFDMA scenario via using utility-based bargain solutions, which demonstrate flexible controllability on user fairness via bargaining powers.
- Propose a full-duplex relaying model to enhance spectrum efficiency for OFDMA-based relaying.
- Propose a novel spectrum sharing model for OCR, and formulate an effective implementation via the introduced accessible interference temperature.

Note that the investigated problems in this thesis mainly focus on physical and Media Access Control (MAC) layers in a vertically layered system profile, as, for ex-

ample, given by the Open Systems Interconnection (OSI) seven-layer model [35]. As a result, some relevant issues in the upper layers are beyond the scope of this thesis. In addition, while per-subcarrier scheduling and power allocation over each subcarrier are studied for OFDMA-based systems, we do not consider resource allocation via some advanced antenna techniques such as Space Division Multiple Access (SDMA) or beamforming [5], [36]. It is also worthwhile to note that this thesis is organized in a topic-based manner, with the above four points discussed in Chapters 2 to 5, respectively.

Chapter 2

Resource allocation for SISO-OFDMA

In this chapter, the general principle of resource allocation in a typical Single Input Single Output (SISO) - OFDMA system is presented in the first section. Then, two sub-issues for partial feedback Channel State Information (CSI) and adjustable Quality-of-Service (QoS) are studied via the proposed schemes.

2.1 Typical downlink system model

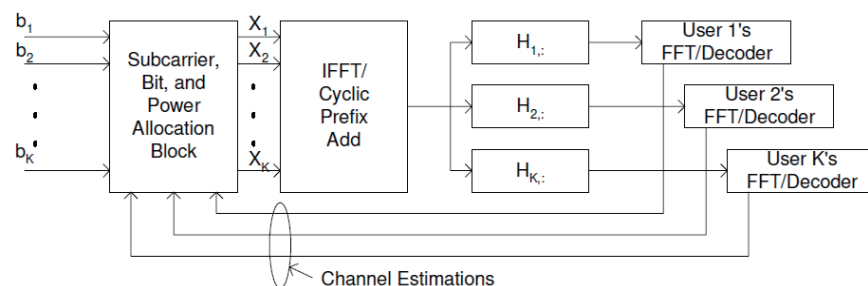


Fig. 2.1: Typical downlink OFDMA system model with K users.

Fig.2.1 shows the general principle of downlink OFDMA resource allocation for K users, where k ($k \in \{1, 2, \dots, K\}$) indicates one particular user. Specifically, the Base

Station (BS) utilizes the instantaneous feedback Channel State Information (CSI) via channel estimation to make resource allocation decisions. Then, these decisions are used to perform a conventional OFDM modulation [6] for each user at the transmitter, which corresponds to modulating the bit data of each user d_k to be the symbol data X_k through a subcarrier-power-bit allocation block, as given in Fig.2.1. After performing Inverse Fast Fourier Transform (IFFT) and adding the cyclic prefix for OFDM symbols, a standard OFDM signal transmission over different channel conditions, denoted as H_k , is carried out. Then, the users decode the received data respectively after performing Fast Fourier Transform (FFT).

For various resource allocation problems formulated from Fig.2.1, many solutions have been proposed in the literature [6], [11], [37]. However, two issues have not been well studied, one is to effectively reduce the maintained CSI at the BS and the other one is to flexibly adjust data-rate distribution according to the specific requirement of each user. As a result, this chapter provides two solutions with low complexity for these two issues, respectively.

To simplify the system modeling, the following assumptions are adopted in the following two sections: Each subcarrier for each user experiences independent fading; The subcarriers are not shared by different users in current system setup¹; The considered system suffers a slowly time-varying frequency selective Rayleigh fading, which means that the channel is constant during one symbol transmission; The BS collects full or partial CSI² via a dedicated feedback channel, while these channel estimates can be used to make resource allocation decisions at the BS without delay.

¹The spectrum sharing problem for such a system will be discussed in Chapter 5.

²Full CSI means the full set of channel gains, while partial CSI means a sub-set of full CSI.

2.2 Partial feedback channel state information

The objective in this section is to maximize the total system capacity with constraints on total available power, Bit Error Rate (BER) and Proportional Fairness (PF) while using a novel partial feedback CSI mechanism.

2.2.1 Review and motivation

As given in [38], [39], it is usually assumed that each user perfectly knows his channel conditions and there exists a reliable mechanism to feedback all the CSI to the BS so that adaptive resource allocation can be performed. This full CSI feedback mechanism may not be practically implementable since the maintained amount of CSI becomes considerable as the number of users increases. In addition, as observed in [11], only a few good subcarriers with strong channel gains are actually allocated to one user even though full CSI of that user is available at the BS, which is mainly due to the multiuser diversity. This phenomenon motivates us to shrink the amount of feedback CSI of each user to a small portion of full CSI with relatively strong channel gains, which is to ask each user to merely feedback the CSI of some most preferable subcarriers having higher probabilities to be allocated to that user at the BS. Although some studies have investigated how to efficiently utilize partial CSI in the literature, however, these methods mainly focus on non-accurate channel estimation [39] or average channel gain [40], which is different from the mechanism proposed in this section. Recently, we find that the study [10] has given a similar idea saying opportunistic feedback over downlink OFDMA networks, nevertheless, the study [10] does not consider user fairness as our scheme in this section.

2.2.2 Problem formulation and opportunistic feedback example

Without loss of generality, the system is assumed to have K users and N subcarriers (SCs), the channel gain of user k on subcarrier n is denoted as g_{kn} , and p_{kn} is the

power on subcarrier n assigned to user k , where $n \in \Gamma = \{1, \dots, N\}$ and $k \in \Delta = \{1, \dots, K\}$. Also, the noise power spectral density is assumed to be z_0 and the total bandwidth of all subcarriers is B . Thus, each subcarrier occupies a spectrum $W = B/N$, the additive white noise power on each subcarrier is $v_0 = z_0 W$ with the associated received Signal-to-Noise Ratio (SNR) being $\gamma_{kn} = p_{kn} g_{kn}^2 / v_0$. When using M-ary Quadrature Amplitude Modulation (MQAM) with Gray bit mapping [41], the Bit Error Rate (BER) can be approximated as a function of the received SNR γ_{kn} , which is given by

$$BER_{\text{MQAM}}(\gamma_{kn}) \approx 0.2 \exp[-1.5\gamma_{kn}/(2^{c_{kn}} - 1)], \quad (2.1)$$

for $\gamma_{kn} \geq 4$ and $BER \leq 10^{-3}$. Then,

$$c_{kn} = \log_2(1 + \gamma_{kn}/\Psi) = \log_2(1 + p_{kn}H_{kn}), \quad (2.2)$$

where $\Psi = -\ln(5BER)/1.5$ is a constant SNR gap [41] and $H_{kn} = g_{kn}^2/(v_0\Psi)$ is the effective channel-to-noise gain of user k on subcarrier n with $p_{kn}H_{kn}$ being the effective SNR. Note that H_{kn} serves as the CSI of user k on subcarrier n in this section, and the matrix \mathbf{H} ($K \times N$) for making subcarrier allocation is as follows

$$\mathbf{H} = \begin{bmatrix} H_{11} & H_{12} & \cdots & H_{1N} \\ H_{21} & H_{22} & \cdots & H_{2N} \\ \vdots & \vdots & \ddots & \vdots \\ H_{K1} & H_{K2} & \cdots & H_{KN} \end{bmatrix}. \quad (2.3)$$

The overall data-rate of user k is then given by

$$r_k = W \sum_{n=1}^N \rho_{kn} \log_2(1 + p_{kn}H_{kn}). \quad (2.4)$$

Based on the problem studied in [11], the total system capacity with proportional fairness can be formulated as

$$\max_{\rho_{kn}, p_{kn}} W \sum_{k=1}^K \sum_{n=1}^N \rho_{kn} \log_2(1 + p_{kn}H_{kn}) \quad (2.5)$$

subject to

$$\sum_{k=1}^K \rho_{kn} = 1 \quad \forall n, \text{ with } \rho_{kn} \in \{0, 1\} \quad \forall k, n \quad (2.6)$$

$$\sum_{k=1}^K \sum_{n=1}^N \rho_{kn} p_{kn} \leq P_{tot}, \text{ with } p_{kn} \geq 0 \quad \forall k, n \quad (2.7)$$

$$\frac{r_1}{r_k} = \frac{\varphi_1}{\varphi_k}, \quad k = 2, 3, \dots, K \quad (2.8)$$

where ρ_{kn} is the subcarrier allocation indicator that means $\rho_{kn} = 1$ if and only if subcarrier n is assigned to user k , otherwise $\rho_{kn} = 0$. In addition, P_{tot} is the total power at the BS and $\varphi_k, k \in \Delta$ are some pre-determined positive values to ensure the proportionalities among users. Specifically, the subcarrier allocation constraint (2.6) ensures that each subcarrier can only be assigned to one user, the power constraint (2.7) limits the transmit power at the BS, and the proportional fairness constraint (2.8) gives the desired normalized rate proportion³ of each user

$$\alpha_k = \varphi_k \Big/ \sum_{k=1}^K \varphi_k. \quad (2.9)$$

The optimization problem in (2.5) is known as a binary integer programming problem, which is generally NP-hard and difficult to obtain the optimal solution [42]. As a result, some suboptimal solutions are proposed for this problem in [11] based on the full knowledge of CSI at the BS. However, the amount of feedback CSI becomes considerable and reduces the feasibility of these existing algorithms, especially when the numbers of users and subcarriers increase. This is also a common and challenging issue in centralized OFDMA resource allocation [38]. Note that, without considering the fairness constraint (2.8), the optimal solution to the problem (2.5) is demonstrated in [43], saying that the capacity of single-hop OFDMA system is maximized when subcarriers are assigned to users with the highest channel gains and power is allocated to subcarriers through water-filling algorithm [44]. In addition, the generalized weighted sum-rate

³In the simulation section, we set the value of each φ_k to be an integer value, while α_k is defined to express the desired fraction of the overall system capacity for user k .

TABLE 2.1: Example for the feasibility of partial feedback CSI

	SC 1	SC 2	SC 3	SC 4
<i>user 1</i>	0.196	0.185	0.258	0.102
<i>user 2</i>	0.327	0.411	0.239	0.098
<i>user 3</i>	0.189	0.272	0.135	0.193

problem with practical optimality is proposed in [45] through a low complexity implementation. With these in mind, this section focuses on designing an efficient mechanism at low complexity to reduce the feedback CSI while maintaining the system performance.

Table 2.1 gives a set of typical channel states with each element being given as $v_0 H_{kn} = g_{kn}^2 / \Psi$ for a four-subcarrier and three-user case when adopting the same simulation settings as [11]. Note that $v_0 \mathbf{H}$ is used as the decision matrix in this example, which does not change the optimal subcarrier allocation as using (2.3)⁴. According to the aforementioned optimal allocation principle [43], the subcarrier allocation should be that SC 1 and SC 2 are both allocated to *user 2*, SC 3 and SC 4 are allocated to *user 1* and *user 3*, respectively. If the BS only knows the best two subcarriers of each user as shown in bold values, it can be easily observed that the optimal subcarrier allocation remains the same. This observation motivates us to realize the fact that it may not be necessary to feedback full CSI of each user to the BS in a multiuser OFDMA system, a portion of full CSI associated with some best subcarriers can also produce an optimal or sub-optimal allocation. In addition, it is worth noting that some subcarriers may not be used and a sub-optimal allocation may be formulated when using this partial feedback mechanism. For instance, if *user 3* does not exist, the usage of SC 4 cannot be determined exactly. Even though SC 4 could be randomly assigned to either *user 1* or *user 2*, the accurate bit-loading becomes difficult without any channel information. In the sequel, the adoption of this partial feedback mechanism into the algorithm in [11] is given in detail.

⁴Multiply all the elements in the matrix \mathbf{H} with the same value does not change the allocation rule, since the location (in which row) of the maximum element in each column remains unchanged.

2.2.3 Proposed scheme

In this sub-section, we propose a novel partial feedback CSI mechanism with its adoption in the conventional algorithm in [11]. This proposed scheme consists of two steps, the first step is to perform a subcarrier allocation with equal power distribution based on partial feedback CSI and the second step is to carry out a power refinement to improve the system capacity.

Firstly, we present the subcarrier allocation method with equal power distribution. According to the optimal subcarrier allocation principle in [43], the selection criterion without fairness concern is to select the maximum value in the n th column of \mathbf{H} in (2.3) for each $n \in \Gamma$. If the maximum value is in the k th row for the n th column, subcarrier n should be allocated to user k . We follow this principle while considering proportional fairness (2.8) in the algorithm design of subcarrier allocation.

Specifically, it is proposed to merely feedback partial values of the elements in the decision matrix \mathbf{H} to the BS. For user k , it feeds back some most highest values in the k th row of \mathbf{H} with the number of these values being given by

$$\min([\xi\alpha_k N], N), \quad (2.10)$$

where $\xi \geq 1$ is defined as the feedback index used to control the amount of feedback CSI, α_k is the normalized rate proportion of user k in (2.9) with $\sum_{k=1}^K \alpha_k = 1$, and $[x]$ means rounding x to the smallest integer larger than or equal to x . Thus, the total amount of feedback CSI can be reduced to be about ξN , which is approximately ξ/K of the original feedback amount requiring all the elements of \mathbf{H} . In addition, the undetermined elements in the decision matrix \mathbf{H} are filled as zero, which gives a modified decision matrix $\hat{\mathbf{H}}$ with each element being \hat{H}_{kn} .

With the modified decision matrix based on partial feedback CSI, the proposed subcarrier allocation algorithm is described in detail as follows. Note that the equal power distribution now becomes allocating equal power to the CSI-available subcarriers

that is less than N for some values of ξ , and some subcarriers named as Null subcarriers (corresponding to the columns with all-zero elements in \mathbf{H}) are allocated to users without usage.

Initialization of parameters:

Let $N_k = \lfloor \alpha_k N \rfloor$ be the total number of subcarriers for user k , and each of the remaining $N_{un} = N - \sum_{k=1}^K N_k$ subcarriers be added to N_k with probability α_k .

Initialize ρ_{kn} and r_k as zero. Note that subcarrier and user indices are $\Gamma = \{1, \dots, N\}$ and $\Delta = \{1, \dots, K\}$, respectively, and α_k can be pre-determined from (2.9).

Implementation of subcarrier allocation:

As shown in Table 2.2.

TABLE 2.2: Implementation of subcarrier allocation

WHILE $\Gamma \neq \emptyset$ DO	
$k = \arg \min_{k \in \Delta} (r_k / \alpha_k);$	(T2.2.1)
IF $N_k > 0$ DO	
$n = \arg \max_{n \in \Gamma} (\hat{H}_{kn});$	(T2.2.2)
$\rho_{kn} = 1;$	(T2.2.3)
$\Gamma \leftarrow \Gamma \setminus n;$	(T2.2.4)
$N_k \leftarrow N_k - 1;$	(T2.2.5)
$r_k \leftarrow r_k + W \log_2 (1 + \hat{p} \hat{H}_{kn});$	(T2.2.6)
ELSE	
$\Delta \leftarrow \Delta \setminus k;$	(T2.2.7)
END IF	
END WHILE	

In above algorithm, \leftarrow stands for updating the value of one specific parameter, $A = A \setminus \{e\}$ is to eliminate the element e from the set A , $\lfloor x \rfloor$ is to round x to the largest integer smaller than or equal to x . Note that the unknown CSI associated with null subcarriers is automatically treated as zero so that the equal power allocation becomes

$\hat{p} = P_{tot}/N_s$, where N_s is the number of actually used subcarriers (the number of non-all-zero columns) in $\hat{\mathbf{H}}$.

To be specific, one user k is selected firstly according to the targeting rate proportion in (T2.2.1), if this user cannot accept more subcarriers, this user is excluded in further iterations (T2.2.7). Otherwise, one subcarrier n with the highest channel gain is selected for this user (T2.2.2) and actually allocated (T2.2.3–5), which is followed by updating the instantaneously achieved data-rate (T2.2.6).

When the subcarrier allocation is obtained, a power refinement can be carried out to further improve the system capacity. The optimal power allocation with known subcarrier allocation is provided in Appendix A. Note that, as shown in many studies [43], [46], [47], the system capacity is not sensitive to the power allocation at high SNR condition due to the logarithmic calculation in the objective function (2.5). Thus, for simplicity, the following simulations with a general high SNR system setup will utilize the equal power allocation for a faster implementation⁵. Note that the average complexity is the same as the scheme in [11] that is in the order of $\mathcal{O}(KN\log_2 N)$, which mainly depends on sorting the decision matrix \mathbf{H} for each user as observed from Table 2.2.

Overall, in this sub-section, we only exemplify the idea on the basis of [11] to propose the above algorithm with partial feedback CSI. To be used in other algorithms for downlink OFDMA systems using full feedback CSI such as [8], [38], [43], [46], [47], similar modifications might be made via the proposed partial feedback mechanism.

2.2.4 Simulation results

This sub-section simulates a typical WLAN scenario the same as that in [11] with the BS located at the centre and several users uniformly distributed within one cell. Specifically, the frequency-selective multipath channel is modeled as 6-tap Rayleigh fading with an

⁵For general SNR scenarios, the power refinement adopting the method in Appendix A should not be omitted, which needs more computational complexity.

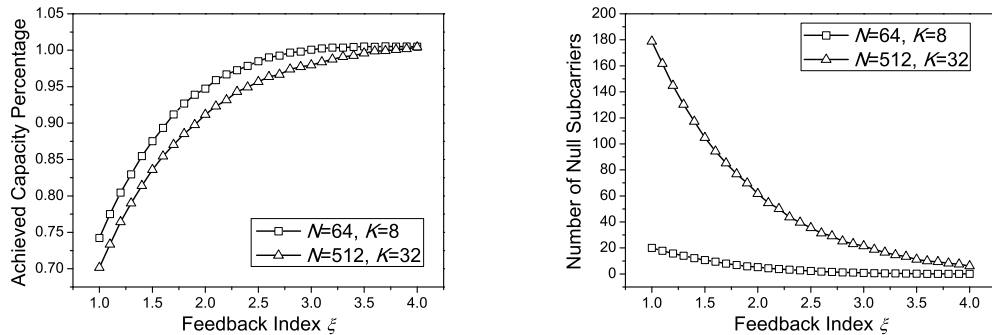


Fig. 2.2: Achieved capacity percentage, and number of null subcarriers.

exponentially decaying profile. The total power at the BS is 1W with the total bandwidth being $B = 1\text{MHz}$. The BER requirement is set as $BER = 10^{-3}$ for each user. In addition, users have independent channel statistics, and the desired rate proportion of each user is calculated by (2.9) with each φ_k being assigned an integer value from the set $\{1, 2, 4\}$ with equal probability. We assume a general high SNR condition by setting the noise power spectral density to be $z_0 = -80\text{dBW/Hz}$.

In the left part of Fig.2.2, the ratio of the system capacity with partial CSI to that with full CSI, denoted as the achieved capacity percentage, is depicted versus the feedback index ξ (2.10) for two settings of different subcarriers and users. It can be seen that the capacity loss of using partial CSI becomes negligible as ξ increases. In the right part, the number of null subcarriers (subcarriers without usage) is given. Similarly, the number of null subcarriers approaches zero when ξ increases. From Fig.2.2, for larger enough ξ (e.g., $\xi = 4$), the system capacity of using partial feedback CSI is shown to be almost the same as that with full CSI even if few null subcarriers may exist. Alternatively speaking, near-optimal resource allocation can be made only from a small portion of full CSI due to the multiuser diversity discussed previously. Note that larger feedback index ξ indicates larger amount of feedback CSI, which is approximately ξ/K of the full CSI required (2.10).

After showing the system capacity and null subcarrier versus different values of

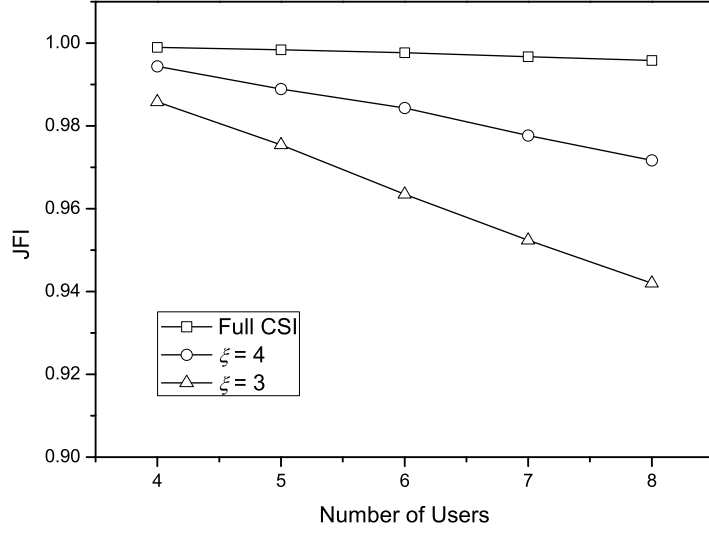


Fig. 2.3: Fairness comparison.

ξ , one question arises: what is the price to pay for maintaining almost the same system capacity when limited CSI is available at the BS in our investigated system. The answer is manifested in Figs.2.3–2.4, focusing on the cases of 64 subcarriers. Specifically, Fig.2.3 compares the fairness achieved by full CSI and the proposed partial CSI implementation with $\xi = 3$ and 4, respectively. The well-known Jain's Fairness Index (JFI) [48] is used for fairness comparison, which is given by

$$JFI = \left(\sum_{k=1}^K x_k \right)^2 / \left(K \sum_{k=1}^K x_k^2 \right), \quad (2.11)$$

where $x_k = r_k/\alpha_k$ is the ratio of practically achieved capacity to the desired rate proportion for user k . Note that absolute fairness is achieved when $JFI = 1$. In Fig.2.3, the use of partial feedback CSI results in certain fairness loss, and less feedback amount gives worse fairness performance. Meanwhile, the overall system fairness decreases as the number of users increases for both full and partial CSI implementations since more users have increased uncertainty in overall fairness. Nevertheless, such degraded fairness

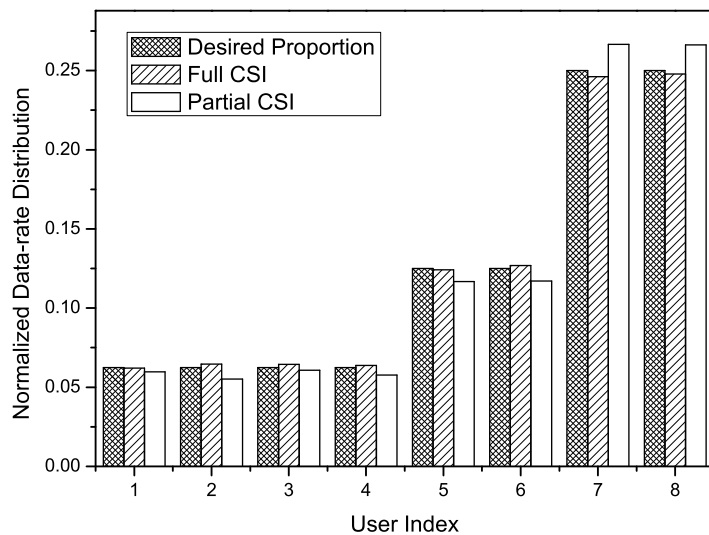


Fig. 2.4: Normalized data-rate distribution.

still lead to the desirable data-rate distribution, which is further shown in Fig.2.4.

Figure 2.4 illustrates a normalized data-rate distribution for the case of $N = 64$, $K = 8$ and $\xi = 3$. In this case, user fairness is directly given by $\alpha_1 = \dots = \alpha_4 = 1/16$, $\alpha_5 = \alpha_6 = 1/8$, and $\alpha_7 = \alpha_8 = 1/4$. As observed in this figure, the fairness performance with partial CSI does not strictly follow the desired proportion as that using full CSI. However, little fairness degradation is not a crucial issue in practical communications since effective data-rate of each user is still achieved. Together with Fig.2.3, we can conclude that the price to pay for maintaining almost same system capacity is the loss of certain proportional fairness among users. With these observations, the feedback index ξ provides a leverage to tradeoff between system capacity and user fairness.

2.3 Adjustable quality-of-service

This sub-section presents a simple implementation that can flexibly adjust system capacity and user fairness at low complexity via using the minimum requested data-rate of each user in the system [15]. This scheme can achieve diverse Quality-of-Service (QoS) requirements of users [48], which is equivalent to properly assigning the requested data-rate to each user in the system.

2.3.1 Problem formulation and motivation

The considered system model is the same as that in the previous section. Accordingly, the objective function considered is the same as (2.5). Three constraints are used, the first and second constraints are in line with (2.6) and (2.7), respectively. Instead of (2.8), the third constraint becomes the minimum requested data-rate of each user, which is given by

$$r_k = \sum_{n=1}^N \rho_{kn} \log_2(1 + p_{kn} H_{kn}) \geq r_k^{\min} \quad \forall k. \quad (2.12)$$

Note that r_k is now defined in spectrum efficiency (bps/Hz) for user k requiring a minimum data-rate r_k^{\min} . In most of existing studies, this minimum data-rates requested by the users are usually pre-determined values. However, they becomes system design variables in this section.

As aforementioned, when $r_k^{\min} = 0$, the capacity optimality of the above modified problem is to assign subcarriers to users with the highest effective SNRs (cf. (2.2)) and to allocate power over subcarriers through the conventional water-filling algorithm [43]. However, this optimality may result in extremely unfair data-rate distribution among users. Although the fairness issue has been discussed in [11], [49], these existing studies normally have deterministic fairness as well as system capacity under certain settings without a flexible factor that can adjust the performance in-between. Motivated by this observation, we have developed a controllable capacity and fairness scheme in [12]. In

which, the shortcoming is that it only fills the gap between [9] and [11] without providing a mechanism to achieve the maximum available system capacity. Thus, in this section, we further propose a simple scheme that can adjust system capacity and user fairness through setting different levels of minimum requested data-rates of users.

2.3.2 Proposed scheme

Specifically, this new scheme consists of two steps. The first step is to allocate subcarriers to all users based on equal power distribution given by $p_{kn} = P_{tot}/N$. Then, the conventional water-filling (WF) algorithm [6], [43] is performed to further improve the capacity on a per user basis. The proposed subcarrier allocation is described in detail in Table 2.3. The notational conventions used here are the same as those for Table 2.2, except that \emptyset indicates the empty set.

To be specific, in Table 2.3, some parameters recording the allocation states are initialized at the beginning. Then, in the first while loop, users are selected by the ratio r_k/r_k^{\min} with fairness consideration, and then assigned with their best subcarriers indicated by the highest available channel-to-noise gain H_{kn} . In the second while loop, each remaining subcarrier is assigned to one user with the best contribution to the system capacity. Note that each state parameter is updated once one subcarrier is allocated.

After carrying out the algorithm in Table 2.3, the allocated subcarriers of each user are available in ρ_{kn} . Then, user k has a total allocated power $p_k = P_{tot}N_k/N$, where N_k is the number of subcarriers actually assigned to this user. Finally, the conventional WF algorithm is utilized to refine user k 's power p_k over the allocated N_k subcarriers to further improve the system capacity. As shown in [49], this performance improvement of the system capacity is quite limited at high SNR condition since WF algorithm approaches equal power allocation.

Together, the subcarrier allocation in Table 2.3 and further power refinement using WF formulate our proposed scheme. In terms of computational complexity, the subcar-

TABLE 2.3: Proposed algorithm for subcarrier allocation

$\Delta = \{1, \dots, K\}$ = user indices;
 $\Gamma = \{1, \dots, N\}$ = subcarrier indices;
 Set $r_k = 0$ and $N_k = 0$ for $k \in \Delta$;
 Set $\rho_{kn} = 0$ for $k \in \Delta, n \in \Gamma$;
WHILE $\Delta \neq \emptyset$
 $k = \arg \min_{k \in \Delta} (r_k / r_k^{\min})$;
 $n = \arg \max_{n \in \Gamma} (H_{kn})$;
 $r_k \leftarrow r_k + q_{kn}$;
 $\Gamma \leftarrow \Gamma \setminus n$; $N_k \leftarrow N_k + 1$; $\rho_{kn} = 1$;
 IF $r_k \geq r_k^{\min}$ **THEN** $\Delta \leftarrow \Delta \setminus k$;
 IF $\Gamma = \emptyset$ **THEN** exits;
END WHILE
 Reset $\Delta = \{1, \dots, K\}$;
WHILE $\Gamma \neq \emptyset$
 Select one subcarrier n from Γ ;
 $k = \arg \max_{k \in \Delta} (H_{kn})$;
 $r_k \leftarrow r_k + q_{kn}$;
 $\Gamma \leftarrow \Gamma \setminus n$; $N_k \leftarrow N_k + 1$; $\rho_{kn} = 1$;
END WHILE

rier allocation has the same worst complexity as [11], which is in a complexity order of $\mathcal{O}(KN \log_2 N)$ when no subcarrier is left for the second while loop. Note that this worst-case complexity mainly depends on sorting H_{kn} for each user. On the other hand, the least complexity is $\mathcal{O}(KN)$, which occurs when no minimum data-rate of each user is set, corresponding to only using the second while loop. Note that r_k^{\min} in the first while loop can make a computational tradeoff inside the algorithm, which will be further shown the ability in adjusting capacity and fairness in the following simulations .

2.3.3 Simulation results

The sub-section also simulates a single-cell scenario with one centered BS and several users uniformly distributed in the cell. For comparison with existing algorithms, main

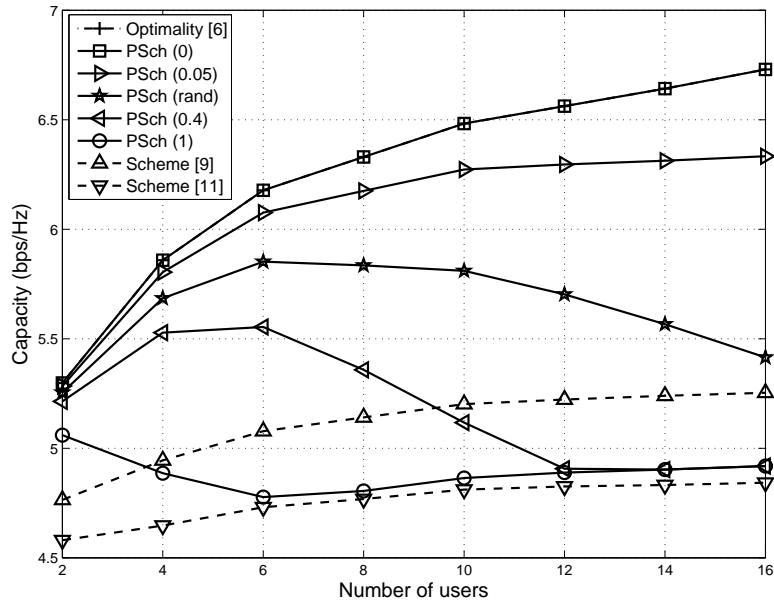


Fig. 2.5: System capacity versus number of users.

system parameters are set the same as [9], [11]. Briefly, the frequency selective multipath channel is modeled as six-path Rayleigh fading channel with an exponentially decaying profile. The total power at the BS is 1 watt, and the total bandwidth, $B=1\text{MHz}$, is occupied by $N=64$ subcarriers. In addition, $BER = 10^{-3}$ is assumed to be required by each user, and the general high SNR condition is given by setting the noise power spectral density as $z_0=-80\text{dBW/Hz}$.

In Fig.2.5, the system capacity against the number of users is depicted. As seen in this figure, two traditional algorithms [9], [11] with an emphasis on user fairness suffer some loss in system capacity compared with the optimal allocation given in [6]. The proposed scheme represented by $\text{PSch}(x)$, where x indicates r_k^{\min} (bps/Hz) for all users and is used to generate different levels of r_k^{\min} settings. Note that $\text{PSch}(\text{rand})$ means each user randomly selects one r_k^{\min} from the set $\{0.1, 0.2, 0.3\}$ (bps/Hz) with equal probability. Obviously, smaller r_k^{\min} produces higher capacity since more subcarriers can be used to enhance the system capacity. As observed from $\text{PSch}(0.4)$ and $\text{PSch}(1)$, when

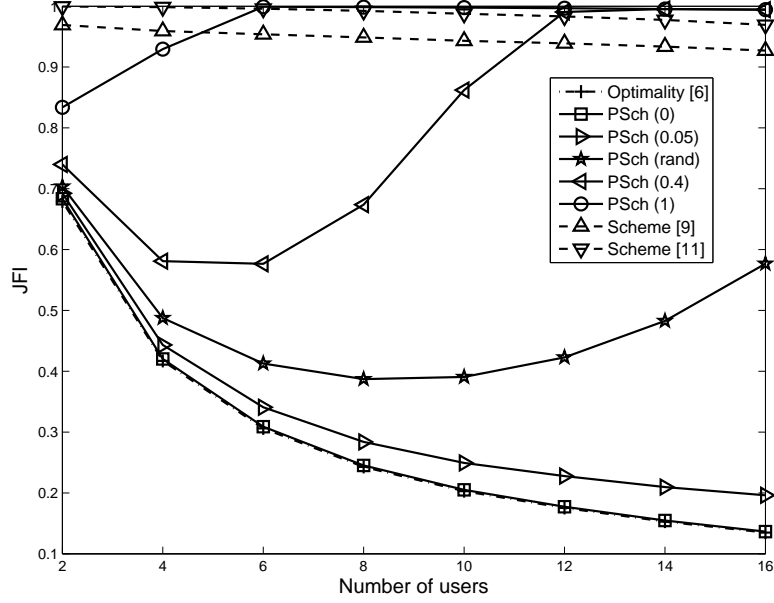


Fig. 2.6: Fairness comparison.

the minimum data-rate of each user cannot be satisfied, the proposed scheme tends to allocate data-rate to users as equal as possible and finally converges to a performance between [9] and [11] since no remaining subcarrier can be used to enhance capacity. This also can explain the gradually decreasing feature of PSch(rand) when the data-rates of users are allocated proportionally to their minimum requirements without being satisfied. In addition, PSch(0) gives almost the maximum system capacity that achieved by the optimality scheme. From this figure, it can be concluded that the proposed scheme is able to provide a flexible factor, r_k^{\min} , to adjust the achieved system capacity.

Figure 2.6 illustrates the fairness comparison among different schemes, where JFI has been defined in (2.11) for comparing user fairness. To make all the investigated algorithms comparable, each element x_k in calculating JFI should be normalized first. Specifically, $x_k = r_k/\alpha_k$ for [9], [11], where α_k is the desired proportionality [11], and $x_k = r_k/\beta_k$ for the proposed scheme, where $\beta_k = r_k^{\min}/(\sum_{k=1}^K r_k^{\min})$. To tackle the problem of being divided by zero, we use a small value 10^{-6} instead of $r_k^{\min} = 0$ in such

a normalization pre-processing, which can be interpreted as assigning an arbitrary small data-rate to the user without data-rate requirement. For the optimality scheme, $x_k = r_k$ is the achieved capacity.

As can be seen in Fig.2.6, the two fairness-emphasized schemes [9], [11] have near optimal fairness for all numbers of users while [9] has worse fairness due to more emphasis on enhanced capacity. For the proposed scheme, the observed features well comply with the system capacity shown in Fig.2.5. Specifically, from PSch(0.4) and PSch(1), the proposed scheme gradually achieves near-optimal fairness when more users request the same minimum data-rate but cannot be satisfied. Another observation is that less r_k^{\min} results in worse fairness, which is compensated by the capacity gain as in Fig.2.5.

2.4 Conclusions

Two efficient schemes are proposed in this chapter for downlink OFDMA-based resource allocation. Firstly, a multiuser diversity enabled partial feedback CSI mechanism is formulated in Section 2.2. As observed from the simulation results, we find that it may not be necessary to feedback full CSI from the users to the BS in terms of system capacity. A small portion of full CSI can be utilized to make near-optimal resource allocation in multiuser OFDMA systems. For instance, exploiting 12.5% of full CSI can achieve almost the same system capacity for the case of $K = 32, \xi = 4$. On the other hand, this partial feedback mechanism may lead to a little fairness loss for users, which is normally acceptable in practical implementations. As a result, Section 2.2 provides an easy method for achieving the tradeoff among system capacity, proportional fairness, and feedback amount of CSI in downlink OFDMA systems. Secondly, Section 2.3 has demonstrated a desirable property for diverse QoS control via properly setting different requested data-rate r_k^{\min} of each user. This r_k^{\min} value is exploited as a system design variable to balance

between system capacity, user fairness, and computational complexity. Overall, two efficient techniques are presented to flexibly balance different system performance metrics, which forms the main contributions in this chapter.

Chapter 3

Resource allocation for MIMO-OFDMA

In this chapter, we consider different utility-based resource allocation schemes for a downlink Multiple Input Multiple Output (MIMO) - OFDMA system. The system optimality and some conventional optimization objectives are reviewed first. Then, two bargaining solutions are utilized to formulate efficient algorithms for flexibly controlling user fairness.

3.1 Review and motivation

Multiple Input Multiple Output (MIMO) is a promising technique that can significantly improve the physical layer performance of wireless communication systems. Many schemes have been proposed for MIMO resource allocation in multiuser environments [17], [18]. In MIMO systems, multiple antennas are used at both transmitter and receiver to exploit spatial diversity. With the need of additional antennas, MIMO transceivers are generally more complex, and are sometimes combined with OFDM or OFDMA to handle the problems induced by multipath fading channel more efficiently. Specifically,

MIMO-OFDMA has been incorporated in the IEEE 802.16e standard [3] and MIMO-OFDM has been recommended in the IEEE 802.11n standard [50].

In high data-rate wireless communication systems, the system utility should be maximized. Meanwhile, fair data-rate distribution should be considered for users in that diverse Quality-of-Service (QoS) requirements with different pricing policies are usually needed [51], which becomes a crucial issue recently in OFDMA-based resource allocation. In dynamic resource allocation, it is known that capacity enhancement, fairness improvement and complexity reduction are usually conflicting in nature. As a result, efficient implementation with low complexity and good balance between system capacity and user fairness is desired.

In the literature, game theoretic approaches have been exploited for resource allocation in OFDMA systems in [52], [53]. In these studies, cooperative and non-cooperative games have been discussed while the Nash equilibrium [54] usually serves as one important algorithm design metric. As one type of cooperative game, bargaining theory is adopted in resource allocation problems for OFDMA systems [55] and multimedia communications [56], in which the bargaining solutions are used to design feasible algorithms. Note that the novel scheme based on Nash Bargaining Solutions (NBS) with equal bargaining powers studied in [55] opens the door for using bargaining theory in OFDMA systems and also motivates the present work with more general considerations. With these in mind, we will investigate the problem of downlink resource allocation for generalized MIMO-OFDMA systems that includes SISO-OFDMA as a special case.

In this chapter, the use of two bargaining solutions, Generalized NBS (GNBS) [54] and Kalai-Smorodinsky Bargaining Solution (KSBS) [57], for efficient MIMO-OFDMA resource allocation will be discussed in detail, which is also the main contribution. In addition, the criteria of utilitarian and egalitarian are briefly described. The generalized bargaining strategies with different bargaining powers are considered, which is different from the pioneering study [55], [56]. Specially, the bargaining powers can

be used to adjust the data-rate distribution of users, which is named as GNBS/KSBS fairness. Note that the introduced GNBS fairness is shown to include the traditional proportional fairness used in [11] as a special case, which gives a more general algorithm design metric. The investigated two bargaining solutions are shown to exhibit important properties for achieving diverse QoS requirements of users.

3.2 MIMO-OFDMA system model

Based on the MIMO systems investigated in [6], [36], this chapter studies the system model shown in Fig. 3.1, which corresponds to a typical downlink channel from the BS to the mobile user k . In this figure, each functional block comply with OFDM transmission [6]. In addition, this figure illustrates the procedure of resource allocation in downlink MIMO-OFDMA, which is similar as in Fig.2.1. Firstly, the BS utilizes the instantaneous feedback Channel State Information (CSI) to make resource allocation decisions. Then, these decisions are used to adjust the transmitter at the BS for loading each user's data onto their allocated subcarriers as well for decoding the received signals at each user end.

Without loss of generality, the number of transmit and receive antennas are denoted as M_t and M_r , respectively, with the number of users being K and the number of subcarriers being N . Also, we assume the total system bandwidth is B and the thermal noise is v_0 over each subcarrier. For convenience, let the user index set be $\Delta = \{1, \dots, K\}$ with user $k \in \Delta$ and the subcarrier index set be $\Gamma = \{1, \dots, N\}$ with subcarrier $n \in \Gamma$. Some other notations used are given as follows: The bold lower case letter, e.g. \mathbf{v} , indicates a vector while the bold upper case letter, e.g. \mathbf{H} , is a matrix; The normal matrix transposition and conjugate transpose are represented by $(\cdot)^T$ and $(\cdot)^H$, respectively.

As shown in Fig. 3.1, let the transmitted signal of user k on subcarrier n be

$$\mathbf{x}_{kn} = [x_{kn}(1), \dots, x_{kn}(M_t)]^T, \quad (3.1)$$

where $x_{kn}(i)$ is the transmitted signal of user k on subcarrier n from the i th antenna.

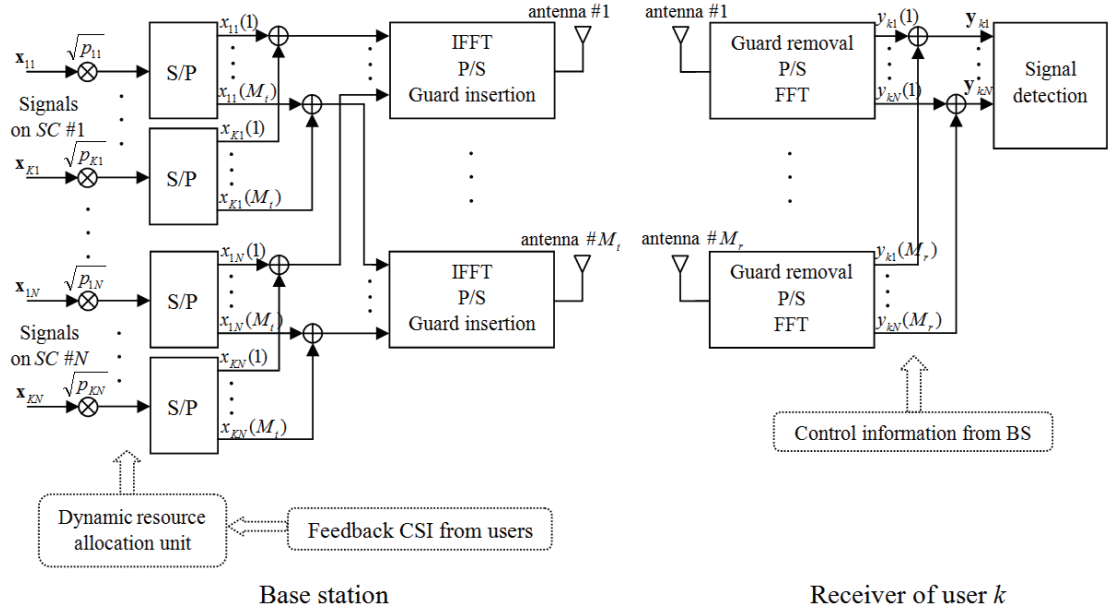


Fig. 3.1: Typical MIMO-OFDMA system model.

Then, the transmitted signal on subcarrier n can be represented as

$$\sum_{k=1}^K \mathbf{x}_{kn} \sqrt{p_{kn}} = \left[\sum_{k=1}^K x_{kn}(1) \sqrt{p_{kn}}, \dots, \sum_{k=1}^K x_{kn}(M_t) \sqrt{p_{kn}} \right]^T. \quad (3.2)$$

Let the received signal of user k on subcarrier n be

$$\mathbf{y}_{kn} = [y_{kn}(1), \dots, y_{kn}(M_r)]^T, \quad (3.3)$$

the channel gain matrix be \mathbf{H}_{kn} ($M_r \times M_t$), and the Additive White Gaussian Noise (AWGN) vector be \mathbf{z}_{kn} ($M_r \times 1$). Each element y_{kn} in (3.3) can be further expressed as

$$\mathbf{y}_{kn} = \sum_{k=1}^K \sqrt{p_{kn}} \mathbf{H}_{kn} \mathbf{x}_{kn} + \mathbf{z}_{kn}, \quad (3.4)$$

with the following assumptions

$$\mathbb{E}(\mathbf{x}_{kn} \mathbf{x}_{kn}^H) = \mathbf{I}, \quad (3.5)$$

$$\mathbb{E}(\mathbf{x}_{in} \mathbf{x}_{jn}^H) = \mathbf{0}, \text{ if } i \neq j, \quad (3.6)$$

$$\mathbb{E}(\mathbf{z}_{kn} \mathbf{z}_{kn}^H) = v_0 \mathbf{I}, \quad (3.7)$$

$$\mathbb{E}(\mathbf{z}_{kn} \mathbf{z}_{kn}^H) = \mathbf{0}, \text{ if } i \neq j. \quad (3.8)$$

Note that \mathbf{I} ($M_r \times M_r$) is the identity matrix. Then,

$$\mathbb{E}(\mathbf{y}_{kn}\mathbf{y}_{kn}^H) = p_n\mathbf{H}_{kn}\mathbf{H}_{kn}^H + v_0\mathbf{I}, \quad (3.9)$$

where $p_n = \sum_{k=1}^K p_{kn}$ is the total power on subcarrier n .

As demonstrated in [6] for MIMO-OFDMA systems, on particular subcarrier n , only one user is allowed to transmit with all the power assigned on this subcarrier to achieve optimality. Thus, the maximum capacity (bps/Hz) of user k on subcarrier n is

$$c_{kn} = \log_2 \left[\det \left(\mathbf{I} + \frac{p_n\mathbf{H}_{kn}\mathbf{H}_{kn}^H}{v_0} \right) \right]. \quad (3.10)$$

Note that \mathbf{H}_{kn} can be decomposed via singular value decomposition given by

$$\mathbf{H}_{kn} = \mathbf{U}_{kn}\Sigma_{kn}\mathbf{V}_{kn}^H, \quad (3.11)$$

where Σ_{kn} ($M_r \times M_t$) is a diagonal matrix, \mathbf{U}_{kn} ($M_r \times M_r$) and \mathbf{V}_{kn} ($M_t \times M_t$) are unitary matrices. Then,

$$\mathbf{H}_{kn}\mathbf{H}_{kn}^H = \mathbf{U}_{kn}\mathbf{\Lambda}_{kn}\mathbf{U}_{kn}^H, \quad (3.12)$$

where $\mathbf{\Lambda}_{kn} = \text{diag}\{\lambda_{kn}^{(1)}, \dots, \lambda_{kn}^{(M_{kn})}\}$ is the eigen-value diagonal matrix of $\mathbf{H}_{kn}\mathbf{H}_{kn}^H$ and $M_{kn} = \text{rank}(\mathbf{H}_{kn})$. When \mathbf{H}_{kn} is available at both transmitter and receiver, a transmitting pre-coding filter of \mathbf{V}_{kn} and a receiving shaping filter of \mathbf{U}_{kn}^H can be used to decouple the MIMO channel of user k on subcarrier n into M_{kn} parallel SISO channels [36]. Note that each $\lambda_{kn}^{(i)}$ corresponds to one decoupled SISO channel. Thus, (3.10) can be simplified

$$c_{kn} = \sum_{i=1}^{M_{kn}} \log_2 \left(1 + \frac{\lambda_{kn}^{(i)}p_n}{v_0} \right). \quad (3.13)$$

With consideration of the SNR gap [58], the total data-rate (bps) of user k can be expressed as

$$r_k = W \sum_{n=1}^N \sum_{i=1}^{M_{kn}} \log_2 \left(1 + \rho_{kn} \frac{\lambda_{kn}^{(i)}p_n}{v_0\Psi} \right), \quad (3.14)$$

where $W = B/N$, and ρ_{kn} is the subcarrier allocation indicator, $\rho_{kn} = 1$ if subcarrier n is allocated to user k , otherwise $\rho_{kn} = 0$. In addition, Ψ is the SNR gap between

the theoretical value of channel capacity and the practically achieved one using some coding-modulation methods. As stated in Chapter 2, $\Psi = -\ln(5BER)/1.5$ that is a function of the required BER when using adaptive MQAM modulation in OFDMA systems [58]. It is also assumed that all users perfectly know their CSI (3.12) and there exists a mechanism to feedback full or partial CSI to the BS in order to make resource allocation decisions. When the CSI is not available at the BS, the MIMO channel cannot be decoupled into M_{kn} SISO channels and other advanced antenna techniques [36] are required to achieve the capacity, which is beyond the scope of this chapter. Note that, with equal power allocation (p_n is a constant value), the capacity in (3.13) holds as long as $M_t \leq M_r$ even without having CSI at the BS. This feature is used for subcarrier allocation in the following section.

3.3 Utility-based resource allocation

In this section, the Dynamic Resource Allocation (DRA) problem of generalized MIMO-OFDMA systems including SISO-OFDMA as a special case is studied. The use of two bargaining solutions, Generalized NBS (GNBS) [54], [57] and Kalai-Smorodinsky Bargaining Solution (KSBS) [59], for designing efficient MIMO-OFDMA resource allocation is discussed in detail. In addition, the criteria of utilitarian and egalitarian are briefly described with their efficient DRA implementations.

3.3.1 Utility-based problem formulation

With the system considered in Fig. 3.1, if all the resources are allocated to a single user, the associated optimization problem is given by

$$\begin{aligned} \max_{p_n} r_s &= W \sum_{n=1}^N \sum_{i=1}^M \log_2 \left(1 + \frac{\lambda_n^{(i)} p_n}{v_0 \Psi} \right) \\ \text{s.t.} \quad &\sum_{n=1}^N p_n \leq P_{tot}, \end{aligned} \quad (3.15)$$

where $M = \min(M_t, M_r)$, P_{tot} is the total power constraint at the BS. The partial Lagrangian of (3.15) is then as follows

$$L_s = W \sum_{n=1}^N \sum_{i=1}^M \log_2 \left(1 + \frac{\lambda_n^{(i)} p_n}{v_0 \Psi} \right) + \lambda_s \left(P_{tot} - \sum_{n=1}^N p_n \right). \quad (3.16)$$

Then, the following partial differential can be obtained

$$\frac{\partial L_s}{\partial p_n} = \frac{W}{\ln 2} \sum_{i=1}^M \frac{\lambda_n^{(i)}}{v_0 \Psi + \lambda_n^{(i)} p_n} - \lambda_s. \quad (3.17)$$

When we set (3.17) equal to zero and assume $\sum_{n=1}^N p_n = P_{tot}$ is satisfied, $(N+1)$ unknown variables with $(N+1)$ equations can be found. This set of non-linear equations could be solved by some existing tools such as Newton-Raphson or quasi-Newton methods [42]. As a result, the optimal capacity in (3.15) can be obtained. In addition, at high SNR, we have $v_0 / \lambda_n^{(i)} \approx 0$, (3.17) then can be approximated as

$$\frac{WM}{p_n \ln 2} - \lambda_s = 0. \quad (3.18)$$

Thus, the power on each subcarrier is

$$p_n = \frac{WM}{\lambda_s \ln 2} = \frac{P_{tot}}{N}, \quad (3.19)$$

and the single-user capacity can be approximated as

$$r_s = W \sum_{n=1}^N \sum_{i=1}^M \log_2 \left(1 + \frac{\lambda_n^{(i)} P_{tot}}{v_0 \Psi N} \right). \quad (3.20)$$

For general SNR scenarios, the multi-dimensional water-filling algorithm [44] can be applied to (3.17) so as to iteratively find the optimal power distribution. However, this iterating process needs more computational complexity. For simplicity, we consider a general high SNR system setup as that in [55].

In the sequel, efficient resource allocation in a multiuser scenario is our focus. Specifically, the problem with multiple users can be formulated as

$$\max_{\rho_{kn}, P_{kn}} U, \text{ s.t. } \begin{cases} \sum_{k=1}^K \rho_{kn} = 1, \forall n \\ r_k \geq r_k^{\min}, \forall k \\ \sum_{k=1}^K \sum_{n=1}^N p_{kn} \leq P_{tot} \end{cases} \quad (3.21)$$

Note that in (3.21), r_k^{\min} is the minimum data-rate requirement of user k , P_{tot} is the total power constraint at the BS. In particular, four utility-based objectives are considered in (3.21). The first one is the *Utilitarian* objective that is $U = \sum_{r=1}^K r_k$, which corresponds to maximizing the sum-rate as much as possible when the minimum data-rate of each user is satisfied [6]. The optimal solution to Utilitarian for $r_k^{\min} = 0$ is provided in the Appendix B. The second one is the *Egalitarian* objective that is $U = \min \{r_1, \dots, r_K\}$, which complies with equally distributing the capacity to users as fairly as possible as the solution given in [55]. In addition, two generalized bargaining objectives, *GNBS* and *KSBS*, are also adopted and will be discussed in detail in the next section. Note that the first two criteria, Utilitarian and Egalitarian, have been often used in the literature to enhance system capacity and user fairness, respectively. Meanwhile, the GNBS and KSBS are two criteria that will be exploited in this chapter for trading off between capacity and fairness.

The problem in (3.21) is a binary integer-programming problem, which is generally NP-hard [60] and usually needs an exhaustive search to find the optimal or one local-optimal point, which does not suit real-time applications. Thus, low complexity algorithms with efficient implementations are the focus of this section.

3.3.2 System optimality and bargaining solutions

The optimality of using Utilitarian criterion in (3.21) has been given in [6] when no minimum data-rate is set for each user that is $r_k^{\min} = 0$. This optimality is briefly given in Appendix B. For convenience of the following description, we define the payoff set as $\mathbf{S} = \{(r_1, \dots, r_K)\} \subset \mathfrak{R}^K$, where r_k is data-rate of user k . From the optimality given in Appendix B, we can obtain the maximum achievable capacity r_{op}^{tot} of the investigated system. Thus, using other objective functions to evaluate U in (3.21) results in a resource re-distribution with a suboptimal sum-rate strictly less than or equal to r_{op}^{tot} , which gives a closed and convex set \mathbf{S} [55]. Furthermore, we assume the disagreement point as

$\mathbf{r}^{\min} = \{(r_1^{\min}, \dots, r_K^{\min})\} \in \mathfrak{R}^K$. Next, the Pareto optimality is introduced as follows [56].

Definition 3.1 (Pareto Optimality): The resource allocation point $(r_1, \dots, r_K) \in \mathbf{S}$ is Pareto optimal, if for each $(r'_1, \dots, r'_K) \in \mathbf{S}$ and $(r'_1, \dots, r'_K) \geq (r_1, \dots, r_K)$, then $(r'_1, \dots, r'_K) = (r_1, \dots, r_K)$.

Note that the equality or inequality between two vectors in this sub-section is component-wise representation. As shown in [56], there might be an infinite number of Pareto optimal points in a bargaining game with multiple users. As a result, other selection criteria are required to decide which Pareto optimal point is the best for a specific system, which is equivalent to finding the corresponding bargaining solution. Subsequently, we adopt two bargaining strategies to analyze the resource allocation with the consideration of Pareto optimality and user fairness.

3.3.2.1 Generalized Nash bargaining solution (GNBS)

Nash bargaining solution has been well studied in cooperative games [54] and can be defined as a unique optimal point that satisfies some axioms. These axioms are known as rationality, feasibility, Pareto optimality, independence of irrelevant alternatives, independence of linear transformations, and symmetry [55]. The first three axioms confine the bargaining set while the others emphasize on fairness. With the violation of symmetry, GNBS has been studied in [56], [57]. This GNBS is used to design the resource allocation in this sub-section since it provides an adjustable fairness for capacity distribution.

Assuming the maximum achievable capacity is r_{GN}^{tot} in this case, the GNBS utility optimization can be formulated as

$$\begin{aligned} \max_{r_k} U &= \prod_{k=1}^K (r_k - r_k^{\min})^{\alpha_k} \\ \text{s.t.} \quad &\sum_{k=1}^K r_k \leq r_{GN}^{tot}, \text{ and } r_k \geq r_k^{\min}. \end{aligned} \quad (3.22)$$

Note that α_k is the generalized bargaining power of user k with their sum being $\sum_{k=1}^K \alpha_k = A$, and the objective U in (3.22) gives the Generalized Nash Product (GNP). Let the GNBS solution be $f_{GN}(\mathbf{S}, \mathbf{r}^{\min}) = \{(r_1^{GN}, \dots, r_K^{GN})\}$, then it can be easily shown that each element r_k^{GN} in this set satisfies [54]

$$r_k^{GN} = r_k^{\min} + \frac{\alpha_k}{A} \left(r_{GN}^{tot} - \sum_{j=1}^K r_j^{\min} \right), \quad (3.23)$$

when $\sum_{k=1}^K r_k = r_{GN}^{tot}$. The physical understanding of (3.23) is to allocate the remaining system capacity to users according to their normalized bargaining powers after satisfying each user's minimum data-rate. Based on (3.23), each user in intermediate bargaining stage with instantaneous data-rate, defined as r_k^{in} , should target an equal value given by $(r_k^{in} - r_k^{\min})/\alpha_k$ to achieve GNBS point, which will be used as the algorithm design criterion in the next section.

Note that (3.23) indicates that the bargaining power of each user can serve as a leverage to adjust the data-rate distribution of users, which is a desired property in diverse QoS systems [48]. In addition, this type of adjustment has been initially discussed in [11] via the Proportional Fairness (PF) defined as follows.

Definition 3.2 (Proportional Fairness): The proportional fairness¹ is defined as that the total system capacity r_{tot} is distributed among users according to their normalized desired proportions given by $\gamma_1, \dots, \gamma_K$ with $\sum_{k=1}^K \gamma_k = 1$. Specifically, user k is allocated the capacity of $\gamma_k r_{tot}$.

The data-rate distribution in (3.23) is named as Generalized NBS (GNBS) fairness, which can be shown to include the above Proportional Fairness (PF) as a special case. Specifically, the GNBS fairness is the same as the PF when $\mathbf{r}^{\min} = \mathbf{0}$, which can be easily observed from (3.23) and the PF definition with $\gamma_k = \alpha_k/A$ when $\mathbf{r}^{\min} = \mathbf{0}$. In addition, the GNBS fairness with consideration of the minimum data-rate of each user is more reasonable than PF with the data-rate distribution strictly according to some

¹There may exist some alternative definitions of proportional fairness as given in [61]. In this section, the definition in [11] is used.

pre-determined proportions since the minimum data-rate of one user usually should be satisfied with high priority in practical systems.

3.3.2.2 Kalai-Smorodinsky bargaining solution (KSBS)

Since GNBS only considers the data-rate distribution from a systematic point of view, KSBS is used to give another designing metric in this sub-section. Specifically, KSBS takes the overall channel condition of each user into account and can enhance efficiency of radio resource utilization [56]. We use the KSBS to design efficient algorithm, more theoretical details about KSBS can be found in [54], [59]. Note that the most important feature of KSBS is individual monotonicity, which states that one user always benefits from increasing the size of bargaining set in a direction preferable for this user.

Let the KSBS result be $f_{KS}(\mathbf{S}, \mathbf{r}^{\min}) = \{(r_1^{KS}, \dots, r_K^{KS})\}$ while assuming the maximum achievable capacity being r_{KS}^{tot} , each element r_k^{KS} can be found by the intersection point of the bargaining set \mathbf{S} and the following set [54], [56]

$$\mathbf{L} = \left\{ \mathbf{r} \left| \begin{array}{l} \frac{r_1 - r_1^{\min}}{\alpha_1 (r_1^{\max} - r_1^{\min})} = \dots = \frac{r_K - r_K^{\min}}{\alpha_K (r_K^{\max} - r_K^{\min})}, \\ \mathbf{r} \geq \mathbf{r}^{\min}, \sum_{k=1}^K \alpha_k = A, \text{ for } k \in \Omega \end{array} \right. \right\}, \quad (3.24)$$

where $\mathbf{r} = (r_1, \dots, r_K)$ is the set of data-rate distribution of users and α_k is the generalized bargaining power of user k . When $\sum_{k=1}^K r_k = r_{KS}^{tot}$, the KSBS of user k is given by

$$r_k^{KS} = r_k^{\min} + \frac{\left(r_{KS}^{tot} - \sum_{k=1}^K r_k^{\min} \right) \alpha_k (r_k^{\max} - r_k^{\min})}{\sum_{k=1}^K \alpha_k (r_k^{\max} - r_k^{\min})}. \quad (3.25)$$

From (3.25), each user in intermediate bargaining stage with instantaneous data-rate r_k^{in} should target an equal value given by $(r_k^{in} - r_k^{\min}) / [\alpha_k (r_k^{\max} - r_k^{\min})]$, which is similar as the designing criterion of GNBS in (3.23). The difference is that KSBS considers both r_k^{\max} and r_k^{\min} while GNBS only considers r_k^{\min} . This user fairness given by (3.25) is named as KSBS fairness in this sub-section. It is also worth noting that the bargaining

power can be easily used to adjust data-rate distribution of users as shown in both (3.23) and (3.25). In addition, r_k^{\max} can be obtained from (3.15) and approximated by (3.20) at high SNR.

For better understanding of these two bargaining solutions, some simple bargaining examples are provided in [54], [55], [56], [62]. After briefly introducing the bargaining results of GNBS and KSBS, efficient implementations of resource allocation will be proposed subsequently.

3.3.3 Implementations of utility-based allocation

In this section, the real-time implementations for the aforementioned four utility-based objectives will be discussed. Note that the maximum system capacity can be achieved by the two conditions summarized in Appendix B, however, it requires high computational complexity. Similar as the study [11], we also separate the subcarrier and power allocation as two independent stages. Specifically, the subcarrier allocation adopts the following sub-optimal selection criterion

$$k_n = \arg \max_k \prod_{i=1}^{M_{kn}} \left(1 + \frac{\lambda_{kn}^{(i)} P_{tot}}{v_0 N} \right), \quad (3.26)$$

where k_n is the allocated user index on subcarrier n that is equivalent to $\rho_{kn} = 1$. This selection criterion corresponds to using equal power allocation in (B.3), which is shown to be near-optimal in Appendix B.

Based on (3.26), the following matrix \mathbf{D} ($K \times N$) can be formulated to make subcarrier allocation

$$\mathbf{D} = \begin{bmatrix} d_{11} & d_{12} & \cdots & d_{1N} \\ d_{21} & d_{22} & \cdots & d_{2N} \\ \vdots & \vdots & \ddots & \vdots \\ d_{K1} & d_{K2} & \cdots & d_{KN} \end{bmatrix}, \quad (3.27)$$

where

$$d_{kn} = \prod_{i=1}^{M_{kn}} \left(1 + \frac{\lambda_{kn}^{(i)} P_{tot}}{v_0 N} \right). \quad (3.28)$$

According to (3.26), the optimal selection criterion for (3.27) is to select the maximum value in the n th column of \mathbf{D} for each $n \in \Gamma$. If the maximum value is in the k th row for the n th column, subcarrier n is then assigned to user k . Once the subcarrier allocation is available, multi-dimensional water-filling can be used to refine the power allocation for further improved capacity [6]. Note that the above processing can be used as a tight approximation of the system optimality and will be used as the capacity upper bound.

Furthermore, we discuss efficient implementations for the aforementioned four utility-based objectives, Egalitarian, Utilitarian, GNBS, and KSBS. Specifically, to efficiently carry out Egalitarian resource allocation, a modified algorithm based on [11] is used. In [11], the authors are concerned with allocating data-rate to users according to some strictly desired proportions. However, this algorithm is designed for a SISO-OFDMA system and must be modified to be suitable for our investigated general SISO/MIMO-OFDMA system. Thus, the channel-to-noise gain matrix used in [11] is replaced by the decision matrix in (3.27). Then, multi-dimensional water-filling algorithm is used to improve the system capacity. We denote this modified algorithm as *Egalitarian* implementation when using equal fairness, otherwise this modified algorithm with proportional fairness as in Definition 3.2 is referred to as *PF* implementation. Note that this modified algorithm becomes the same as that in [11] when $M_r = M_t = 1$ and has an asymptotic complexity of $O(KN \log_2 N)$.

For the *Utilitarian* implementation, the minimum data-rate requirement of each user should be satisfied with top priority. Thus, the associated low complexity implementation is proposed as the following two steps. Firstly, users take turns to select one best subcarrier at one time until all users have gained their minimum data-rates. Specifically, one subcarrier is selected by $n = \arg \max_{n \in \Gamma_{av}} (d_{kn})$ for user k , where n is in the set of currently available subcarriers given by Γ_{av} . Note that users who have gained

TABLE 3.1: GNBS/KSBS implementation of resource allocation

$\Delta = \{1, \dots, K\}$ = user indices;	
$\Gamma = \{1, \dots, N\}$ = subcarrier indices;	
Set $r_k = 0$ for $k \in \Delta$ and $\mathbf{r}^{\min} = (r_1^{\min}, \dots, r_K^{\min})$;	
Set $\rho_{kn} = 0$ for $k \in \Delta, n \in \Gamma$;	
WHILE $\Delta \neq \emptyset$	
$k = \arg \min_{k \in \Delta} (r_k)$;	(T3.1.1)
$n = \arg \max_{n \in \Gamma} (d_{kn})$;	(T3.1.2)
$r_k \leftarrow r_k + W \sum_{i=1}^{M_{kn}} \log_2 \left(1 + \frac{\lambda_{kn}^{(i)} p}{v_0 \Psi} \right)$;	(T3.1.3)
IF $r_k \geq r_k^{\min}$ THEN $\Delta \leftarrow \Delta \setminus k$;	(T3.1.4)
$\Gamma \leftarrow \Gamma \setminus n$; $\rho_{kn} = 1$;	(T3.1.5)
IF $\Gamma = \emptyset$ THEN exits;	(T3.1.6)
END WHILE	
Reset $\Delta = \{1, \dots, K\}$;	
WHILE $\Gamma \neq \emptyset$	
$k = \arg \min_{k \in \Delta} \left(\frac{r_k - r_k^{\min}}{\alpha_k} \right)_{GN}$	
<i>or</i> $\arg \min_{k \in \Delta} \left[\frac{r_k - r_k^{\min}}{\alpha_k (r_k^{\max} - r_k^{\min})} \right]_{KS}$;	(T3.1.7)
$n = \arg \max_{n \in \Gamma} (d_{kn})$;	(T3.1.8)
$r_k \leftarrow r_k + W \sum_{i=1}^{M_{kn}} \log_2 \left(1 + \frac{\lambda_{kn}^{(i)} p}{v_0 \Psi} \right)$;	(T3.1.9)
$\Gamma \leftarrow \Gamma \setminus n$; $\rho_{kn} = 1$;	(T3.1.10)
END WHILE	

their minimum data-rates is excluded in further allocation of this step. Secondly, allocate the rest of the subcarriers according to (3.26) to increase the system capacity as much as possible.

Based on the above implementations, the resource allocation with GNBS/KSBS fairness is proposed in Table 3.1 in detail. Note that \emptyset represents the empty set, $\Gamma \setminus n$ means deleting the element n from the set Γ while $a \leftarrow b$ stands for updating the value of a by b . To be specific, some parameters are initialized first including the user and subcarrier indices, instantaneously achieved data-rate r_k , minimum data-rate of each user

r_k^{\min} , and the allocation indicator ρ_{kn} . In addition, equal power allocation, $p = P_{tot}/N$ is used and $\Psi = -\ln(5BER)/1.5$ can be pre-calculated for one particular BER level [58].

The first while loop is to roughly ensure the minimum data-rate of each user, corresponding to the first step of *Utilitarian*. In this loop, the user with the minimum instantaneous data-rate (T3.1.1) is allocated with the best available subcarrier (T3.1.2) according to (3.26), this user's instantaneous data-rate is then updated (T3.1.3). Once user k has reached r_k^{\min} , this user is excluded in further operation (T3.1.4). Also, each allocated subcarrier is removed from Γ with ρ_{kn} updated (T3.1.5). When all subcarriers run out, this loop breaks and the whole algorithm stops (T3.1.6). In this loop, it functions as allocating data-rate to each user proportional to r_k^{\min} . In the second while loop, bargaining fairness is emphasized while each user targets the GNBS/KSBS point (T3.1.7), the adopted two selection criteria have been discussed in the previous section. Then, the best available subcarrier of this user is chosen (T3.1.8) with the instantaneous data-rate being updated (T3.1.9).

The proposed algorithm in Table 3.1 corresponds to emphasizing GNBS/KSBS fairness as given by in (3.23) and (3.25). The complexity of this algorithm is dominated by the sorting process (T3.1.2) or (T3.1.8) within each iteration, and can be further reduced by pre-sorting the decision matrix (3.27) for each row (or for each user). This pre-sorting needs a total complexity order of $O(KN\log_2 N)$ by using some conventional sorting methods such as heap sort or merge sort [60].

In above proposed implementations, the equal power allocation is assumed, which only demonstrates near-optimal power allocation in high SNR scenarios. For general SNR cases, a power refinement after implementing the algorithm in Table 3.1 should be further followed to improve the system capacity. We have shown this power refinement method in [63] as an extension of [11], which bears the similar feature as the optimal power distribution given in Appendix A. Since a general high SNR system setup is used in the simulation section, this power refinement is not exploited in current chapter for a

faster implementation. Interested readers may refer to our work in [63] for more details. In addition, it can be observed that all four utility objectives will converge to almost the same performance when the system becomes infeasible (cannot satisfy the minimum data-rate requirements of all the users). This case makes the system allocate data-rates to users proportional to their minimum data-rate requirements, which complies with the proportional fairness [11].

Note that the decision matrix (3.27) should be available at the BS in advance to perform dynamic resource allocation, which requires all the users to feedback their CSI to the BS. However, the amount of feedback CSI becomes considerable and reduces the feasibility of our proposed implementations when the number of users increases. Thus, an efficient mechanism is required to reduce the feedback CSI without severe performance loss. Note that in Chapter 2 [64], we have presented the idea of reducing feedback CSI via opportunistic feedback since only a small number of subcarriers with relatively strong channel gains are actually used by each user under independent multiuser fading environment. This technique can also be exploited here for CSI reduction.

3.3.4 Simulation results

Based on the physical layer setup in [3], we simulate one single cell with radius being 1.6 kilometers. In this cell, a total bandwidth of 5MHz divided into 512 subcarriers is considered. In addition, each user has slow mobility that is 30Hz Doppler frequency, and the total power constraint at the BS is set to be 43.1dBm. We also assume enough separation between antennas so that the fading for transmit and receive antenna pairs are independent.

For other system settings, the large-scale propagation loss factor is assumed as three [55] and the log-normal shadowing is zero mean with standard deviation of 8 dB. In addition, the multi-path channel is modeled as 6-tap Rayleigh fading with an exponential decaying profile [36] while each user experiences an independent channel statistics. The

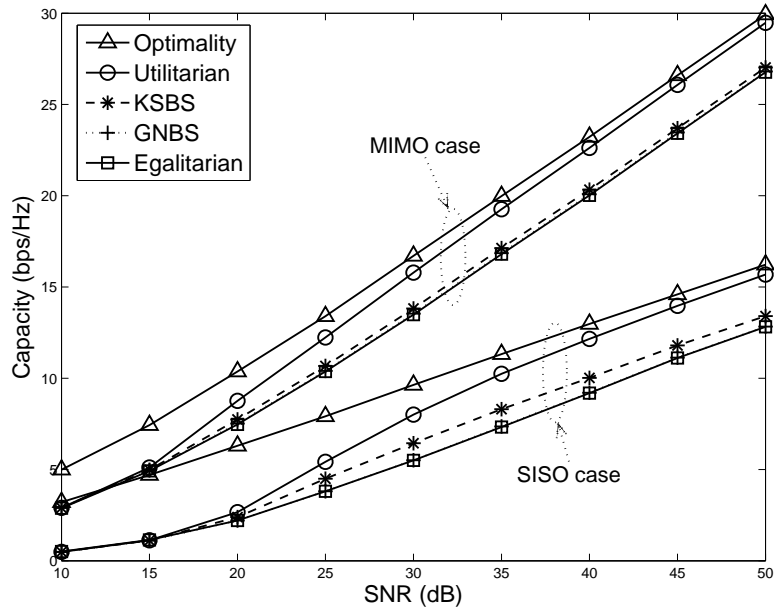


Fig. 3.2: System capacity versus average SNR.

SNR gap in (3.14) is calculated by setting $BER = 10^{-3}$, and adaptive modulation based on MQAM in [58] is used. Note that the thermal noise v_0 on each subcarrier is set according to the average SNR measured at the half radius of the cell in the following simulation results. Unless otherwise stated, these results are averaged over 10^3 channel realizations with users randomly located within the cell for each channel realization. The generalized bargaining power, α_k in (3.23) and (3.25), of user k is assigned with a value from the set $\{1, 2, 4\}$ with equal probability.

Figure 3.2 shows the system capacity against the average SNR for different implementations when $K=10$ users are in the system. Both MIMO ($M_t = M_r = 2$) and SISO ($M_t = M_r = 1$) cases are considered, each user's $r_k^{\min} = 0.5\text{bps/Hz}$ for the MIMO case and $r_k^{\min} = 0.25\text{bps/Hz}$ for the SISO case. This figure also presents the generalization of the proposed and modified algorithms for SISO- and MIMO-OFDMA. To be specific, in the MIMO case, it can be observed that the implementations of *Egalitarian* and *GNBS* have almost the same performance. When average SNR is larger than 15dB, *KSBS* shows

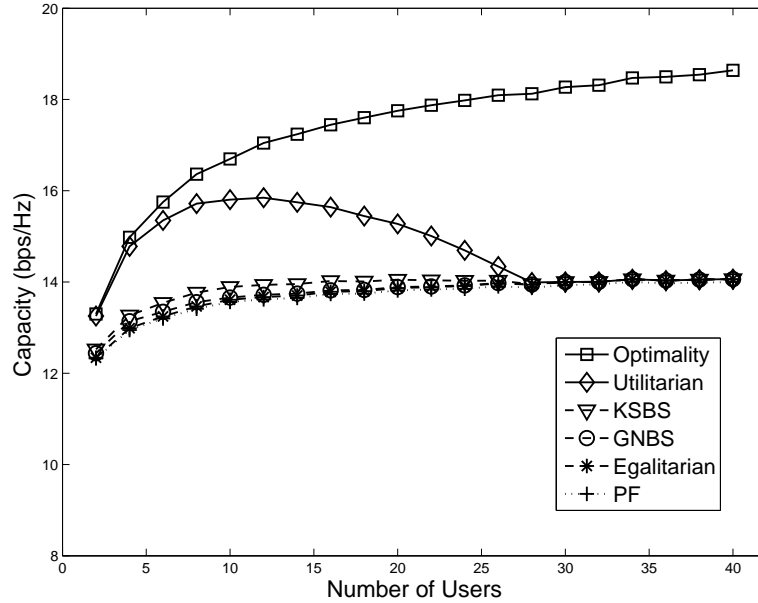


Fig. 3.3: System capacity versus number of users.

little advantage than both *Egalitarian* and *GNBS*, while *Utilitarian* gradually approaches the *Optimality*. Note that the four utility-based implementations converge when at moderate SNR region (10–15dB) since the system cannot satisfy r_k^{\min} of each user and is implemented in an equal fairness manner. This convergence complies with our analysis in the previous sub-section (Page 46), which happens when the system becomes infeasible. Moreover, similar observations can be obtained in the SISO case. To illustrate other features of the proposed implementations, the MIMO case, $M_t = M_r = 2$, is focused in the following results.

Figure 3.3 illustrates the system capacity versus the number of users for the average SNR=30dB, while the minimum data-rate of each user is fixed at 0.5bps/Hz. Specifically, most algorithms have a performance increasing with the increased number of users due to the multiuser diversity except for *Utilitarian*. In the implementation of *Utilitarian*, the system capacity increases first then gradually goes down for continuously increased number of users until converges to almost the same performance as *GNBS* and *KSBS*.

This is because the system gradually becomes infeasible and cannot satisfy r_k^{\min} of each user when more users request the same minimum data-rate. On the other hand, the *Optimality* implementation shows the highest performance, especially when more users are existing. However, this optimal implementation can lead to extremely unfair data-rate distribution, which is to concentrate the system capacity to a small number of users with relatively better channel conditions regardless of other users [6]. Fig.3.3 demonstrates that all four utility-based implementations give a little better capacity than the modified *PF* algorithm, which also shows the disadvantage of imposing strict proportional fairness as [11] in terms of system capacity. This observation verifies the significance of introducing other fairness criteria in the studied system. From Figs.3.2 and 3.3, it can be concluded that spectrum allocation is more dominant in system capacity than power allocation since equal power allocation is used in *GNBS* and *KSBS* without further refinement, which is in line with the observations in [49]. In addition, it can be seen that capacity and fairness are conflicting in nature since imposing fairness degrades system capacity to some extent, especially for a large number of users.

In Fig.3.4, the data-rate distribution of 8 users is plotted for one channel realization with relatively fixed user-locations given by the average distances from the BS as 1.30, 1.23, 1.06, 0.38, 0.24, 0.87, 0.33, 0.59 kilometers, respectively. In addition, we set $r_k^{\min} = 1\text{bps/Hz}$ and the generalized bargaining powers of these 8 users to be $\alpha_1 = \alpha_2 = 1, \alpha_3 = \alpha_4 = 2, \alpha_5 = \alpha_6 = 4, \alpha_7 = \alpha_8 = 8$. In this figure, it can be observed that *Optimality* results in a few users (indices 4, 5, 7) with better channel conditions occupy most of the radio resources without any consideration of user fairness. This unfair allocation is usually dominated by the relative distance from users to the BS. When some users always have worse channel conditions than other users over all subcarriers, the *Optimality* implementation leads to zero data-rate for these users (indices 1, 2) as shown in Fig.3.4. In contrast, the *PF* implementation according to [11] gives almost ideal fairness as the ratios of the bargaining powers. However, this algorithm does not

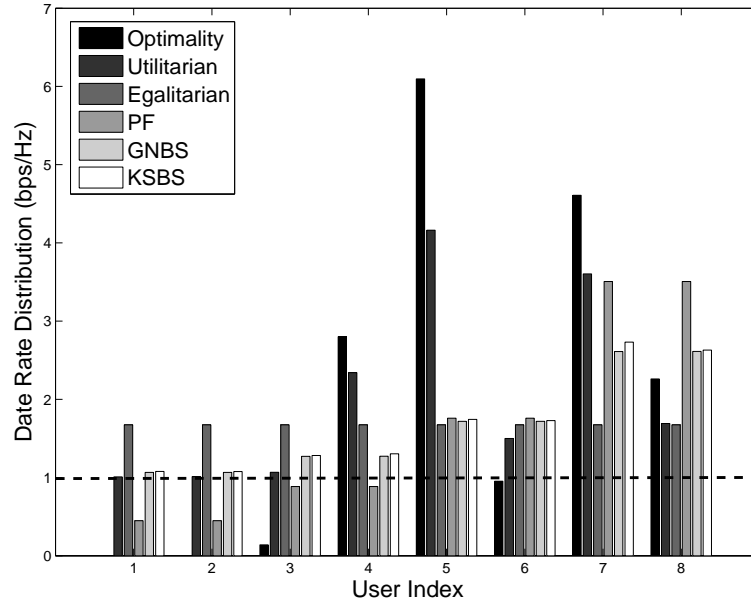


Fig. 3.4: Data-rate distribution for 8 users.

consider the minimum data-rate requirement of each user and results in half number of the users without satisfying their minimum required data-rates.

On the other hand, all the four utility-based implementations can ensure each user's r_k^{\min} in Fig.3.4, which should be considered with high priority in practical systems. In addition, *Egalitarian* provides almost the same data-rate for each user, and *Utilitarian* allocates the resources to users with better channel conditions to increase the system capacity after satisfying r_k^{\min} of each user. The *GNBS* demonstrates that the remaining system capacity is distributed proportionally according to the bargaining powers when the minimum data-rate of each user is achieved. Note that *KSBS* can give a little better capacity gain than *GNBS* over all the users since it considers the overall channel condition of each user.

To illustrate the effect of bargaining power, the bargaining results of two users located at half distance of cell radius under the average SNR of 20dB and 30dB are depicted in Fig.3.5. The minimum data-rates of these two users are set as $\mathbf{r}^{\min} = (r_1^{\min}, r_2^{\min}) =$

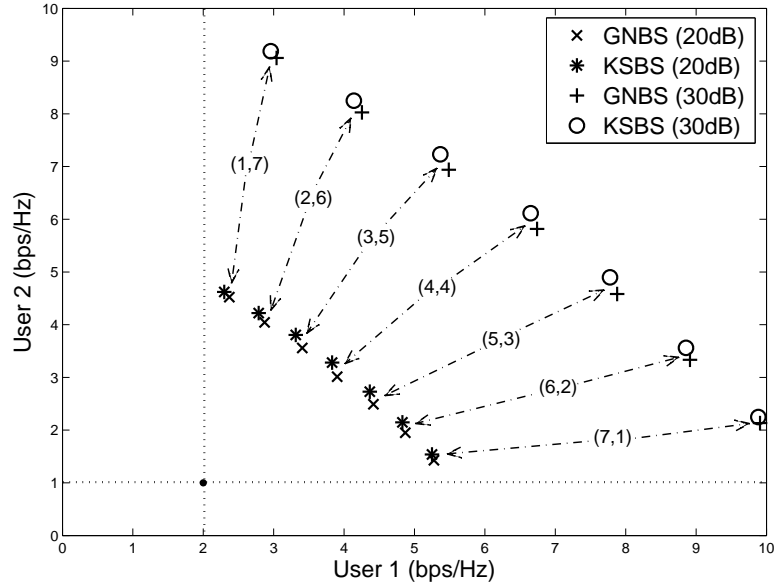


Fig. 3.5: Effect of bargaining power for two-user case.

(2, 1)bps/Hz. With current system realization, the maximum achievable data-rates of these two users are $(r_1^{\max}, r_2^{\max}) = (6.84, 7.12)$ bps/Hz for 20dB SNR scenario, and $(r_1^{\max}, r_2^{\max}) = (11.68, 12.02)$ bps/Hz for 30dB SNR case. The bargaining powers of user 1 and user 2 are given in vector form as (α_1, α_2) in Fig.3.5, with $\alpha_1 + \alpha_2 = 8$ for simplicity. As observed, these two users can bargain for the rest of the system capacity according to their bargaining powers when their minimum data-rates are achieved. Under one specific setting of SNR and bargaining powers, it can be seen that the *GNBS* and *KSBS* are two close points and *KSBS* tends to allocate more data-rate to user 2 with better overall channel conditions than user 1. This data-rate adjustment feature is well-suited for diverse QoS systems.

3.4 Conclusions

In this chapter, we have discussed the general resource allocation problems in downlink MIMO-OFDMA multiuser cellular systems with various system optimization constraints. Four utility-based objectives are studied that are Egalitarian, Utilitarian, and two bargaining solutions, GNBS and KSBS. Based on the system optimality, we propose some efficient algorithms with low complexity in polynomial time for implementing dynamic resource allocation. Furthermore, the generalized bargaining power is shown the ability in adjusting the data-rate distribution of users, which is referred to as GNBS/KSBS fairness. Thus, the proposed algorithms are well suited for satisfying diverse QoS requirements and have a general applicability to downlink SISO/MIMO-OFDMA systems.

Chapter 4

OFDMA-based relaying

This chapter studies a relay-assisted OFDMA cellular system with joint consideration of the direct and relaying paths. In this system, a novel implementation adopting full-duplex relaying is proposed for joint relay-destination selection, subcarrier and power allocation. This new implementation can be shown to significantly improve the system spectrum efficiency compared with the conventional half-duplex relaying mode. In addition, the proposed scheme enables flexible controllability on the tradeoff between system capacity and user fairness.

4.1 Review and motivation

Fixed or mobile Relay Station (RS) is used in Mobile Multi-hop Relay (MMR) systems to extend the network coverage and improve system capacity [24], [65]. Specifically, in MMR systems, each destination node have the ability to combine the signals received from all the previous nodes for better signal detection [22], [66]. As shown in [20], Amplify-and-Forward (AF) and Decode-and-Forward (DF) are two relaying strategies that are often exploited in practical systems. In AF relaying, the relay amplifies the received signal and transmits the amplified signal directly to the destination node. In DF

relaying, the received signal is decoded first and then forwarded to the destination node.

As shown in the previous chapters, OFDMA has an inherent capability of exploiting frequency selectivity enabled multiuser diversity to improve system capacity. The basic principle behind OFDMA-based relaying is thus to utilize the benefits of both multiuser diversity in OFDMA systems and cooperative diversity in relaying systems. In particular, many schemes have been proposed for cellular systems exploiting OFDMA-based relaying [24], [67], which usually models a relay-assisted OFDMA system as an optimization problem with various constraints.

In conventional multi-hop relaying systems, the direct path is usually ignored with the assumption that the destination node is far away from the source node [23]. This conventional relaying mode can make each RS transmit signals in a full-duplex manner via independent sub-channel over individual hops. However, in a relay-assisted cellular system, users may not be always far away from the Base Station (BS) so that the direct path may be strong enough to carry information. As a result, the direct path should not be simply ignored in cellular systems. The authors in [24] initially investigate a joint scenario of direct and relaying paths for uplink OFDMA. Based on [24], many studies for such type of relay-assisted OFDMA systems have been presented [25], [68]. Nevertheless, for simplicity, these studies usually assume that each RS adopts a half-duplex transmission protocol to avoid interference since the same subcarrier is used in successive two hops of the relaying path. In addition, the authors in [26] recently show a novel implementation model, in which the user node can communicate with the BS either through direct path or half-duplex relaying path intelligently. With these in mind, in this chapter, a new system model with joint consideration of direct path and relaying path via using full-duplex RSs is studied so as to fill the gap in the literature.

To be specific, a downlink relay-assisted OFDMA cellular system consisting of one BS, several fixed RSs and a number of user nodes is investigated. In this system, each

RS adopts AF relaying and full-duplex transmission¹ while assuming that direct paths exist between user nodes and the BS. The joint optimization of relay-destination selection and subcarrier pairing in two hops is emphasized. Meanwhile, the power allocation over each subcarrier and fair data-rate distribution of users are considered jointly. Note that, in this new model, the relaying path is always utilized to enhance the direct path, which differs from existing studies either without considering direct path or adopting half-duplex RS.

4.2 System model and problem formulation

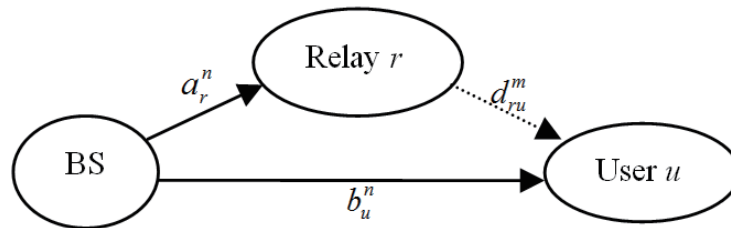


Fig. 4.1: Basic transmission paths in a relay-assisted OFDMA cellular system.

A typical cellular system is considered within a single cell, which has total bandwidth B , one centered BS, R fixed RSs and U users in this section. The basic transmission paths from the BS to user u with the help of RS r in such a relay-assisted OFDMA cellular system are illustrated in Fig. 4.1. As shown by the solid lines, the BS transmits signals to both RS and user nodes. Also, as indicated by the dotted line, RS relays the signal received from the BS to the user node via AF relaying. Note that the BS-RS and RS-User paths adopt different subcarriers, given by n and m , in this model. Thus, each RS can work in a full-duplex manner. For simplicity, the delay between the direct path and the relaying path is assumed to be negligible² compared with symbol duration so

¹One possible method for subcarrier switching via AF in this full-duplex model is given in [69].

²The radio transmission delay in each path is negligible compared with symbol duration. However, each RS may have a processing delay. For simplicity, the adopted AF relaying at each RS is assumed to

that each user node can combine the received signals from both paths for a joint detection. Since the relaying path strictly uses two different subcarriers and the direct path shares the same subcarrier with the first hop of relaying path, the implementation of this novel model is inter-node-interference free once the orthogonalities of subcarriers are maintained [24].

In Fig. 4.1, the channel fading gain from the BS to RS r on subcarrier n is assumed to be a_r^n . The gains from the BS to user u on subcarrier n and from RS r to user u on subcarrier m are b_u^n and d_{ru}^m , respectively. Essentially, subcarriers n and m could form one subcarrier pair, (n, m) , with each value selected from the set $\Gamma = \{1, \dots, N\}$ and $n \neq m$. Similarly, u and r range from 1 to U and 1 to R , respectively. Then, we use (r, u, n, m) to represent one particular subcarrier allocation. Given these parameters, the relayed and received signals at each RS and each user are given by

$$y_{ru}^n = a_r^n x_u^n + v_r^n, \quad (4.1)$$

$$y_{u1}^n = b_u^n x_u^n + v_1^n, \quad (4.2)$$

$$\hat{x}_{ru}^m = \mu_{ru}^m y_{ru}^n, \quad (4.3)$$

$$y_{ru\text{II}}^m = d_{ru}^m \hat{x}_{ru}^m + v_{\text{II}}^m. \quad (4.4)$$

Specifically, in (4.1)–(4.4), x_u^n is the signal transmitted to user u on subcarrier n from the BS with power $E\{\|x_u^n\|^2\} = p_u^n$, \hat{x}_{ru}^m is the signal transmitted to user u on subcarrier m from RS r with power $E\{\|\hat{x}_{ru}^m\|^2\} = p_{ru}^m$. Note that y_{ru}^n is the signal received at RS r , y_{u1}^n and $y_{ru\text{II}}^m$ are the signals received by user u in direct path and relaying path, respectively. In addition, v_r^n , v_1^n , and v_{II}^m are the corresponding noises, and μ_{ru}^m is the amplification factor at RS r for user u on subcarrier m . As a result, with RS r assisting signal transmission for user u on the allocated subcarrier pair (n, m) , the capacity (bps)

be fast enough to load the received signals onto another subcarrier meanwhile sending these signals to the destination users [69], [70].

via using AF relaying is³

$$C_{\text{AF}(r,u)}^{(n,m)} = W \log_2 f(r, u, n, m), \quad (4.5)$$

where

$$f(r, u, n, m) = 1 + \frac{p_u^n \|b_u^n\|^2}{v_0} + \frac{p_u^n p_{ru}^m \|a_r^n\|^2 \|d_{ru}^m\|^2}{v_0^2 + v_0 \|a_r^n\|^2 p_u^n + v_0 \|d_{ru}^m\|^2 p_{ru}^m}, \quad (4.6)$$

with $v_0 = z_0 W$ being the noise power on each subcarrier, and $W = B/N$ being the bandwidth of one subcarrier. Note that z_0 is the power spectrum density of thermal noise. For simplicity⁴, $f(r, u, n, m)$ is used as a notation to represent the right-hand-side of (4.6), which is actually a function of channel gains and allocated powers.

Based on (4.5), the objective function of maximizing the total system capacity can be formulated as

$$\max \sum_{u=1}^U \sum_{r=1}^R \sum_{n=1}^N \sum_{m=1}^N \rho_{ru}^{nm} C_{\text{AF}(r,u)}^{(n,m)} \quad (4.7)$$

subject to

$$\rho_{ru}^{nm} = \{0, 1\}, \quad \forall r, u, n, m, \quad (4.8)$$

$$\sum_{n=1}^N \sum_{r=1}^R \sum_{u=1}^U \rho_{ru}^{nm} = 1, \quad \forall m, \quad (4.9)$$

$$\sum_{m=1}^N \sum_{r=1}^R \sum_{u=1}^U \rho_{ru}^{nm} = 1, \quad \forall n, \quad (4.10)$$

$$\sum_{u=1}^U \sum_{n=1}^N p_u^n \leq P_{BS} \text{ with } p_u^n \geq 0, \quad (4.11)$$

$$\sum_{u=1}^U \sum_{m=1}^N p_{ru}^m \leq P_{FR} \text{ with } p_{ru}^m \geq 0, \quad \forall r. \quad (4.12)$$

For the objective function (4.7), the conditions in (4.8)–(4.10) correspond to subcarrier allocation constraints, and (4.11)–(4.12) correspond to independent power constraints at the BS and each fixed RS respectively. Note that each allocated power should be

³To prove this capacity, we can refer to a similar derivation for uplink OFDMA via half-duplex RS in [24]. For completeness, we provide such a proof in Appendix C.

⁴This type of simplification is also applied later in (4.13) for $L(r, u, n, m)$.

non-negative, and $n \neq m$ with each value ranging from 1 to N . In (4.8), ρ_{ru}^{nm} is the subcarrier pair allocation indicator, $\rho_{ru}^{nm} = 1$ if and only if the subcarrier pair (n, m) is allocated to one particular RS-User pair (r, u) . Since each subcarrier cannot be shared, the conditions (4.9)–(4.10) are used to ensure that one subcarrier pair (n, m) can only be associated with one particular RS-User pair (r, u) once. However, these constraints result in a mixed integer programming problem that is usually NP-hard [60].

Based on the formulated problem, two key questions can now be posed more explicitly. The first one is how to form relay-user and subcarrier pair, (r, u, n, m) , so that each RS can best assist in the signal transmission. The second one is how to allocate transmission power over each subcarrier. These two sub-issues are discussed in the following section.

4.3 System analysis and proposed scheme

For mathematical tractability of the problem (4.7), the constraint (4.8) could be relaxed to be a continuous value between 0 and 1 as the technique used in [71]. With this simplification and using Lagrangian method, the objective function in (4.7) can be transformed into

$$\begin{aligned}
L(r, u, n, m) = & W \sum_{u=1}^U \sum_{r=1}^R \sum_{n=1}^N \sum_{m=1}^N \rho_{ru}^{nm} \log_2 f(r, u, n, m) \\
& - \sum_{n=1}^N \mu_n \left(\sum_{m=1}^N \sum_{r=1}^R \sum_{u=1}^U \rho_{ru}^{nm} - 1 \right) - \sum_{m=1}^N \lambda_m \left(\sum_{n=1}^N \sum_{r=1}^R \sum_{u=1}^U \rho_{ru}^{nm} - 1 \right) \\
& - \xi \left(\sum_{u=1}^U \sum_{n=1}^N p_u^n - P_{BS} \right) - \sum_{r=1}^R \eta_r \left(\sum_{u=1}^U \sum_{m=1}^N p_{ru}^m - P_{FR} \right),
\end{aligned} \tag{4.13}$$

where $\mu_n, \lambda_m, \eta_r, \xi$ are non-negative Lagrangian multipliers. The solution to (4.7) should satisfy Karush-Kuhn-Tucker (KKT) conditions⁵, two of which are given as follows

$$\frac{\partial L(r, u, n, m)}{\partial \rho_{ru}^{nm}} = W \log_2 f(r, u, n, m) - \mu_n - \lambda_m \leq 0, \quad (4.14)$$

$$\rho_{ru}^{nm} [W \log_2 f(r, u, n, m) - \mu_n - \lambda_m] = 0, \quad (4.15)$$

If one particular allocation, (r, u, n, m) , is determined, $\rho_{ru}^{nm} > 0$ should be satisfied. In this case, the following equation can be obtained from (4.15)

$$W \log_2 f(r, u, n, m) = \mu_n + \lambda_m. \quad (4.16)$$

On the other hand, if such allocation does not exist ($\rho_{ru}^{nm} = 0$), it has

$$W \log_2 f(r, u, n, m) \leq \mu_n + \lambda_m, \quad (4.17)$$

which can be observed from (4.14) and (4.15). These two conditions given in (4.16) and (4.17) imply that one particular subcarrier allocation should maximize the left-hand-side of (4.16). Thus, we can conclude that the subcarrier allocation should be selected according to

$$\arg \max [W \log_2 f(r, u, n, m)] = \arg \max f(r, u, n, m). \quad (4.18)$$

Alternatively, the maximum or one of the maximum $f(r, u, n, m)$ values could be used to guide the assignment of subcarriers and RS-User pairs with an additional consideration $n \neq m$ for full-duplex RS implementation.

When the subcarrier allocation for each RS-User pair is determined, several power allocation methods can be adopted, in which, the simplest method is to use equal power allocation at the BS and each RS. The most complicated method is to solve a set of non-linear equations derived from KKT conditions, however the convergence cannot be

⁵Note that only necessary KKT conditions are presented here, it can refer to [72] to easily derive a full set of KKT conditions. The method of deriving KKT conditions is briefly included in Appendix D.

guaranteed due to the non-convexity⁶ of (4.7). Thus, an efficient power allocation is proposed subsequently.

In the sequel, a high SNR condition is assumed so that the channel gains in Fig. 4.1 and the allocated powers p_u^n, p_{ru}^m are far more than the noise power v_0 . Under this condition, let $\partial L(r, u, n, m)/\partial p_u^n = 0$ and $\partial L(r, u, n, m)/\partial p_{ru}^m = 0$ based on (4.13), the following suboptimal power allocation can be derived when ignoring the high-order items of noise power v_0^2 . To be specific, the power allocation for user u on subcarrier n should follow

$$p_u^n = \Delta_{BS} \left(1 - \frac{1}{g_u^n} \right), \quad (4.19)$$

where

$$g_u^n = \frac{\|b_u^n\|^2}{\|d_{ru}^m\|^2} \left(\frac{p_u^n}{p_{ru}^m} \right) + \left(\frac{\|b_u^n\|^2 \|d_{ru}^m\|^2}{\|a_r^n\|^4} + \frac{\|d_{ru}^m\|^2}{\|a_r^n\|^2} \right) \left(\frac{p_{ru}^m}{p_u^n} \right) + \frac{2\|b_u^n\|^2}{\|a_r^n\|^2} + 1. \quad (4.20)$$

Since the total power at the BS is constrained by

$$\sum_{u=1}^U \sum_{n=1}^N p_u^n = P_{BS}, \quad (4.21)$$

substituting (4.19) into (4.21) and simplifying the results will lead to Δ_{BS} given by

$$\Delta_{BS} = \frac{P_{BS}}{N - \sum_{(n,u) \in \Omega_{nu}} \frac{1}{g_u^n}}, \quad (4.22)$$

where Ω_{nu} is the set of users with their allocated subcarriers in the direct paths. Note that g_u^n is larger than one since all the parameters in (4.20) are non-negative. From this observation, it is easy to see that the power allocation in (4.19) always give a positive power p_u^n allocated to user u on subcarrier n .

Similarly, the power distribution of user u on subcarrier m via RS r can be shown as follows

$$p_{ru}^m = \Delta_r \left(\frac{1}{q_{ru}^m} - \frac{1}{g_{ru}^m} \right), \quad (4.23)$$

⁶This can be easily shown through Jacobian and Hessian of (4.7) with the relaxed constraint (4.8) being a continuous value.

where

$$q_{ru}^m = \frac{\|b_u^n\|^2}{\|d_{ru}^m\|^2} \left(\frac{p_u^n}{p_{ru}^m} \right) + \frac{\|b_u^n\|^2}{\|a_r^n\|^2} + 1, \quad (4.24)$$

$$g_{ru}^m = \frac{\|a_r^n\|^2 \|b_u^n\|^2}{\|d_{ru}^m\|^4} \left(\frac{p_u^n}{p_{ru}^m} \right)^2 + \left(\frac{\|b_u^n\|^2}{\|d_{ru}^m\|^2} + \frac{\|a_r^n\|^2}{\|d_{ru}^m\|^2} \right) \left(\frac{p_u^n}{p_{ru}^m} \right) + q_{ru}^m, \quad (4.25)$$

and

$$\Delta_r = \frac{P_{FR}}{\sum_{(m,u) \in \Omega_{rmu}} \left(\frac{1}{q_{ru}^m} - \frac{1}{g_{ru}^m} \right)}. \quad (4.26)$$

At high SNR, (4.19) and (4.23) show the optimization of power distribution over subcarriers with joint consideration of channel conditions in both hops. The main difficulty is that these power allocation equations depend on the parameters g_u^n , q_{ru}^m and g_{ru}^m that are in turn dependent on the power allocation itself and the channel conditions a_r^n , b_u^n and d_{ru}^m . As seen in the non-linear relationships in (4.20), (4.24) and (4.25), it is not possible to obtain an explicit expression for the power allocation on each subcarrier in general. Nevertheless, it can be observed that once the set of ratios $\gamma_{ru}^{nm} = p_u^n/p_{ru}^m$ is available, the power allocation in (4.19) and (4.23) can be easily obtained. This observation motivates us to design an iterative algorithm so that the power allocation can be refined in an iterative manner with the initial ratios given by

$$\gamma_{ru}^{nm} = \frac{p_u^n}{p_{ru}^m} = \frac{P_{BS}}{RP_{FR}}, \quad (4.27)$$

which corresponds to an equal power allocation at the BS and each RS with balanced relaying⁷. Specifically, this equal power allocation is given by $p_u^n = 2P_{BS}/N$ and $p_{ru}^m = P_{FR}/N_r$ with N_r being the number of subcarrier pairs assisted by RS r . Note that in (4.25), $N_r = N/(2R)$ is assumed since the same number of subcarrier pairs should be assisted at each RS in an ideally balanced relaying [24].

Based on the selection criterion given in (4.18), a subcarrier allocation algorithm is then proposed with flexible user fairness control, which may be suited for diverse QoS

⁷This feature requires each RS to relay roughly the same number of subcarrier pairs.

requirements [46], [73]. In this proposed algorithm, balanced relaying is considered as aforementioned. However, the number of subcarrier pairs must be an integer in practical implementation, approximated values are then adopted. In addition, we assume that any subcarrier pair (n, m) itself indicates $n \neq m$, and that each $f(r, u, n, m)$ used for subcarrier pair allocation is pre-calculated based on instantaneous channel conditions. Once having the subcarrier allocation, power refinement could be carried out according to (4.19) and (4.23), where the initial power distribution is given in (4.27). The details of this algorithm are described as below.

Initialization of parameters:

Let the number of assisted subcarrier pairs at each RS be $N_r = \lfloor N/(2R) \rfloor$, with the remaining $N_{un} = \lfloor N/2 \rfloor - \sum_{r=1}^R N_r$ pairs being randomly used by some RSs having more users nearby, where $\lfloor x \rfloor$ means rounding x to the largest integer less than or equal to x . Set the minimum number of subcarrier pairs must be satisfied for each user as N_u , where $N_u \geq \beta$ with β being an integer between 0 and $N/(2U)$. In addition, initialize each allocation indicator as $\rho_{ru}^{nm} = 0$, and denote the RS, user and subcarrier indices as $\Delta = \{1, \dots, R\}$, $\Lambda = \{1, \dots, U\}$ and $\Gamma = \{1, \dots, N\}$, respectively.

Implementation of subcarrier allocation:

As shown in Table 4.1.

In above proposed subcarrier allocation, some parameters are initialized first such as N_r, N_u and the index sets. Then, the implementation of subcarrier assignment is carried out via two steps, where equal power allocation is used whenever needed. Specifically, Step I tries to satisfy each user with their minimum desired subcarrier pairs, and Step II tends to increase the total system capacity as much as possible using the remaining subcarrier pairs according to (4.18). Note that, in this allocation, the value β can be used to control user fairness. Larger β gives stricter fairness due to less freedom in diversity gain of selecting users. In addition, some other notations used in this algorithm are:

TABLE 4.1: Implementation of subcarrier allocation

Step I - Satisfy the minimum number of required subcarrier pairs for each user

FOR $i = 1 \dots \beta$ **DO**

$u = 1;$

WHILE $u \leq U$ **DO**

$(r, n, m) = \arg \max_{r \in \Delta, \{n, m\} \in \Gamma} f(r, u, n, m);$ (T4.1.1)

IF $N_r = 0$ **THEN**

$\Delta \leftarrow \Delta \setminus \{r\};$ (T4.1.2)

ELSE

$\rho_{ru}^{nm} = 1; N_r \leftarrow N_r - 1; \Gamma \leftarrow \Gamma \setminus \{n, m\}; u \leftarrow u + 1;$ (T4.1.3)

END IF

END WHILE

END FOR

Step II - Use the remaining subcarrier pairs to improve system capacity

calculate $N_{re} = \lfloor N/2 \rfloor - U\beta;$

WHILE $N_{re} > 0$ **DO**

$(r, u, n, m) = \arg \max_{r \in \Delta, u \in \Lambda, \{n, m\} \in \Gamma} f(r, u, n, m);$ (T4.1.4)

IF $N_r = 0$ **THEN**

$\Delta \leftarrow \Delta \setminus \{r\};$ (T4.1.5)

ELSE

$\rho_{ru}^{nm} = 1; N_{re} \leftarrow N_{re} - 1; \Gamma \leftarrow \Gamma \setminus \{n, m\};$ (T4.1.6)

END IF

END WHILE

\leftarrow means updating one particular parameter; $\Gamma \setminus \{n, m\}$ stands for deleting subcarrier n and m from the set Γ ; N_{re} is the remaining subcarrier pairs that can be practically used in Step II.

Given the subcarrier allocation, power distribution can be iteratively refined from the initial equal power allocation according to (4.19) and (4.23). This iterative process continues until there is no significant improvement⁸ in system capacity. Eventually, the subcarrier allocation and power refinement form the proposed scheme.

The computational complexity of the proposed resource allocation scheme is

⁸The stop condition of practical implementation is normally controlled by a small tolerance value. When the capacity improvement of one iteration is below this tolerance value, the whole implementation stops. Generally, a smaller tolerance value results in longer iterations.

TABLE 4.2: Basic system settings

Parameters	Values
Cell radius	1.6 km
System bandwidth	5 MHz
FFT size	512
Doppler frequency	30 Hz
Total power at the BS	43.1 dBm
Total power at each RS	35.3 dBm
Large-scale propagation	$128.1+37.6\log D$ dB
Thermal noise density	-174 dBm/Hz

dominated by the searching step of finding the maximum value of $f(r, u, n, m)$ in the subcarrier allocation stage, which makes the whole algorithm have a complexity order of $O(RUN^2)$. In addition, the power refinement method has a complexity proportional to the number of subcarriers N and the number of iterations. Note that when there exist a large number of users, the maintained CSI at the BS may be enormous so as to prevent the feasibility of the proposed scheme. In this case, some well-studied CSI reduction techniques [74] may be utilized to facilitate our implementation.

4.4 Simulation results and conclusion

The performance of the proposed scheme is further studied through some simulation results in this section. The physical channels are modeled according to [75], which is partially compatible with 802.16 standard. Some system settings are given in Table 4.2, where D in kilometers (km) is the length of one particular link for calculating large-scale propagation path loss. For other settings used, the log-normal shadowing is set as zero mean with standard deviation of 8dB for BS-User and RS-User paths⁹, and the multipath channel is modeled as 6-tap Rayleigh fading with an exponential decaying profile. As illustrated in Fig. 4.2, it is assumed that 6 RSs are uniformly located in a circle 0.6km

⁹It assumes no log-normal shadowing in BS-RS paths.

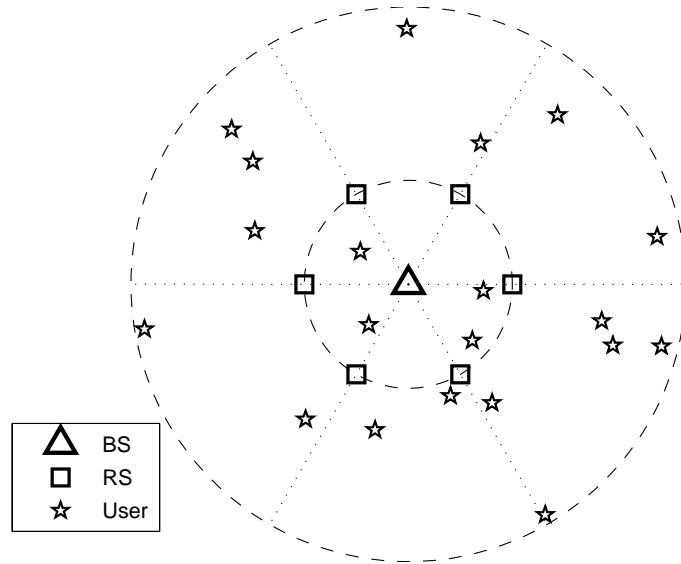


Fig. 4.2: Example for illustrating geo-locations of the BS, 6 RSs, and 20 users.

away from the BS, and each RS has a total power approximately $1/6$ of that of the BS. Note that all 512 subcarriers are utilized in the proposed resource allocation scheme regardless of the fact that some subcarriers may be reserved for signaling purposes in practice. In addition, in each channel realization¹⁰, users generated in the following simulations are assumed to have a probability of 20% to be randomly located within the 0.6km RS-circle. Otherwise, users are randomly located between the RS-circle and the cell-border as in Fig. 4.2.

In Fig. 4.3, the use of iterative power refinement, as given in (4.19) and (4.23), to improve system capacity is presented for the case of 16 users. Specifically, the proposed scheme adopts three levels of fairness control as follows: the maximum fairness (Max Fair) sets $\beta = \lfloor N/(2U) \rfloor$, the medium fairness (Med Fair) sets $\beta = \lfloor N/(4U) \rfloor$, and the minimum fairness (Min Fair) sets $\beta = 1$. As seen in this figure, the proposed power

¹⁰For smooth presentations, all simulation results are averaged over 1000 channel realizations.

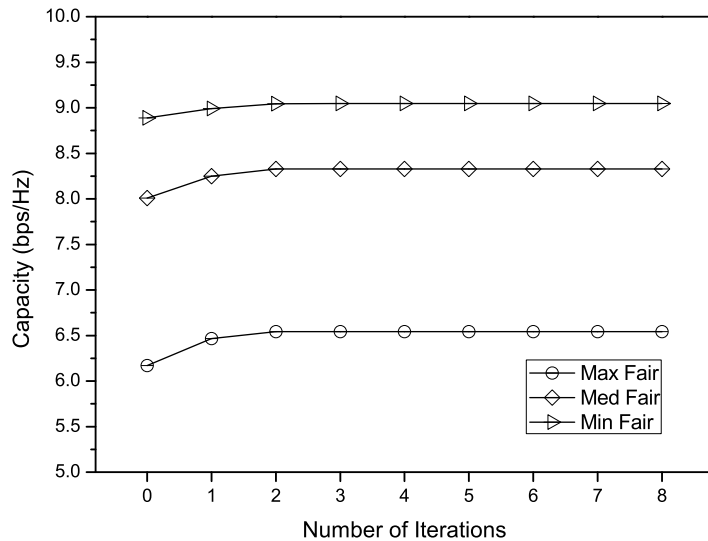


Fig. 4.3: Iterative power refinement for improving system capacity.

allocation has a fast convergence and the most significant performance improvement occurs in the first two iterations. After which, the capacity improvement is negligible. For instance, the capacity increases 0.0097bps/Hz from the 4th iteration to the 5th iteration when adopting medium fairness level, which is undistinguishable in Fig. 4.3. Note that iteration 0 indicates equal power allocation initially used for one particular subcarrier allocation, which also shows that the system performance without power refinement is degraded to some extent. In the following two results, 6 iterations of power refinement are adopted for individual subcarrier allocation.

Fig. 4.4 shows the system capacity against the number of users ranging from 8 to 20. The half-duplex scheme represents using the conventional implementation with half-duplex RS in [24]. The optimal¹¹ case is obtained without considering the minimum subcarrier pairs of each user, which corresponds to merely utilizing (4.18) to enhance

¹¹This is not the optimality of the original problem (4.7), however, it is the maximum achievable capacity under the mentioned two constraints. Thus, the *optimal* means the performance limit of the proposed suboptimal resource allocation scheme.

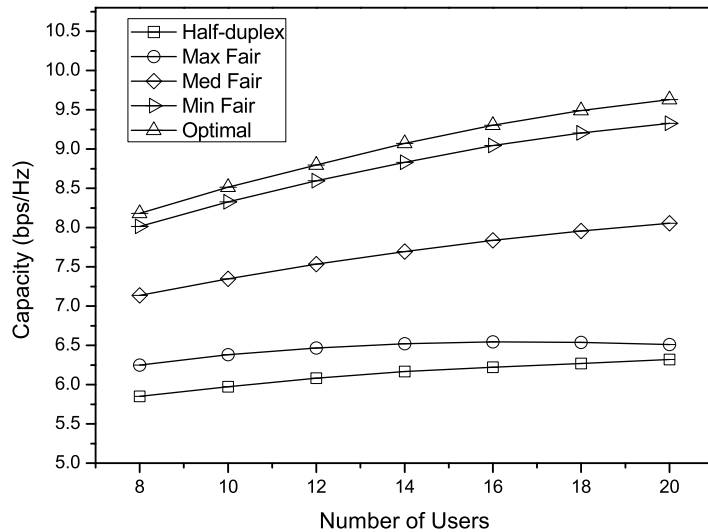


Fig. 4.4: System capacity versus number of users.

system capacity as much as possible under the two constraints of balanced relaying and full-duplex RS. In Fig. 4.4, it can be observed that the proposed scheme with full-duplex RS can outperform the conventional implementation with half-duplex RS. Note that the capacity of Max Fair tends to reduce when exceeding 16 users, which indicates that imposing strict fairness over larger number of users may decrease the system capacity without further exploiting multiuser diversity.

In Fig. 4.5, Jain's Fairness Index (JFI) is used to compare the fairness of data-rate distribution among users for different schemes as done in previous chapters. This JFI is similarly defined as $JFI = \left(\sum_{u=1}^U r_u \right)^2 / \left(U \sum_{u=1}^U r_u^2 \right)$, where r_u is the practically achieved capacity of user u . This figure demonstrates that the capacity loss shown in Fig. 4.4 can be compensated by the fairness gain, which complies with the observation in [46]. Note that the maximum fairness level achieves almost the same performance as Half-duplex with balanced relaying, and the optimal capacity method leads to the most unfair resource allocation since it does not consider user fairness. In addition, the

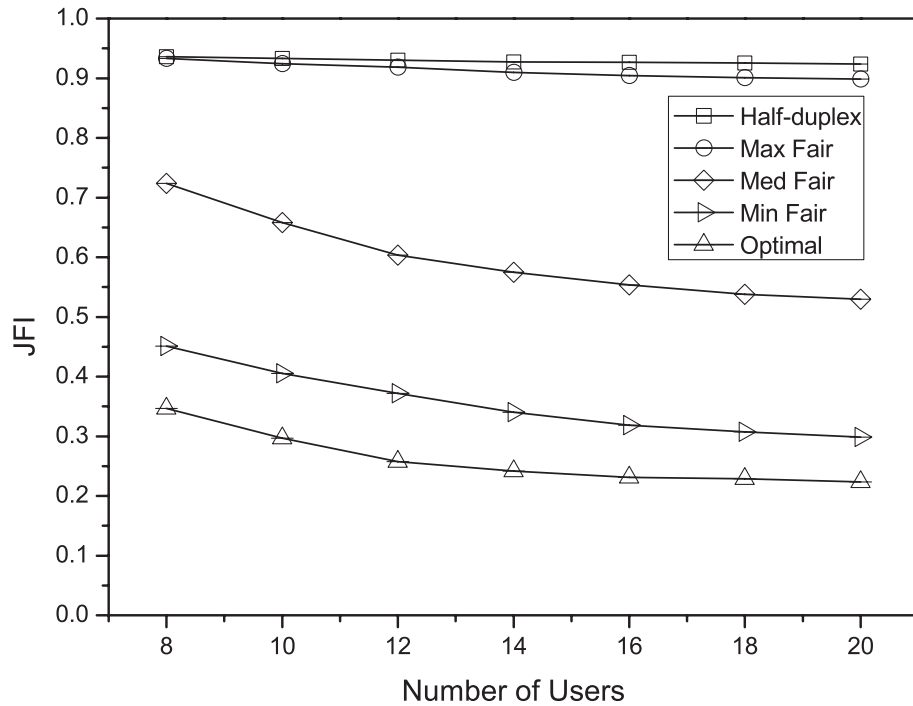


Fig. 4.5: Fairness comparison.

proposed scheme with different levels of fairness tends to have the same decreasing trend when more users existing in the system, which may be attributed to increased channel variability. Essentially, as shown in this figure, the proposed scheme is able to flexibly adjust user fairness via the introduced system design parameter β , which is the desired property of satisfying diverse quality-of-service requirements in OFDMA relaying.

4.5 Conclusions

In this chapter, we jointly consider direct and relaying paths in a relay-assisted OFDMA cellular system, with full-duplex RS being exploited to enhance the system performance. To formulate efficient system implementation, the optimal subcarrier allocation is derived first, and a suboptimal power allocation with fast convergence is proposed. Meanwhile, we introduce a system design variable to enables flexible controllability on the

tradeoff between system capacity and user fairness. Overall, this new implementation model can significantly improve the system spectrum efficiency as compared with the conventional half-duplex relaying mode.

Chapter 5

OFDMA-based cognitive radio

In this chapter, two issues are investigated for OFDMA-based Cognitive Radio (OCR) systems. Firstly, a novel spectrum sharing model is proposed to implement OCR in a conventional downlink OFDMA system. We analyze this model based on duality theory and present some efficient resource allocation schemes. Secondly, the method of exploiting Accessible Interference Temperature (AIT) is introduced to effectively implement a simplified OCR model with extremely low complexity.

5.1 Spectrum sharing in OFDMA-based cognitive radio

As studied in [76], a Cognitive Radio (CR) network architecture has two groups, which are the primary network (or licensed network) and the secondary network (also called CR network, dynamic spectrum access network, or unlicensed network). Specifically, the primary network is referred to as an existing network, where the primary users have a license to operate in a certain frequency band. The secondary network does not have a license to operate in a desired band. Hence, additional functionality is required for CR users in secondary network to share the licensed frequency band.

In this section, we mainly study the OFDMA-based cognitive radio network. The

secondary network is assumed to be underlaid in a Conventional Downlink OFDMA System (CDOS), which formulates an implementation of cognitive radio without modifying existing OFDMA system architecture [77], [78]. This implementation is applied to the scenario when the number of active users is larger than the number of subcarriers, which usually cannot be achieved in traditional OFDMA systems. To properly allocate radio resources, some solutions are proposed based on duality theory. The proposed solutions are partially distributed implementations that can dynamically allocate radio resources to the Secondary Users (SUs) (users in the secondary network) with the cooperation of Primary Users (PUs) (users in the primary network) so that the capacity of secondary network can be maximized and the co-channel interference can be minimized. In addition, the effect of interference temperature limit on the capacity of secondary network is studied, which may serve as a leverage to balance the performance between the primary users and the secondary network.

5.1.1 Review and motivation

Due to the reported low spectrum utilization in traditional fixed spectrum allocation [79], Cognitive Radio (CR) has emerged as a new paradigm for spectrum sharing in modern wireless communications [80]. In the past decade, many fundamental researches have been performed to promote the realization of CR so that high spectrum efficiency can be achieved [76].

Spectrum underlay and overlay techniques are the basis of designing Cognitive Radio Networks (CRNs) [29]. In a typical CRN, PUs should be protected when SUs access the same spectrum. In the case of spectrum underlay, the Interference Temperature Limit (ITL) is used to constrain the received interference level at the end of PUs as well as the transmitting power at the end of SUs. On the other hand, spectrum overlay allows SUs to opportunistically access the radio resources owned by PUs if these frequency bands are not being used. The transmission opportunities are usually detected by spectrum

sensing techniques [30], [31].

In recent years, OFDMA has been adopted to facilitate the implementations of CR systems, resulting in OFDMA-based CR (OCR) [81], [82], [83]. Note that traditional OFDMA systems normally do not allow spectrum sharing within its communication region, however, OCR makes conditional spectrum sharing possible if the communication qualities of PUs are not affected.

In this section, an underlay network known as secondary network is added into a CDOS. Spectrum sharing is enabled in this new system model, which is expected to increase the overall spectrum utilization [84]. In the literature, it is known that the studies about CDOS tend to avoid co-channel interference [6]. However, our study will show that if all co-channel transmissions are regarded as noises and powers over subcarriers are properly distributed, system performance of secondary network can be significantly improved via dynamic spectrum sharing under CR paradigm. Thus, designing efficient resource allocation algorithms for this new system model is our focus in this chapter. Note that the MAC and higher layer issues are beyond the scope of this section, which may refer to [82], [84] for some potential solutions.

The main contributions of this section are summarized as follows. A new model is presented to implement OCR without changing the fundamental CDOS structure. Based on duality theory, some algorithms are proposed to be applicable to the scenario when the number of active users is larger than the number of subcarriers, which usually cannot be achieved in traditional OFDMA systems. In addition, the proposed algorithms are partially distributed implementations that can dynamically allocate radio resources to SUs via PUs' cooperation, and the effect of ITL values on the achieved capacity of secondary network is demonstrated for OCR exploiting dynamic spectrum sharing.

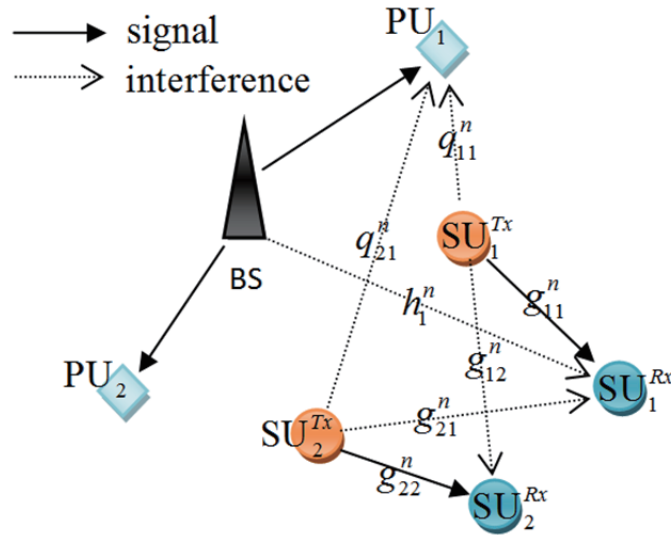


Fig. 5.1: System model for two PUs and two SUs.

5.1.2 Dynamic spectrum sharing model

We consider a Conventional Downlink OFDMA System (CDOS) with one centered Base Station (BS) and several surrounding PUs, where a secondary network having some SUs is co-located. To better illustrate this system, Fig. 5.1 shows a simplified model with two PUs and two SUs.

Without loss of generality, the numbers of PUs, SUs and subcarriers in this system are assumed to be U , K and N , respectively. For convenience, PU, SU and subcarrier are indexed by the following sets: $u \in \Lambda = \{1, 2, \dots, U\}$, $k \in \Delta = \{1, 2, \dots, K\}$ and $n \in \Gamma = \{1, 2, \dots, N\}$. Note that each SU¹ pair has one transmitter (Tx) and one receiver (Rx), which are represented by SU_k^{Tx} and SU_k^{Rx} for k th SU as shown in Fig. 5.1. Also, we assume that each subcarrier can be shared by multiple SUs as long as the ITL of each PU is not violated, which makes our system model different from current studies of OCR that normally assume exclusive spectrum occupation by SUs without considering a CDOS infrastructure. Note that this spectrum sharing feature makes our system model applicable to the scenario when the number of active users is larger than the number of

¹Unless specifically stated, one SU indicates both SU-Tx and SU-Rx in the rest of this chapter.

subcarriers.

In addition, the total system bandwidth and the noise power spectral density are assumed to be B and z_0 , respectively. Hence, the spectrum of individual subcarrier is $W = B/N$ and the noise power on each subcarrier is $v_0 = z_0W$. Following the system modelling in [81], [84], the channel gains of SU-Tx to SU-Rx, BS to SU-Rx and SU-Tx to PU are denoted by g_{kk}^n , h_k^n , and q_{ku}^n , respectively², which are also assumed to be available for dynamic resource allocation discussed in this section. Note that the estimation of these channel state information (CSI) is beyond our scope, which may refer to some well-documented techniques [85]. Since the maintained CSI may become huge when large number of users exist, some CSI reduction techniques could be adopted [74]. Furthermore, the achieved capacity in bit-per-second (bps) is used to measure the utilities of data-rates by PUs or SUs over each subcarrier.

Existing studies usually assume that OCR transmissions in secondary network do not interference with each other since only one SU is allowed to operate over one given sub-channel. If SUs cannot share the same subcarriers, our model becomes similar to the problem studied in [81]. However, spectrum sharing among SUs is allowed in present system, which may enable boosted spectrum reuse for higher capacity in secondary network with the possible cost of increased complexity. A similar type of spectrum sharing has been studied in [84] for a model without considering the CDOS infrastructure. However, the algorithms shown in [84] cannot be directly applicable to our system, and a possible transformation will be discussed in the next section.

In traditional downlink OFDMA systems, optimal resource allocation schemes can be used to assign subcarriers and powers to PUs [43], [86]. For simplicity, we assume that the resource allocation for PUs is fixed and available for SUs. As shown in [32], [87], this type of cooperation could facilitate the resource allocation in secondary network for better utilities. Specifically, the subcarrier allocation of PUs is denoted as

²For simplicity, the channel gains used in chapter are amplitude square.

$\Omega = \{(u, n) | p_u^n > 0, u \in \Lambda, n \in \Gamma\}$, where p_u^n is an allocated positive power for u th PU on n th subcarrier. Thus, the total power at the BS is $P_{BS} = \sum_{u=1}^U \sum_{n=1}^N p_u^n$. Similarly, it is assumed that the allocated non-negative power for k th SU on n th subcarrier is p_k^n . If $p_k^n > 0$, it means n th subcarrier is being used by k th SU, otherwise, not being used. As a result, for any values of $k \in \Delta$ and $n \in \Gamma$, the Signal-to-Interference-plus-Noise-ratio (SINR) is

$$SINR_k^n = \frac{g_{kk}^n p_k^n}{M_k^n + \sum_{j \in \Delta, j \neq k} g_{jk}^n p_j^n + v_0}, \quad (5.1)$$

where $M_k^n = h_k^n p_n$ and $\sum_{j \in \Delta, j \neq k} g_{jk}^n p_j^n$ are PU-to-SU and SU-to-SU interferences, which are assumed to be capable of being detected by each SU [84]. Note that $p_n = \sum_{u=1}^U p_u^n$ is the allocated power on n th subcarrier since each PU has an exclusive subcarrier allocation. The overall capacity of k th SU is then given by

$$R_k = \sum_{n=1}^N r_k^n = \sum_{n=1}^N W \log_2 \left(1 + \frac{g_{kk}^n p_k^n}{\eta_k^n} \right), \quad (5.2)$$

where $r_k^n = W \log_2 (1 + SINR_k^n)$ is the achieved capacity of k th SU on n th subcarrier, and $\eta_k^n = M_k^n + \sum_{j \in \Delta, j \neq k} g_{jk}^n p_j^n + v_0$.

With above discussions, two generalized optimization problems for any numbers of SUs, PUs and subcarriers can be formulated for the secondary network. The first problem is to simultaneously maximize the utility of individual SU, which is given by

$$\max \{R_k\}, \text{ for any } k \in \Delta. \quad (5.3)$$

Another problem is to maximize a generalized weighted-sum-rate utility function, which is given by

$$\max \left\{ \sum_{k=1}^K w_k R_k \right\}. \quad (5.4)$$

Given above two convex objectives³, the following three constraints are used to formulate

³As defined in (5.2), r_k^n can be easily shown to be convex via checking its first and second derivatives [72]. These two objectives are the linear combinations of r_k^n , thus being convex.

the individual and global optimization problems.

$$p_k^n \geq 0, \text{ for any } k \in \Delta, n \in \Gamma, \quad (5.5)$$

which is the individually allocated power for SU k on subcarrier n .

$$\sum_{n=1}^N p_k^n \leq P_k^{\max}, \text{ for any } k \in \Delta, \quad (5.6)$$

which is the total power constraint of each SU, where P_k^{\max} is the power constraint of k th SU.

$$\frac{\sum_{k=1}^K q_{ku}^n p_k^n}{W} \leq T_u^n, \text{ for any } (u, n) \in \Omega, \quad (5.7)$$

which is the ITL constraint at each PU end, where T_u^n is one specific ITL value. As a result, the objective function in (5.3) with the constraints (5.5)–(5.7) is referred to as the individual optimization problem, while the objective function in (5.4) with the constraints (5.5)–(5.7) is a global optimization.

Besides the constraints given in (5.5)–(5.7), a minimum $SINR_k^n$ should be considered to ensure effective data-rate over each subcarrier for each SU. However, numerically including this condition makes the investigated problem extremely intractable, we use a minimum allocated power instead to limit the usability of each subcarrier⁴. In (5.6), P_k^{\max} should be technically different for SUs in a general case, we adopt the same value in the simulation section for simplicity. Note that the unknown variables, p_k^n , also indicate the subcarrier sharing feature in above two optimization problems. For instance, if $p_k^n > 0$, k th SU uses the n th subcarrier. For the individual and global optimization objectives in (5.3) and (5.4), both optimal and suboptimal solutions are analyzed in the following section.

⁴Calculating the instantaneous SINR to determine the usability of any subcarrier for any SU is a waste of computational capability. Since the effective signals and the mutual interferences are normally in the same scale (5.1), thus it is reasonable to assume a minimum allocated power to limit subcarrier usability. In other words, for simplicity, the subcarrier allocated a power less than such a minimum amount is not used.

5.1.3 System analysis and solutions

The objective (5.3) is to individually maximize the capacity of each SU, however, the overall capacity achieved by (5.3) would be worse than the optimal solution of the global optimization (5.4) in practice⁵. As shown in [84], the technique of applying pricing function can be used to force the solution of (5.3) to get closer to that of (5.4), where the linear pricing function is the simplest form with easy implementation [88]. When adopting a linear pricing function into the objective (5.3), the overall capacity of each SU becomes

$$\tilde{R}_k = \sum_{n=1}^N (r_k^n - \lambda_k^n p_k^n), \quad (5.8)$$

As a result, (5.3) is equivalent to

$$\max \left\{ \tilde{R}_k \right\}, \text{ for any } k \in \Delta. \quad (5.9)$$

For k th SU in (5.9) with the constraints (5.5)–(5.7), for any $k \in \Delta$, the Lagrangian function can be expressed as

$$\begin{aligned} L_k = & w_k \tilde{R}_k + \sum_{n=1}^N \alpha_k^n p_k^n - \beta_k \left(\sum_{n=1}^N p_k^n - P_k^{\max} \right) \\ & - \sum_{(u,n) \in \Omega} \gamma_u^n \left(\sum_{k=1}^K q_{ku}^n p_k^n - WT_u^n \right), \end{aligned} \quad (5.10)$$

where w_k , α_k^n , β_k , γ_u^n are dual variables. Similarly, the Lagrangian function of the global optimization (5.4) associated with the constraints (5.5)–(5.7) is given by

$$\begin{aligned} L_g = & \sum_{k=1}^K w_k R_k + \sum_{k=1}^K \sum_{n=1}^N \alpha_k^n p_k^n - \sum_{k=1}^K \beta_k \left(\sum_{n=1}^N p_k^n - P_k^{\max} \right) \\ & - \sum_{(u,n) \in \Omega} \gamma_u^n \left(\sum_{k=1}^K q_{ku}^n p_k^n - WT_u^n \right), \end{aligned} \quad (5.11)$$

⁵The individual and global solutions are usually denoted as Nash equilibrium (NE) and Pareto optimality in the literature. It is known that NE is strictly less than or equal to Pareto optimality [32].

Based on (5.10) and (5.11), we can simply compare the results of $\partial L_k / \partial p_k^n$ and $\partial L_g / \partial p_k^n$ so as to find the following optimal linear pricing function⁶

$$\lambda_k^n = -\frac{1}{w_k} \sum_{j \in \Delta, j \neq k} w_j \frac{\partial r_j^n}{\partial p_k^n} = \frac{W}{\ln 2} \sum_{j \in \Delta, j \neq k} \frac{w_j}{w_k} \left[\frac{g_{jj}^n g_{kj}^n p_j^n}{\eta_j^n (\eta_j^n + g_{jj}^n p_j^n)} \right], \quad (5.12)$$

where $\eta_j^n = M_j^n + \sum_{i \in \Delta, i \neq j} g_{ij}^n p_i^n + v_0$. Note that (5.12) can be used to individually adjust resource allocation for better utilities of SUs in (5.9).

In the rest of this section, Lagrangian duality theory [72] is adopted to derive power allocation solutions for the studied two objectives. If only consider the constraint (5.6) for the revised individual objective (5.9), the following partial Lagrangian can be obtained

$$\widehat{L}_k = w_k \sum_{n=1}^N (r_k^n - \lambda_k^n p_k^n) - \beta_k \left(\sum_{n=1}^N p_k^n - P_k^{\max} \right), \quad (5.13)$$

where β_k is the dual variable associated with (5.6). For k th SU, the dual problem is then given by

$$\min_{\beta_k \geq 0} \left(\max_{p_k^n \geq 0} \widehat{L}_k \right). \quad (5.14)$$

With fixed dual variable β_k , the dual problem (5.14) can be simplified as

$$\max_{p_k^n \geq 0} \widehat{L}_k. \quad (5.15)$$

Let the derivative of (5.13) w.r.t p_k^n be zero, which leads to

$$\frac{\partial \widehat{L}_k}{\partial p_k^n} = w_k \frac{\partial r_k^n}{\partial p_k^n} - w_k \lambda_k^n - \beta_k = 0. \quad (5.16)$$

From (5.2), it can derive

$$\frac{\partial r_k^n}{\partial p_k^n} = \frac{W g_{kk}^n}{\ln 2 \times (\eta_k^n + g_{kk}^n p_k^n)}. \quad (5.17)$$

Then, substitute (5.17) into (5.16), p_k^n can be shown as follows

$$p_k^n = \left(\frac{W w_k}{\ln 2 \times (\beta_k + w_k \lambda_k^n)} - \frac{\eta_k^n}{g_{kk}^n} \right)^+. \quad (5.18)$$

⁶A similar derivation of calculating the linear pricing function is given in [84].

As observed in (5.18), β_k could be iteratively adjusted to find a set of non-negative p_k^n over all subcarriers of k th SU. For each SU, this iterative processing can be achieved by the traditional subgradient-based (e.g., bi-section) methods [44] and the whole processing should stop when the conditions of non-negative p_k^n and the largest possible total power constrained by P_k^{\max} are both satisfied. Afterwards, the ITL of each PU should be ensured, which is achieved by the following proposed methods.

The power mask constraint is used in [84] to restrict the transmission power of k th SU over n th subcarrier, which is defined as $p_k^n \leq P_{kn}^{\text{mask}}$. In [84], these power mask constraints $P_{kn}^{\text{mask}}, k \in \Delta, n \in \Gamma$ are given as pre-determined values without considering the specific channel conditions. We propose to transfer the ITL constraint (5.7) into the power mask constraints via an explicit relation with channel conditions. Specifically, we set $q_{ku}^n p_k^n \leq WT_u^n / K$ for k th SU sharing n th subcarrier based on the ITL constraint (5.7). The associated power masks then become

$$P_{kn}^{\text{mask}} = \frac{WT_u^n}{K q_{ku}^n}, \text{ for any } k \in \Delta, n \in \Gamma. \quad (5.19)$$

With the power masks given in (5.19), the first method is to adopt the algorithm⁷ in [84] to ensure the ITL of each PU, while the individual optimization (5.9) is achieved. This method gives a suboptimal distributed implementation. Note that the values in (5.19) can be interpreted as restricting the generated interference from SU to PU to be below the same level.

The second method is formulated based on the possible cooperation between PUs and SUs as studied in [87]. Specifically, it is assumed that PUs could feedback some indices about ITL violation on each subcarrier to SUs given by

$$V_u^n = \hat{T}_u^n / T_u^n, \quad (5.20)$$

where \hat{T}_u^n is the instantaneously measured ITL at PUs and T_u^n is the maximum allowable values. Then, based on these ITL violation feedbacks, SUs can adjust their transmitting

⁷For completeness, the details of this algorithm is given in Appendix E.

powers simply by a normalization process as follows

$$\widehat{p}_k^n = p_k^n / V_u^n. \quad (5.21)$$

Since P_k^{\max} has been satisfied via adjusting β_k in (5.18), either using the first or second method could determine the final power allocation. For the rest of this section, these two methods of ensuring ITL at PUs are named as Pmask (5.19) and Violation Feedback Index (VFI) (5.21), respectively. Note that Pmask is purely distributed implementation while VFI is partially distributed with the cooperation of PUs.

After presenting the power allocation based on the individual objective (5.3), we proceed to discuss the allocation strategies for the global objective (5.4). When considering both constraints (5.6) and (5.7), the partial Lagrangian in this case can be expressed as

$$\begin{aligned} \widehat{L}_g &= \sum_{k=1}^K w_k \sum_{n=1}^N r_k^n - \sum_{k=1}^K \beta_k \left(\sum_{n=1}^N p_k^n - P_k^{\max} \right) - \sum_{(u,n) \in \Omega} \gamma_u^n \left(\sum_{k=1}^K q_{ku}^n p_k^n - WT_u^n \right) \\ &= \sum_{k=1}^K \sum_{n=1}^N (w_k r_k^n - \beta_k p_k^n - \gamma_u^n q_{ku}^n p_k^n) + \sum_{k=1}^K \beta_k P_k^{\max} + W \sum_{n=1}^N \gamma_u^n T_u^n. \end{aligned} \quad (5.22)$$

As observed in (5.22), different per-subcarrier-per-user Lagrangian functions,

$$l_k^n = w_k r_k^n - \beta_k p_k^n - \gamma_u^n q_{ku}^n p_k^n, \text{ for any } k \in \Delta, n \in \Gamma \quad (5.23)$$

can be obtained and independent with each other. Therefore, the original global optimization could be decoupled into KN sub-problems maximizing (5.23). Taking the derivatives of (5.23) *w.r.t* to p_k^n and let them be zero, we have

$$\frac{\partial l_k^n}{\partial p_k^n} = w_k \frac{\partial r_k^n}{\partial p_k^n} - \beta_k - \gamma_u^n q_{ku}^n = 0, \text{ for any } k \in \Delta, n \in \Gamma. \quad (5.24)$$

Then, p_k^n can be derived as below by substituting (5.17) into (5.24)

$$p_k^n = \left(\frac{W w_k}{\ln 2 \times (\beta_k + \gamma_u^n q_{ku}^n)} - \frac{\eta_k^n}{g_{kk}^n} \right)^+. \quad (5.25)$$

When $\beta_k \neq 0$, the dual variables β_k, γ_u^n in (5.25) should be properly adjusted so as to find the optimal power allocation, which can be regarded as the benchmark for other

algorithms proposed in this section. Essentially, this power adjustment can be efficiently achieved via some subgradient-based methods (e.g., Ellipsoid method) [44].

On the other hand, when $\beta_k = 0$ that is equivalent to only considering the constraint (5.7), (5.25) thus becomes

$$p_k^n = \left(\frac{W}{\ln 2} \frac{w_k}{\gamma_u^n q_{ku}^n} - \frac{\eta_k^n}{g_{kk}^n} \right)^+. \quad (5.26)$$

Based on (5.26), another iterative algorithm can be designed via adjusting γ_u^n gradually as does in (5.18). Note that if the equality is satisfied in (5.7), we have

$$\sum_{k=1}^K q_{ku}^n p_k^n = WT_u^n. \quad (5.27)$$

Substitute (5.26) into (5.27) will lead to γ_u^n given by

$$\gamma_u^n = \frac{W \sum_{k=1}^K w_k}{\ln 2 \times \left[\sum_{k=1}^K \left(q_{ku}^n \frac{\eta_k^n}{g_{kk}^n} \right) + WT_u^n \right]}. \quad (5.28)$$

As observed in (5.26) and (5.28), these two equations are intertwined, p_k^n can be derived once γ_u^n are available while γ_u^n requires deterministic p_k^n for measuring mutual interferences. Based on this observation, a heuristic suboptimal power allocation having four steps is proposed as follows:

- (a) Each SU equally distributes his/her total power P_k^{\max} over all subcarriers, then the co-channel interference can be detected by each SU to calculate γ_u^n .
- (b) Adjust the power allocation according to (5.26) via using γ_u^n for each SU.
- (c) Use VFI method to refine the power allocation so that the ITL of each PU is satisfied.
- (d) Assume current total power of k th SU is P_k^{tot} after (a)–(c), each SU then performs a self-check for the power constraint P_k^{\max} . Specifically, if $P_k^{\text{tot}} \leq P_k^{\max}$,

the whole processing steps. Otherwise, normalize the powers p_k^n over all subcarriers of each SU to have a sum-power being P_k^{\max} , which corresponds to $\tilde{p}_k^n = p_k^n P_k^{\max} / P_k^{\text{tot}}$.

The above four-step processing gives an initial power for all subcarrier of each SU first, then calculate γ_u^n based on (5.28) followed by using (5.26) to compute each p_k^n . Finally, far-end ITL and local total power constraints are examined.

In this section, suboptimal and optimal solutions are discussed based on duality theory [72]. To briefly refer to these solutions, the resource allocation via (5.18) using VFI adjustment is denoted as **P1**, while using Pmask is referred to as **Fan08** [84]. The four-step power allocation method based on (5.26)–(5.28) are named as **P2**, and the solution given by (5.25) through Ellipsoid method [44] is regarded as the **Optimal** solution. In addition, when instantaneous P_{kn}^{mask} are known, the simplest power allocation is to equally distribute power over the subcarriers of each SU under ITL constraint, $p_k^n = \min(\bar{p}_k, P_{kn}^{\text{mask}})$, where $\bar{p}_k = P_k^{\max} / N$, which is an equal power (**EP**) method that may serve as another benchmark in our system. Note that the proposed two algorithms, P1 and P2, are both partially distributed implementations.

5.1.4 Simulation results

In this sub-section, a few simulation results are presented to verify previously discussed resource allocation algorithms. Based on the system modelling for downlink OFDMA in [75], the basic system settings are: total bandwidth considered is 5MHz divided into 512 subcarriers; cell radius is 1.6 kilometers; the noise power spectral density z_0 is -174 dBm/Hz; each SU-Tx has the same total power constraint that is $P_k^{\max} = 1$ watt, and the power limit of subcarrier usability is 0.001 mW. To model the fading channels, the large-scale fading factor is assumed to be 4 as used in [84] while the multipath small-scale fading uses a 6-tap Rayleigh fading with an exponential decaying profile as used in [11]. For evenly generating the SUs, the cell is separated into six sectors, and each

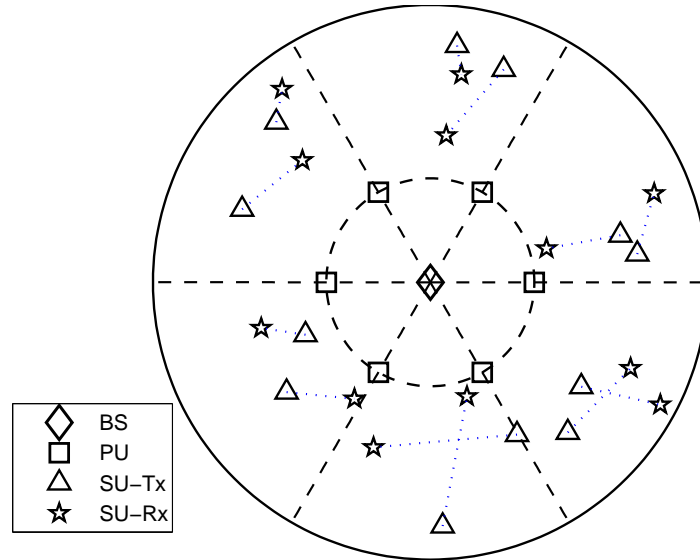


Fig. 5.2: Geo-location snapshot of the system.

SU is assumed to be generated in each sector with equal probability. When one SU is generated, its Tx and Rx ends will suffer a slow mobility with a Doppler frequency being 30Hz. In addition, six fixed PUs are assumed to be located uniformly at a circle 600 meters away from the BS. One example for the geo-locations of BS, PUs and SUs is illustrated in Fig.5.2, which is actually a snapshot of the simulated system. Note that all 512 subcarriers are used to carry signals, regardless the fact that some subcarriers might be reserved for signaling purpose. Also, the ITL of PUs is normalized by Boltzman constant $\bar{k} = 1.38 \times 10^{-23}$, which corresponds to dividing each T_u^n by \bar{k} to formulate the values used in the following simulations. Unless otherwise stated, these simulation results are averaged over 1000 channel realizations.

With the assumption that the same ITL value equal to 10^3 is applied to each PU, Fig. 5.3 illustrates the total capacity of SUs against the number of SUs. As observed in this figure, P2 gives a performance close to the optimality and higher than other imple-

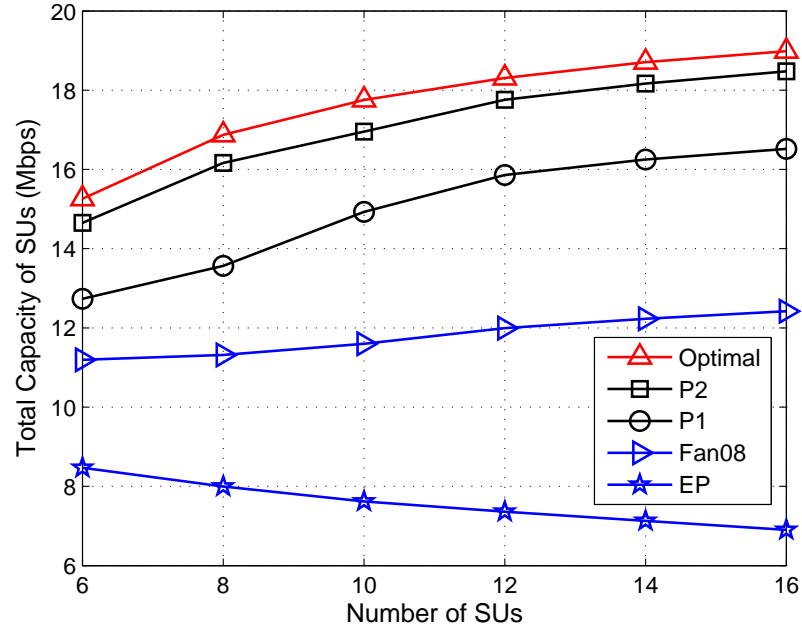


Fig. 5.3: Total capacity of secondary users.

mentations. P1 shows an advantage over Fan08 algorithm since the cooperation between SUs and PUs is utilized in our system model while Fan08 does not have this feature. Except for the simplest EP method, all other algorithms present improved capacities as the number of users increases, which demonstrates that multiuser diversity still exists even in a constrained underlay environment. The decreasing property of EP may be attributed to the fact that increased mutual interference in (5.1) becomes severe when more SUs are active in the system without adaptive power control.

Fig. 5.4 shows the total capacity of SUs against different values of ITL for 12 SUs. This figure demonstrates similar performance relations of the investigated algorithms as shown in Fig. 5.3. In this figure, all algorithms tend to have higher total capacities for larger ITL values, which could be regarded as a leverage to balance the performance between PUs and SUs. When PUs are relatively idle, they can provide larger ITL for SUs to allow higher capacity in secondary network, otherwise, PUs can lower down ITL

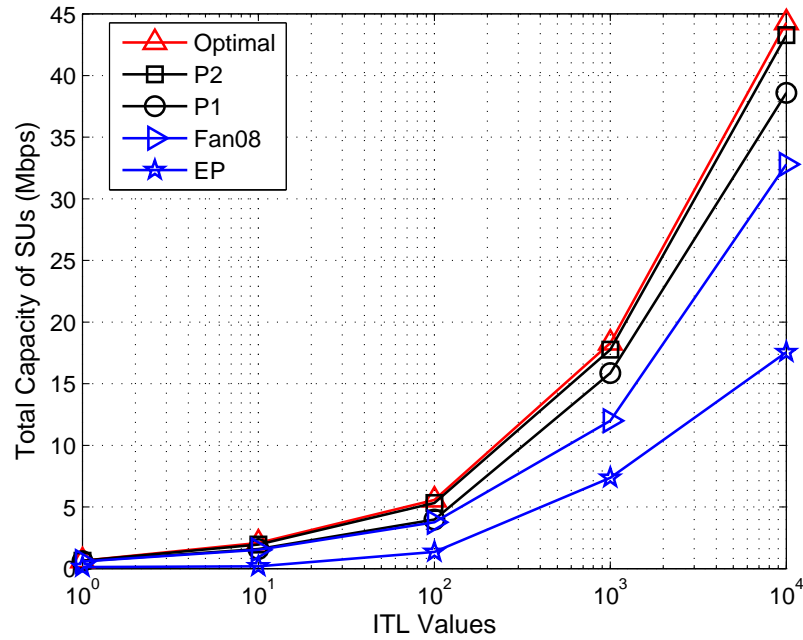


Fig. 5.4: Effect of interference temperature limit.

to restrict the activity of SUs.

To numerically express the spectrum sharing feature of different algorithms, a subcarrier sharing index is introduced as $SSI = \left(\sum_{k=1}^K N_k \right) / N$, where N_k is the actually used subcarriers of k th SU. Obviously, SSI can indicate an averaged degree of subcarrier sharing, which is given in Fig. 5.5. As seen in this figure, more SUs leads to higher spectrum sharing that may be the reason besides multiuser diversity for improved performance. In addition, it is worth mentioning that the SSI of EP has the same value as the number of SUs, which is the highest possible subcarrier sharing index that is equivalent to using all the subcarriers. However, EP gives the lowest capacity performance as shown in the previous two figures. The reason might be severe mutual interference and lack of adaptive power control. Regarding EP as a benchmark, all other algorithms have smaller SSI values, which demonstrates that a proper spectrum sharing should be accompanied by an appropriate power control. Based on this observation, higher spectrum

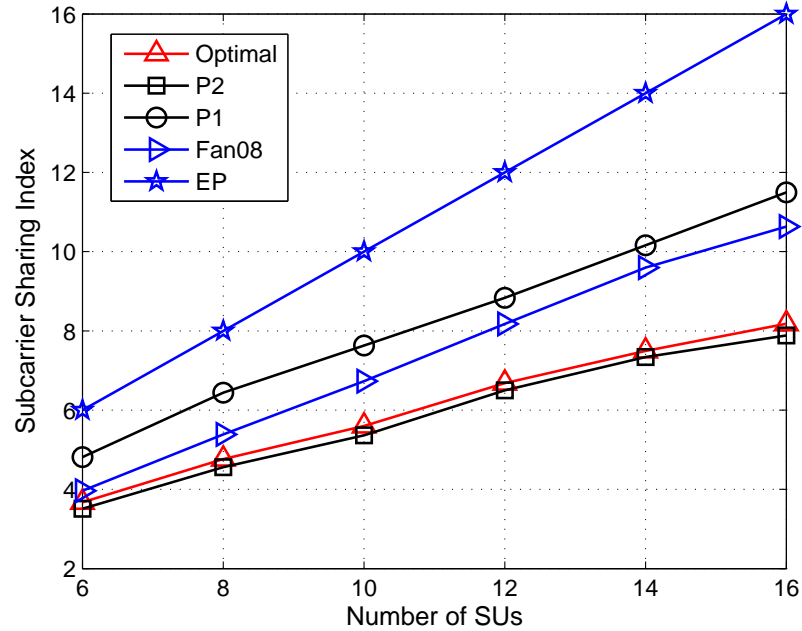


Fig. 5.5: Subcarrier sharing index.

sharing does not definitely lead to higher utilities and some subcarriers without usage are necessary to lower down mutual interference via dynamic power control, which also can be further verified from the Optimal and P2 algorithms that have the least spectrum sharing.

5.2 OCR implementation via accessible interference temperature

As aforementioned, in the case of spectrum underlay, Interference Temperature Limit (ITL) can be utilized to constrain the received interference at the Primary Users (PUs) so that these PUs could be protected from sharing their spectra with some Secondary Users (SUs). In this section, we consider a simplified OFDMA-based Cognitive Radio (OCR) model compared with that studied in the previous section, where one particular subcarrier

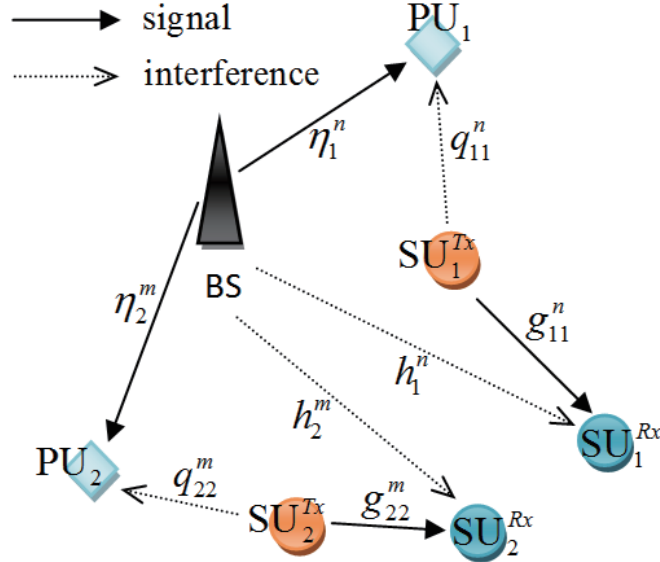


Fig. 5.6: System model with two PUs and two SUs.

of PU is restricted to be used by only one SU. This simplification makes the interference control more convenient and is suitable for extremely low complexity implementation (the proposed algorithm is with the complexity order of $\mathcal{O}(1)$). In addition, the concept of Accessible Interference Temperature (AIT) is introduced to implement this simplified OCR without modifying the conventional infrastructure of downlink OFDMA [89].

5.2.1 Accessible interference temperature and proposed implementation

We consider a simplified model compared with that shown in Fig. 5.1, with basic system settings being the same as those in the previous section. To be specific, Fig. 5.6 illustrates this simplified model with two PUs and two SUs, where PU_1 and SU_1 share n th SC, PU_2 and SU_2 share m th subcarrier (SC), with $n, m \in \Gamma = \{1, 2, \dots, N\}$ and $n \neq m$. Note that k th SU consists of one transmitter (Tx) and one receiver (Rx) denoted by SU_k^{Tx} and SU_k^{Rx} , and for simplicity, one SU indicates both SU-Tx and SU-Rx unless otherwise

stated. To avoid mutual interferences among SUs, it is also assumed that each SC of PUs could be shared by only one SU as long as the interference temperature of PUs is not violated. As shown in Fig. 5.6, the channel gain from the BS to u th PU on n th SC is assumed to be η_u^n , while the gains from k th SU-Tx to SU-Rx, from the BS to k th SU-Rx and from k th SU-Tx to u th PU are represented by g_{kk}^n , h_k^n and q_{ku}^n , respectively.

In traditional downlink OFDMA systems, optimal resource allocation schemes can be used to assign SCs and powers to PUs [11]. For simplicity, we assume that the resource allocation for PUs is pre-determined and expressed by

$$\Omega = \{(u, n) | p_u^n > 0, u \in \Lambda, n \in \Gamma\}, \quad (5.29)$$

where p_u^n is the allocated power for u th PU on n th SC. Thus, the total power at the BS is $P_{BS} = \sum_{u=1}^U \sum_{n=1}^N p_u^n$. In addition, p_k^n is used to denote the allocated non-negative power for k th SU on n th SC. When $p_k^n > 0$, n th SC is being used by k th SU. As a result, the Signal-to-Interference-plus-Noise Ratio (SINR) for k th SU on n th SC in present case is

$$SINR_k^n = \frac{g_{kk}^n p_k^n}{M_k^n + v_0}, \quad (5.30)$$

where $M_k^n = h_k^n p_n$ is the PU-to-SU interference (from the BS to k th SU on n th SC), which is assumed to be capable of being detected by each SU. Note that $p_n = \sum_{u=1}^U p_u^n$ is the overall allocated power on n th subcarrier. Then, the total capacity of k th SU is given by

$$R_k = \sum_{n=1}^N r_k^n = W \sum_{n=1}^N \log_2(1 + SINR_k^n), \quad (5.31)$$

where $r_k^n = W \log_2(1 + SINR_k^n)$ is the achievable capacity of k th SU on n th SC.

Similarly, the SINR for u th PU on n th SU is

$$SINR_u^n = \frac{\eta_u^n p_u^n}{I_u^n + v_0} \quad (5.32)$$

where $I_u^n = \sum_{k=1}^K q_{ku}^n p_k^n$ is the aggregate interference to u th PU on n th SC from all the SUs. When $I_u^n = 0$, (5.32) becomes the traditional Signal-to-Noise Ratio (SNR) given

by

$$SNR_u^n = \eta_u^n p_u^n / v_0. \quad (5.33)$$

However, a minimum SINR value in (5.32) should be maintained for the usability of one particular SC at each PU, which is given by

$$SINR_{un}^{\min} = \frac{\eta_u^n p_u^n}{I_{un}^{\max} + v_0}, \quad (5.34)$$

where I_{un}^{\max} corresponds to the maximum allowable interference to u th PU on n th SC. Comparing (5.33) and (5.34) will lead to

$$\frac{SNR_u^n}{SINR_{un}^{\min}} = \frac{I_{un}^{\max} + v_0}{v_0}. \quad (5.35)$$

Thus, I_{un}^{\max} can be expressed as

$$I_{un}^{\max} = v_0 \left(\frac{SNR_u^n}{SINR_{un}^{\min}} - 1 \right), \quad (5.36)$$

which is defined as Accessible Interference Temperature (AIT) that functions as an interference gap. This gap indicates the maximum SNR degradation for PUs due to spectrum sharing with SUs⁸. Note that this relationship has not been explicitly utilized for resource allocation in the literature.

The values in (5.36) can be generated by PUs according to their channel qualities over SCs, which can be further used to constrain the activities of SUs in the system. Specifically, k th SU using n th SC must satisfy

$$\sum_{k=1}^K q_{ku}^n p_k^n \leq I_{un}^{\max}. \quad (5.37)$$

As aforementioned, for simplicity, n th SC is assumed to be shared by one SU, which gives that only one element in the set $\{p_1^n, p_2^n, \dots, p_K^n\}$ is positive with others being zero. Given $p_k^n > 0$, (5.37) can be further simplified, the transmission power constraint for k th SU-Tx on n th SC then becomes

$$p_k^n \leq \hat{p}_k^n = I_{un}^{\max} / q_{ku}^n. \quad (5.38)$$

⁸When the $SINR_{un}^{\min}$ is set to be larger than SNR_u^n , I_{un}^{\max} is assumed to be zero, which indicates the n th subcarrier of u th PU cannot be shared.

TABLE 5.1: AIT values

	SC 1	SC 2	SC 3	SC 4	SC 5	SC 6
PU 1	i_{11}	0	i_{13}	0	i_{15}	0
PU 2	0	i_{22}	0	i_{24}	0	i_{26}

Based on I_{un}^{\max} defined in (5.36), a constraint table named as AIT table can be formulated, which is actually a U -by- N matrix used to limit the allowable interference introduced by SUs through (5.38). An example for 2 PUs with 6 SCs is given in Table 5.1, where the first PU occupies SCs 1, 3, 5, and the second PU has SCs 2, 4, 6. In this table, i_{un} represents I_{un}^{\max} for short, and 0 means one particular SC is not assigned to one PU.

The AIT table is assumed to be maintained and updated by a central referee such as the BS, and is utilized to allocate resources to SUs. When one SU attempts to access into the system, this SU could apply for some SCs based on the AIT table. To fast implement the allocation, one SU randomly selects β SCs, where β is an integer between 0 and $\lfloor N/K \rfloor$. Without considering the reserved SCs for signalling purpose, we set $\beta = \lfloor N/K \rfloor$ by default for the rest of this section.

To be specific, the studied OCR model can be conveniently implemented via the introduced AIT by the following two steps:

- (Step 1) - PUs calculate the maximum allowable AIT values on their occupied SCs (5.36) and formulate a U -by- N matrix as in Table 5.1.
- (Step 2) - SUs apply for some SCs from the central referee, where each SU tends to attain β SCs at most. Based on the AIT table, the central referee randomly assigns available SCs to SUs while informing them the transmission power constraints \widehat{p}_k^n (5.38). With these assigned SCs, each SU performs a conventional water-filling algorithm [11] to distribute the total power at SU-Tx over their assigned SCs, which results in the power for k th SU-Tx on n th SC being \bar{p}_k^n . Then, k th SU starts using the allocated SCs to transmit signals until a pre-determined timeout, where the transmission power is constrained by $\min(\widehat{p}_k^n, \bar{p}_k^n)$.

Note that the above two steps needs a centrally maintained AIT table, and the activities between PUs and SUs are mutually independent, which enables the extremely fast implementation of this proposed algorithm with an order of $\mathcal{O}(1)$ in one particular allocation slot.

5.2.2 Simulation results

In this sub-section, one simple set of simulation results is presented for OCR resource allocation via AIT table. The system settings used are the same as that in Section 5.1.4. Note that one example of the geo-location snapshot has been illustrated in Fig. 5.2.

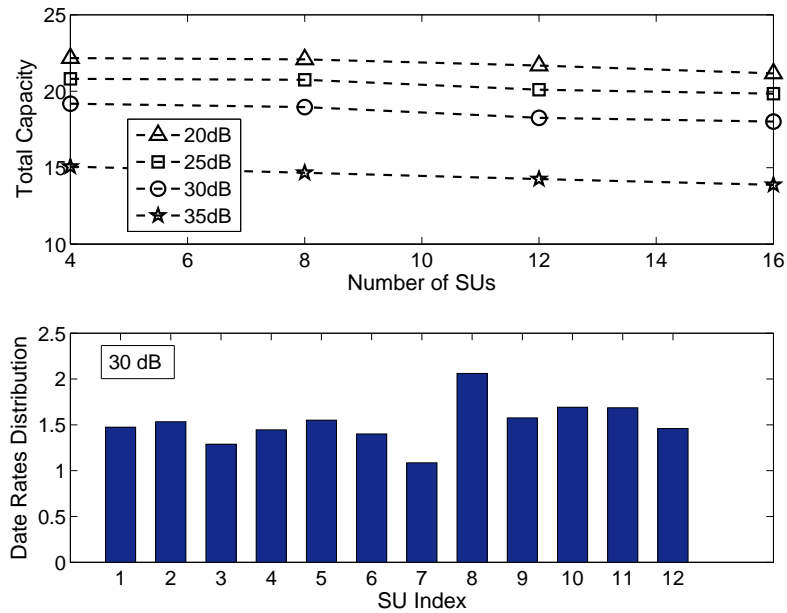


Fig. 5.7: Performance of secondary network.

Fig. 5.7 includes two sub-figures to show the performance of the secondary network. The upper figure gives the total capacity (Mbps) versus the number of SUs under different minimum SINR values, $SINR_{un}^{\min}$. As given in (5.34), these minimum SINRs are used to maintain the usability of each SC for PUs. Specifically, the upper figure

demonstrates the fact that higher SINR requirements of PUs over each SC results in lower performance of SUs due to stricter interference constraint as indicated by I_{un}^{\max} in (5.37). Note that the multiuser diversity may not be available in this simplified model as that in conventional OFDMA systems or in the multiple sharing model in Section 5.1, which may be attributed to random SC selection for SUs without optimized subcarrier scheduling. However, it is computationally efficient and only has a little performance degradation as the number of users increases. In addition, the lower figure presents a sampled data-rate distribution of 12 SUs for one channel realization with SINR being 30 dB. From this figure, it can be seen that SUs achieve relatively fair capacities, which could be regarded as a fairness control by limiting each SU to request the same number of SCs.

5.3 Conclusions

In this chapter, a new system model is first presented to implement OFDMA-based cognitive radio without modifying the fundamental structure of conventional downlink OFDMA systems in Section 5.1. Some solutions are discussed for this new system based on duality theory. With proper spectrum sharing, the proposed algorithms can be applied to the scenario when the number of active users is larger than the number of subcarriers in the system. These proposed algorithms are formulated as partially distributed implementations, which can dynamically allocate radio resources to Secondary Users (SUs) with the cooperation of Primary Users (PUs). In addition, the effect of Interference Temperature Limit (ITL) on the achieved capacity of secondary network is demonstrated, which reveals that a properly selected ITL value may serve as a leverage to balance the performance between PUs and SUs. Generally, Section 5.1 shows that if all co-channel interfering transmissions are regarded as noises and powers over subcarriers are appropriately distributed, the system performance of secondary network can be significantly

improved via dynamic spectrum sharing.

In Section 5.2, the Accessible Interference Temperature (AIT) is introduced to rapidly implement a simplified OCR model as compared with the model used in Section 5.1. In this simplified model, the activities between PUs and SUs are mutually independent. When AIT constraints are guaranteed in the secondary network, each SU can flexibly access the available frequency bands without introducing deleterious interferences to PUs.

Chapter 6

Conclusions

6.1 Summary of contributions

This thesis may contribute to design efficient algorithms for Orthogonal Frequency Division Multiple Access (OFDMA) - based resource allocation in wireless communication systems such as Single Input Single Output (SISO) - OFDMA, Multiple Input Multiple Output (MIMO) - OFDMA, OFDMA relaying and OFDMA-based Cognitive Radio (OCR). More specifically, the main contributions made in each chapter are summarized as follows:

- In Chapter 2, two low-complexity methods are proposed for downlink SISO - OFDMA resource allocation, with a flexible balance of different system performance metrics. Specifically, a multiuser diversity enabled partial feedback Channel State Information (CSI) mechanism is formulated in Section 2.2. We have shown that it may not be necessary to feedback full CSI of each user in terms of system capacity. Alternatively, a small portion of full CSI can be utilized to generate near-optimal resource allocation in multiuser OFDMA systems. This partial feedback mechanism may lead to a little fairness loss for users, which is normally acceptable in practical implementations. This section provides an easy method

to achieve the tradeoff over system capacity, proportional fairness, and feedback amount of CSI in OFDMA systems. Furthermore, in Section 2.3, we have demonstrated another method for satisfying diverse Quality-of-Service (QoS) requirements via exploiting the minimum requested data-rate of each user as a system design variable. The method in Section 2.3 also can easily trade off over system capacity, user fairness and computational complexity in OFDMA systems. Note that the above two methods both require accurate channel estimations for CSI, which may limit their applications in scenarios without accurate CSI.

- In Chapter 3, the general resource allocation problems in multiuser downlink MIMO - OFDMA cellular systems are investigated. Specifically, four utility-based objectives are studied, Egalitarian, Utilitarian, and two bargaining solutions, Generalized Nash Bargaining Solution (GNBS) and Kalai-Smorodinsky Bargaining Solution (KSBS). Based on the system optimality given in Appendix B, we have presented some low-complexity algorithms, which can be implemented in polynomial time for dynamic resource allocation. Furthermore, the generalized bargaining power is demonstrated to be able to flexibly control the data-rate distribution of users, which formulates the introduced GNBS/KSBS fairness. As observed from the simulation section, one disadvantage of applying these two fairness criteria is to cause certain loss in overall system capacity. In brief, the proposed algorithms in this chapter are well suited for satisfying diverse QoS requirements and have a general applicability to downlink SISO/MIMO-OFDMA systems.
- In Chapter 4, we study a relay-assisted OFDMA cellular system with joint consideration of the direct and relaying paths. A novel implementation adopting full-duplex relaying is proposed for relay-destination selection, subcarrier and power allocation. This implementation can achieve higher spectrum efficiency than the conventional half-duplex relaying mode. Meanwhile, it has effective controllability on the tradeoff between system capacity and user fairness. One limitation of

this work might be the high deployment complexity of full-duplex relaying, which requires a demanding condition for subcarrier switching at each relaying station.

- In Chapter 5, OFDMA-based Cognitive Radio (OCR) systems are investigated. Firstly, a novel spectrum sharing model is proposed to implement OCR in a conventional downlink OFDMA system in Section 5.1. This model can dynamically allocate radio resources to the Secondary Users (SUs) with the cooperation of Primary Users (PUs) so that the capacity of secondary network is maximized and the co-channel interference is minimized. In addition, the effect of Interference Temperature Limit (ITL) on the overall capacity of the secondary network is illustrated, which demonstrates that properly selecting different ITL values can balance the performance between the primary and secondary networks. This feature may be exploited to flexibly control the activities of the secondary network according to the instantaneous data transmission requirements of PUs. Secondly, in Section 5.2, the Accessible Interference Temperature (AIT) is introduced for fast implementation of a simplified OCR model. In this simplified model, the activities between PUs and SUs are mutually independent. When AIT constraints are guaranteed in the secondary network, each SU could rapidly access the available frequency bands without introducing deleterious interferences to PUs.

6.2 Future research

In this section, some possible extensions and future researches are outlined. In our studies, the proposed schemes generally assume accurate channel estimations for CSI. However, there may exist some CSI estimation errors. Thus, it is worthwhile to further investigate the sensitivities of the proposed schemes in this thesis to CSI estimation errors in the future. Furthermore, as given in Chapter 4, the Amplify-and-Forward (AF) relaying mode is discussed via adopting full-duplex relaying. However, in the Decode-

and-Forward (DF) relaying mode, each Relay Station (RS) should take some time to decode the received signals before relaying these signals to the destination users. Therefore, the time delay must be considered and may make the system implementation more complicated. As a result, it is worth developing a new model to deal with this delay for the full-duplex DF relaying mode. We have conceived a way to realize this implementation. Specifically, the BS transmits the signals to each RS in the first hop of the relaying path¹. Meanwhile, each RS transmits the signals received from the BS in the previous time-slot to its destination users on different subcarriers in the second hop of the relaying path. Finally, each destination user combines the signals directly received from the BS in the previous time-slot with the relayed signals received in the current time-slot to make joint signal detection. This implementation needs an additional buffering function at each destination user and could enable full-duplex DF relaying.

In recent years, many efforts have been made to realize OFDMA-based Cognitive Radio (OCR) systems [83]. This OCR technique has high potential to be practically used in future wireless communication systems since it has a low implementation complexity and can be easily deployed in conventional OFDMA systems. We have shown some methods to effectively implement spectrum sharing in OCR systems in Chapter 5. Nevertheless, many crucial issues, such as spectrum sensing, spectrum decision, spectrum handoff, and primary user protection, are open for investigations. In addition, fairness should be considered in OCR systems so that the shared spectrum can be fairly used in the secondary network. Furthermore, interference control is another concern that should be taken into account with dynamic power allocation.

In the sense of ergodic capacity, the interference diversity in cognitive radio systems is recently revealed in [90], which may motivate us to study a two-dimensional interference diversity for OCR systems in both time and frequency domains. In addition, the multiuser interference diversity should be exploited for OCR systems in multiuser

¹Fig. 4.1 has an illustration of this relaying path.

scenarios, which are more complicated than the single narrow-band case studied in [91]. In the near future, the OCR technique is expected to be adopted in conventional cellular systems. Thus, the cooperative interference control² among different cells should be further investigated.

In summary, the development of OCR applications compatible with the current network architectures will be our future research focus, which may include the following aspects:

- Agile spectrum handoff mechanisms.
- Spectrum sharing via dynamic power control and interference avoidance.
- Distributed OCR implementations.
- Joint spectrum sensing and radio resource management via cross-layer design.
- Two-dimensional interference diversity in both time and frequency domains.
- Cooperation between the primary and secondary users for mutual benefits.
- Cooperative interference control and multiuser interference diversity in multi-cell OCR systems.

²This work has been finished in [92] before the final submission of this thesis.

References

- [1] J. Proakis and M. Salehi, *Digital Communications, 5th Edition*. McGraw-Hill Science, 2007.
- [2] D. Agrawal, H. Gossain, D. Cavalcanti, and P. Mohapatra, "Recent advances and evolution of WLAN and WMAN standards," *IEEE Transactions on Wireless Communications*, vol. 15, no. 5, pp. 54–55, Oct. 2008.
- [3] "IEEE standard for local and metropolitan area networks part 16: Air interface for fixed and mobile broadband wireless access systems amendment 2: Physical and medium access control layers for combined fixed and mobile operation in licensed bands and corrigendum 1," *IEEE Std 802.16e-2005 and IEEE Std 802.16-2004/Cor 1-2005 (Amendment and Corrigendum to IEEE Std 802.16-2004)*, pp. 1–822, 2006.
- [4] C. Stevenson, G. Chouinard, Z. Lei, W. Hu, S. Shellhammer, and W. Caldwell, "Ieee 802.22: The first cognitive radio wireless regional area network standard," *IEEE Communications Magazine*, vol. 47, no. 1, pp. 130–138, Jan. 2009.
- [5] D. Tse and P. Viswanath, *Fundamentals of Wireless Communication*. Cambridge University Press, 2005.
- [6] H. Liu and G. Li, *OFDM-Based Broadband Wireless Networks - Design and Optimization*. NY: Wiley, Nov. 2005.
- [7] K. Letaief and Y. J. Zhang, "Dynamic multiuser resource allocation and adaptation for wireless systems," *IEEE Transactions on Wireless Communications*, vol. 13, no. 4, pp. 38–47, Aug. 2006.
- [8] C. Y. Wong, R. Cheng, K. Lataief, and R. Murch, "Multiuser OFDM with adaptive subcarrier, bit, and power allocation," *IEEE Journal on Selected Areas in Communications*, vol. 17, no. 10, pp. 1747–1758, Oct. 1999.
- [9] J. Hui and Y. Zhou, "Enhanced rate adaptive resource allocation scheme in downlink OFDMA system," in *IEEE 63rd Vehicular Technology Conference (VTC Spring)*, vol. 5, May 2006, pp. 2464–2468.
- [10] R. Agarwal, V. Majjigi, Z. Han, R. Vannithamby, and J. Cioffi, "Low complexity resource allocation with opportunistic feedback over downlink OFDMA networks," *IEEE Journal on Selected Areas in Communications*, vol. 26, no. 8, pp. 1462–1472, Oct. 2008.
- [11] Z. Shen, J. Andrews, and B. Evans, "Adaptive resource allocation in multiuser OFDM systems with proportional rate constraints," *IEEE Transactions on Wireless Communications*, vol. 4, no. 6, pp. 2726–2737, Nov. 2005.

- [12] B. Da and C. C. Ko, "A new scheme with controllable capacity and fairness for OFDMA downlink resource allocation," in *IEEE 66th Vehicular Technology Conference (VTC Fall)*, Sep. 2007, pp. 1817–1821.
- [13] I. Wong, Z. Shen, B. Evans, and J. Andrews, "A low complexity algorithm for proportional resource allocation in OFDMA systems," in *IEEE Workshop on Signal Processing Systems (SIPS)*, Oct. 2004, pp. 1–6.
- [14] B. Da and C. C. Ko, "A new scheme for downlink MIMO-OFDMA resource allocation with proportional fairness," in *14th Asia-Pacific Conference on Communications (APCC)*, Oct. 2008, pp. 1–5.
- [15] —, "Dynamic resource allocation in OFDMA systems with adjustable QoS," *IEICE Transactions on Communications*, vol. E92-B, no. 12, pp. 3586–3588, Dec. 2009.
- [16] —, "Resource allocation in downlink MIMO-OFDMA with proportional fairness," *Journal of Communications*, vol. 4, no. 1, pp. 8–13, Feb. 2009.
- [17] Y. J. Zhang and K. Letaief, "An efficient resource allocation scheme for spatial multiuser access in MIMO-OFDM systems," *IEEE Transactions on Communications*, vol. 53, no. 1, pp. 107–116, Jan. 2005.
- [18] Y.-H. Pan, K. Letaief, and Z. Cao, "Dynamic spatial subchannel allocation with adaptive beamforming for MIMO-OFDM systems," *IEEE Transactions on Wireless Communications*, vol. 3, no. 6, pp. 2097–2107, Nov. 2004.
- [19] B. Da and C. C. Ko, "Utility-based dynamic resource allocation in multi-user MIMO-OFDMA cellular systems," in *15th Asia-Pacific Conference on Communications (APCC)*, Oct. 2009, pp. 113–117.
- [20] J. Laneman, D. Tse, and G. Wornell, "Cooperative diversity in wireless networks: Efficient protocols and outage behavior," *IEEE Transactions on Information Theory*, vol. 50, no. 12, pp. 3062–3080, Dec. 2004.
- [21] Y. Liu, R. Hoshyar, X. Yang, and R. Tafazolli, "Integrated radio resource allocation for multihop cellular networks with fixed relay stations," *IEEE Journal on Selected Areas in Communications*, vol. 24, no. 11, pp. 2137–2146, Nov. 2006.
- [22] A. K. Sadek, W. Su, and K. J. R. Liu, "Multinode cooperative communications in wireless networks," *IEEE Transactions on Signal Processing*, vol. 55, no. 1, pp. 341–355, Jan. 2007.
- [23] L. Chen and B. Krongold, "An efficient resource allocation algorithm for OFDMA-based multihop wireless transmission," in *IEEE 18th International Symposium on Personal, Indoor and Mobile Radio Communications (PIMRC)*, Sep. 2007, pp. 1–5.

- [24] G. Li and H. Liu, "Resource allocation for OFDMA relay networks with fairness constraints," *IEEE Journal on Selected Areas in Communications*, vol. 24, no. 11, pp. 2061–2069, Nov. 2006.
- [25] M. Salem, A. Adinoyi, M. Rahman, H. Yanikomeroglu, D. Falconer, Y. Kim, E. Kim, and Y. Cheong, "An overview of radio resource management in relay-enhanced OFDMA-based networks," *IEEE Communications Surveys Tutorials*, 2010.
- [26] K. Jitvanichphaibool, R. Zhang, and Y.-C. Liang, "Optimal resource allocation for two-way relay-assisted OFDMA," *IEEE Transactions on Vehicular Technology*, vol. 58, no. 7, pp. 3311–3321, Sep. 2009.
- [27] B. Da, R. Zhang, and C. C. Ko, "Dynamic channel switching for downlink relay-aided OFDMA system," in *12th IEEE International Conference on Communication Technology (ICCT)*, submitted.
- [28] B. Da and C. C. Ko, "Dynamic resource allocation in relay-aided OFDMA cellular system," *European Transactions on Telecommunications*, conditionally accepted.
- [29] L. B. Le and E. Hossain, "Resource allocation for spectrum underlay in cognitive radio networks," *IEEE Transactions on Wireless Communications*, vol. 7, no. 12, pp. 5306–5315, Dec. 2008.
- [30] T. Yucek and H. Arslan, "A survey of spectrum sensing algorithms for cognitive radio applications," *IEEE Communications Surveys Tutorials*, vol. 11, no. 1, pp. 116–130, First Quarter 2009.
- [31] S.-Y. Tu, K.-C. Chen, and R. Prasad, "Spectrum sensing of OFDMA systems for cognitive radio networks," *IEEE Transactions on Vehicular Technology*, vol. 58, no. 7, pp. 3410–3425, Sep. 2009.
- [32] D. Niyato and E. Hossain, "Competitive pricing for spectrum sharing in cognitive radio networks: Dynamic game, inefficiency of nash equilibrium, and collusion," *IEEE Journal on Selected Areas in Communications*, vol. 26, no. 1, pp. 192–202, Jan. 2008.
- [33] —, "Spectrum trading in cognitive radio networks: A market-equilibrium-based approach," *IEEE Transactions on Wireless Communications*, vol. 15, no. 6, pp. 71–80, Dec. 2008.
- [34] D. Niyato, E. Hossain, and Z. Han, "Dynamics of multiple-seller and multiple-buyer spectrum trading in cognitive radio networks: A game-theoretic modeling approach," *IEEE Transactions on Mobile Computing*, vol. 8, no. 8, pp. 1009–1022, Aug. 2009.
- [35] T. Lammle, *Cisco Certified Network Associate Study Guide, 3rd Edition*. Sybex Inc, 2002.
- [36] V. Kuhn, *Wireless Communications over MIMO Channels*. NY: Wiley, 2006.
- [37] I. Wong and B. Evans, "Optimal downlink OFDMA resource allocation with linear complexity to maximize ergodic rates," *IEEE Transactions on Wireless Communications*, vol. 7, no. 3, pp. 962–971, Mar. 2008.

- [38] Y. Ma, "Rate maximization for downlink OFDMA with proportional fairness," *IEEE Transactions on Vehicular Technology*, vol. 57, no. 5, pp. 3267–3274, Sep. 2008.
- [39] I. Wong and B. Evans, "Optimal resource allocation in the OFDMA downlink with imperfect channel knowledge," *IEEE Transactions on Communications*, vol. 57, no. 1, pp. 232–241, Jan. 2009.
- [40] A. Alsawah and I. Fijalkow, "Fair service provision in OFDMA with partial channel-state information," in *IEEE 9th Workshop on Signal Processing Advances in Wireless Communications (SPAWC)*, Jul. 2008, pp. 106–110.
- [41] S. T. Chung and A. Goldsmith, "Degrees of freedom in adaptive modulation: a unified view," *IEEE Transactions on Communications*, vol. 49, no. 9, pp. 1561–1571, Sep. 2001.
- [42] E. K. P. Chong and S. H. Zak, *An Introduction to Optimization*. NY: Wiley, 2001.
- [43] J. Jang and K. B. Lee, "Transmit power adaptation for multiuser OFDM systems," *IEEE Journal on Selected Areas in Communications*, vol. 21, no. 2, pp. 171–178, Feb. 2003.
- [44] S. Boyd and L. Vandenberghe, *Convex Optimization*. Cambridge, U.K.: Cambridge Univ. Press, 2004.
- [45] K. Seong, M. Mohseni, and J. Cioffi, "Optimal resource allocation for OFDMA downlink systems," in *IEEE International Symposium on Information Theory*, Jul. 2006, pp. 1394–1398.
- [46] C. Bae and D.-H. Cho, "Fairness-aware adaptive resource allocation scheme in multihop OFDMA systems," *IEEE Communications Letters*, vol. 11, no. 2, pp. 134–136, Feb. 2007.
- [47] K. Kim, Y. Han, and S.-L. Kim, "Joint subcarrier and power allocation in uplink OFDMA systems," *IEEE Communications Letters*, vol. 9, no. 6, pp. 526–528, Jun. 2005.
- [48] N. Ruangchaijatupon and Y. Ji, "OFDMA resource allocation based on traffic class-oriented optimization," *IEICE Transactions on Communications*, vol. E92-B, no. 1, pp. 93–101, Jan. 2009.
- [49] H.-W. Lee and S. Chong, "Downlink resource allocation in multi-carrier systems: frequency-selective vs. equal power allocation," *IEEE Transactions on Wireless Communications*, vol. 7, no. 10, pp. 3738–3747, Oct. 2008.
- [50] E. Perahia, "Ieee 802.11n development: History, process, and technology," *IEEE Communications Magazine*, vol. 46, no. 7, pp. 48–55, Jul. 2008.
- [51] H. Yaiche, R. Mazumdar, and C. Rosenberg, "A game theoretic framework for bandwidth allocation and pricing in broadband networks," *IEEE/ACM Transactions on Networking*, vol. 8, no. 5, pp. 667–678, Oct. 2000.

- [52] G. Scutari, D. Palomar, and S. Barbarossa, "MIMO cognitive radio: A game theoretical approach," in *IEEE 9th Workshop on Signal Processing Advances in Wireless Communications (SPAWC)*, Jul. 2008, pp. 426–430.
- [53] ———, "Competitive design of multiuser MIMO systems based on game theory: A unified view," *IEEE Journal on Selected Areas in Communications*, vol. 26, no. 7, pp. 1089–1103, Sep. 2008.
- [54] A. Muthoo, *Bargaining Theory with Applications*. Cambridge, U.K.: Cambridge University Press, 1999.
- [55] Z. Han, Z. Ji, and K. Liu, "Fair multiuser channel allocation for OFDMA networks using nash bargaining solutions and coalitions," *IEEE Transactions on Communications*, vol. 53, no. 8, pp. 1366–1376, Aug. 2005.
- [56] N. Mastrorarde and M. van der Schaar, "A bargaining theoretic approach to quality-fair system resource allocation for multiple decoding tasks," *IEEE Transactions on Circuits and Systems for Video Technology*, vol. 18, no. 4, pp. 453–466, Apr. 2008.
- [57] E. Kalai, "Nonsymmetric Nash solutions and replications of 2-person bargaining," *Intl. Journal of Game Theory*, vol. 6, no. 3, pp. 129–133, 1975.
- [58] A. Goldsmith and S.-G. Chua, "Variable-rate variable-power MQAM for fading channels," *IEEE Transactions on Communications*, vol. 45, no. 10, pp. 1218–1230, Oct. 1997.
- [59] J. Dubra, "An asymmetric Kalai-Smorodinsky solution," *Economics Letters*, vol. 73, no. 2, pp. 131–136, 2001.
- [60] T. H. Cormen, C. E. Leiserson, R. L. Rivest, and C. Stein, *Introduction to Algorithms, 2nd ed.* MIT Press, 2001.
- [61] F. Kelly, A. Maulloo, and D. Tan, "Rate control for communication networks: shadow prices, proportional fairness and stability," *Journal of the Operational Research Society*, vol. 49.
- [62] M. Nokleby and A. Swindlehurst, "Bargaining and multi-user detection in MIMO interference networks," in *17th International Conference on Computer Communications and Networks (ICCCN)*, Aug. 2008, pp. 1–6.
- [63] B. Da, C. C. Ko, and Y. Liang, "An enhanced capacity and fairness scheme for MIMO-OFDMA downlink resource allocation," in *International Symposium on Communications and Information Technologies (ISCIT)*, Oct. 2007, pp. 495–499.
- [64] B. Da and C. C. Ko, "Fairness-aware resource allocation in downlink OFDMA systems with partial feedback CSI," in *15th Asia-Pacific Conference on Communications (APCC)*, Oct. 2009, pp. 131–134.

- [65] M. Salem, A. Adinoyi, H. Yanikomeroglu, and D. Falconer, "Opportunities and challenges in ofdma-based cellular relay networks: A radio resource management perspective," *IEEE Transactions on Vehicular Technology*, vol. 59, no. 5, pp. 2496–2510, Jun. 2010.
- [66] G. Kramer, M. Gastpar, and P. Gupta, "Cooperative strategies and capacity theorems for relay networks," *IEEE Transactions on Information Theory*, vol. 51, no. 9, pp. 3037–3063, Sep. 2005.
- [67] T. C.-Y. Ng and W. Yu, "Joint optimization of relay strategies and resource allocations in cooperative cellular networks," *IEEE Journal on Selected Areas in Communications*, vol. 25, no. 2, pp. 328–339, Feb. 2007.
- [68] L. You, M. Song, J. Song, Q. Miao, and Y. Zhang, "Adaptive resource allocation in OFDMA relay-aided cooperative cellular networks," in *IEEE Vehicular Technology Conference (VTC Spring)*, May 2008, pp. 1925–1929.
- [69] T. Riihonen, K. Haneda, S. Werner, and R. Wichman, "SINR analysis of full-duplex ofdm repeaters," in *IEEE 20th International Symposium on Personal, Indoor and Mobile Radio Communications (PIMRC)*, 2009, pp. 3169–3173.
- [70] A. Nosratinia, T. Hunter, and A. Hedayat, "Cooperative communication in wireless networks," *IEEE Communications Magazine*, vol. 42, no. 10, pp. 74–80, Oct. 2004.
- [71] L. Hoo, B. Halder, J. Tellado, and J. Cioffi, "Multiuser transmit optimization for multicarrier broadcast channels: Asymptotic FDMA capacity region and algorithms," *IEEE Transactions on Communications*, vol. 52, no. 6, pp. 922–930, Jun. 2004.
- [72] Z.-Q. Luo and W. Yu, "An introduction to convex optimization for communications and signal processing," *IEEE Journal on Selected Areas in Communications*, vol. 24, no. 8, pp. 1426–1438, Aug. 2006.
- [73] M. Salem, A. Adinoyi, M. Rahman, H. Yanikomeroglu, D. Falconer, and Y.-D. Kim, "Fairness-aware radio resource management in downlink ofdma cellular relay networks," *IEEE Transactions on Wireless Communications*, vol. 9, no. 5, pp. 1628–1639, May 2010.
- [74] S. Sanayei and A. Nosratinia, "Opportunistic downlink transmission with limited feedback," *IEEE Transactions on Information Theory*, vol. 53, no. 11, pp. 4363–4372, Nov. 2007.
- [75] C.-F. Tsai, C.-J. Chang, F.-C. Ren, and C.-M. Yen, "Adaptive radio resource allocation for downlink OFDMA/SDMA systems with multimedia traffic," *IEEE Transactions on Wireless Communications*, vol. 7, no. 5, pp. 1734–1743, May 2008.
- [76] I. Akyildiz, W.-Y. Lee, M. Vuran, and S. Mohanty, "A survey on spectrum management in cognitive radio networks," *IEEE Communications Magazine*, vol. 46, no. 4, pp. 40–48, Apr. 2008.

- [77] B. Da and C. C. Ko, "Dynamic spectrum sharing in OFDMA-based cognitive radio," *IET Communications*, to appear.
- [78] D. Ngo, C. Tellambura, and H. Nguyen, "Efficient resource allocation for ofdma multicast systems with spectrum-sharing control," *IEEE Transactions on Vehicular Technology*, vol. 58, no. 9, pp. 4878–4889, Nov. 2009.
- [79] "FCC 02-155 : Spectrum policy task force report," Nov. 2002.
- [80] S. Haykin, "Cognitive radio: Brain-empowered wireless communications," *IEEE Journal on Selected Areas in Communications*, vol. 23, no. 2, pp. 201–220, Feb. 2005.
- [81] P. Cheng, Z. Zhang, H. Huang, and P. Qiu, "A distributed algorithm for optimal resource allocation in cognitive OFDMA systems," in *IEEE International Conference on Communications (ICC)*, May 2008, pp. 4718–4723.
- [82] Y. Zhang and C. Leung, "Cross-layer resource allocation for mixed services in multiuser OFDM-based cognitive radio systems," *IEEE Transactions on Vehicular Technology*, vol. 58, no. 8, pp. 4605–4619, Oct. 2009.
- [83] R. Wang, V. Lau, L. Lv, and B. Chen, "Joint cross-layer scheduling and spectrum sensing for ofdma cognitive radio systems," *IEEE Transactions on Wireless Communications*, vol. 8, no. 5, pp. 2410–2416, May 2009.
- [84] W. Fan, M. Krunz, and S. Cui, "Price-based spectrum management in cognitive radio networks," *IEEE Journal of Selected Topics in Signal Processing*, vol. 2, no. 1, pp. 74–87, Feb. 2008.
- [85] M. Ozdemir and H. Arslan, "Channel estimation for wireless OFDM systems," *IEEE Communications Surveys Tutorials*, vol. 9, no. 2, pp. 18–48, Second Quarter 2007.
- [86] K. Seong, M. Mohseni, and J. Cioffi, "Optimal resource allocation for OFDMA downlink systems," in *IEEE International Symposium on Information Theory*, Jul. 2006, pp. 1394–1398.
- [87] A. T. Hoang, Y.-C. Liang, and M. Islam, "Power control and channel allocation in cognitive radio networks with primary users' cooperation," *IEEE Transactions on Mobile Computing*, vol. 9, no. 3, pp. 348–360, Mar. 2010.
- [88] C. Saraydar, N. Mandayam, and D. Goodman, "Efficient power control via pricing in wireless data networks," *IEEE Transactions on Communications*, vol. 50, no. 2, pp. 291–303, Feb. 2002.
- [89] B. Da and C. C. Ko, "Implementation of OFDMA-based cognitive radio via accessible interference temperature," *IEICE Transactions on Communications*, conditionally accepted.

- [90] R. Zhang, "On peak versus average interference power constraints for protecting primary users in cognitive radio networks," *IEEE Transactions on Wireless Communications*, vol. 8, no. 4, pp. 2112–2120, april 2009.
- [91] R. Zhang and Y.-C. Liang, "Investigation on multiuser diversity in spectrum sharing based cognitive radio networks," *IEEE Communications Letters*, vol. 14, no. 2, pp. 133–135, Feb. 2010.
- [92] B. Da and R. Zhang, "Cooperative interference control for spectrum sharing in cellular OFDMA systems," in *IEEE International Conference on Communications (ICC)*, accepted.
- [93] T. M. Cover and J. A. Thomas, *Elements of Information Theory*. NY: Wiley.

Appendix A

Optimal power allocation to Problem (2.5)

If the subcarrier allocation for user k is given by the set Γ_k , where the number of elements in Γ_k is N_k i.e., the practically allocated number of subcarriers to user k , the optimal power allocation solution to Problem (2.5) is given by solving the following set of equations [11]:

$$\begin{aligned} & \frac{1}{\alpha_1} \frac{N_1}{N} \left(\log_2 \left(1 + H_{11} \frac{P_{1,tot} - V_1}{N_1} \right) + \log_2 W_1 \right) \\ & = \frac{1}{\alpha_k} \frac{N_k}{N} \left(\log_2 \left(1 + H_{k1} \frac{P_{k,tot} - V_k}{N_k} \right) + \log_2 W_k \right), \quad k = 2, 3, \dots, K, \end{aligned} \quad (\text{A.1})$$

and

$$\sum_{k=1}^K P_{k,tot} = P_{tot}, \quad (\text{A.2})$$

where $P_{k,tot}$ is the total allocated power of each user, and

$$V_k = \sum_{n=2}^{N_k} \frac{H_{kn} - H_{k1}}{H_{kn} H_{k1}}, \quad (\text{A.3})$$

$$W_k = \left(\prod_{n=2}^{N_k} \frac{H_{kn}}{H_{k1}} \right)^{\frac{1}{N_k}}. \quad (\text{A.4})$$

Note that in (A.1) and (A.2), there are K variables i.e., $P_{k,tot}, k \in \Delta$ with K equations, some iterative methods such as Newton-Raphson or quasi-Newton methods [44] can be used to find the solutions efficiently.

Once $P_{k,tot}, k \in \Delta$ are known, we can use the following two equations to easily derive the optimal power allocation across the assigned subcarriers of user k :

$$\sum_{n=1}^{N_k} p_{kn} = P_{k,tot}, \quad (\text{A.5})$$

$$p_{kn} = p_{k1} + \frac{H_{kn} - H_{k1}}{H_{kn}H_{k1}}, \quad n = 2, \dots, N_k. \quad (\text{A.6})$$

Appendix B

MIMO-OFDMA optimality

For the investigated MIMO-OFDMA system, the total system capacity is maximized when the following conditions are satisfied [6].

Condition 1: The user assigned to subcarrier n has the highest value of $\prod_{i=1}^{M_{kn}} \left(1 + \frac{\lambda_{kn}^{(i)} p_n^*}{\mu}\right)$ over all k , i.e.,

$$k_n = \arg \max_k \prod_{i=1}^{M_{kn}} \left(1 + \frac{\lambda_{kn}^{(i)} p_n^*}{\mu}\right), \quad (\text{B.1})$$

where k_n is the allocated user index on subcarrier n , M_{kn} is the rank of \mathbf{H}_{kn} , and $\lambda_{kn}^{(1)}, \dots, \lambda_{kn}^{(M_{kn})}$ are the eigen-values of $\mathbf{H}_{kn} \mathbf{H}_{kn}^H$ and p_n^* is the optimal power assigned to subcarrier n that satisfies the following condition.

Condition 2: The power distribution over subcarriers is $p_n^* = \max(0, p_n)$, where p_n is the root of the following equations,

$$\sum_{i=1}^{M_{k_n n}} \frac{\lambda_{k_n n}^{(i)}}{\lambda_{k_n n}^{(i)} p_n + \mu} + \beta = 0, n = 1, \dots, N, \quad (\text{B.2})$$

where β complies with $\sum_{n=1}^N p_n^* = P_{tot}$.

Proposition 1: Under high SNR condition, the allocation of equal power over all subcarriers is a near-optimal power allocation method.

Proof: Each $\lambda_{k_n n}^{(i)}$ in (B.2) will be much larger than μ i.e., $\mu / \lambda_{k_n n}^{(i)} \approx 0$ under the

condition of high SNR. Thus, (B.2) can be approximated as

$$\frac{M_{k_n n}}{p_n} + \beta = 0, n = 1, \dots, N. \quad (\text{B.3})$$

Then, it has $p_i = p_j$ for $i \neq j$, which gives the allocated power of each subcarrier is equal in this case.

Appendix C

Proof of achievable capacity in equation (4.5)

Based on the equations in (4.1)–(4.4), the received signal of user k in two hops are

$$y_{u_I}^n = b_u^n x_u^n + v_I^n, \quad (\text{C.1})$$

and

$$y_{ru_{II}}^m = \mu_{ru}^m a_r^n d_{ru}^m x_u^n + \mu_{ru}^m d_{ru}^m v_r^n + v_{II}^m, \quad (\text{C.2})$$

respectively. When joint estimation is adopted at each user via relaying path, (C.1) and (C.2) are equivalent to the following representation are equivalent to the following representation

$$\mathbf{y}^{(n,m)} = \begin{pmatrix} y_{u_I}^n \\ y_{ru_{II}}^m \end{pmatrix} = \mathbf{A}\mathbf{x} + \mathbf{B}\mathbf{v}, \quad (\text{C.3})$$

where

$$\mathbf{A} = \begin{bmatrix} b_u^n \\ \mu_{ru}^m a_r^n d_{ru}^m \end{bmatrix}, \quad (\text{C.4})$$

$$\mathbf{x} = [x_u^n], \quad (\text{C.5})$$

$$\mathbf{B} = \begin{bmatrix} 1 & 0 & 0 \\ 0 & 1 & \mu_{ru}^m d_{ru}^m \end{bmatrix}, \quad (\text{C.6})$$

$$\mathbf{v} = \begin{bmatrix} v_{\text{I}}^n \\ v_{\text{II}}^m \\ v_r^n \end{bmatrix}. \quad (\text{C.7})$$

Then, the achieved capacity (bps/Hz) can be calculated [93]

$$\begin{aligned} C_{ru}^{mm} &= I(\mathbf{y}^{(n,m)}; \mathbf{x}) = \log_2 \det \left[\mathbf{I} + \frac{\mathbf{A}E(\mathbf{x}\mathbf{x}^H)\mathbf{A}^H}{\mathbf{B}E(\mathbf{v}\mathbf{v}^H)\mathbf{B}^H} \right] \\ &= \log_2 \left[1 + \frac{p_u^n \|b_u^n\|^2}{v_0} + \frac{p_k^n \|a_r^n\|^2 \|d_{ru}^m\|^2 \|\mu_{ru}^m\|^2}{v_0 (1 + \|d_{ru}^m\|^2 \|\mu_{ru}^m\|^2)} \right]. \end{aligned} \quad (\text{C.8})$$

where

$$\|\mu_{ru}^m\|^2 = \frac{p_{ru}^m}{\|a_r^n\|^2 p_u^n + v_0}, \quad (\text{C.9})$$

is the amplification factor at r th RS for user k on subcarrier m . Then, substitute (C.9) into (C.8) while considering the full-duplex relaying and multiplying the bandwidth W of each subcarrier will lead to the achievable capacity (bps) given as in (4.5).

Appendix D

Lagrangian duality and Karush-Kuhn-Tucker conditions

In this appendix, Lagrangian duality and Karush-Kuhn-Tucker condition are introduced, which are selected from [72]. More details and examples about these two concepts can further refer to [42].

Specifically, consider the following (not necessarily convex) optimization problem:

$$\begin{aligned}
 & \min f_0(x) \\
 & \text{s.t. } f_i(x) \leq 0, \quad i = 1, 2, \dots, m, \\
 & \quad h_j(x) = 0, \quad j = 1, 2, \dots, r, \\
 & \quad x \in S.
 \end{aligned} \tag{D.1}$$

Let p^* denote the global minimum value of (D.1). For symmetry reason, we will call (D.1) the primal optimization problem, and call x the primal vector. Introducing dual variables $\lambda \in \mathfrak{R}^m$ and $v \in \mathfrak{R}^r$, we can form the Lagrangian function

$$L(x, \lambda, v) := f_0(x) + \sum_{i=1}^m \lambda_i f_i(x) + \sum_{j=1}^r v_j h_j(x). \tag{D.2}$$

The so-called dual function $g(\lambda, v)$ associated with (D.1) is defined as

$$g(\lambda, v) := \min_{x \in S} L(x, \lambda, v). \quad (\text{D.3})$$

Notice that, as a pointwise minimum of a family of linear functions (in (λ, v)), the dual function $g(\lambda, v)$ is always concave. We will say (λ, v) is dual feasible if $\lambda \geq 0$ and $g(\lambda, v)$ is finite. The well-known weak duality result says the following.

Proposition 1: For any primal feasible vector and any dual feasible vector (λ, v) , there holds

$$f_0(x) \geq g(\lambda, v). \quad (\text{D.4})$$

In other words, for any dual feasible vector (λ, v) , the dual function value $g(\lambda, v)$ always serves as a lower bound on the primal objective value $f_0(x)$. Note that x and (λ, v) are chosen independent from each other (so long as they are both feasible). Thus, $p^* \geq g(\lambda, v)$ for all dual feasible vector (λ, v) . The largest lower bound for p^* can be found by solving the following dual optimization problem:

$$\begin{aligned} \max \quad & g(\lambda, v) \\ \text{s.t.} \quad & \lambda \geq 0, v \in \Re^r. \end{aligned} \quad (\text{D.5})$$

Notice that the dual problem (D.5) is always convex regardless of the convexity of the primal problem (D.1), since $g(\lambda, v)$ is concave. Let us denote the maximum value of (D.5) by d^* . Then, we have $p^* \geq d^*$. For most convex optimization problems (satisfying some mild constraint qualification conditions, such as the existence of a strict interior point), we actually have $p^* = d^*$, which is called strong duality.

Next, we present a local optimality condition for the optimization problem (D.1). For ease of exposition, let us assume $S = \Re$. Then, a necessary condition for x^* to be a local optimal solution of (D.1) is that there exists some (λ^*, v^*) such that

$$f_i(x^*) \leq 0, \quad \forall i = 1, 2, \dots, m, \quad (\text{D.6})$$

$$h_j(x^*) = 0, \quad \forall j = 1, 2, \dots, r, \quad (\text{D.7})$$

$$\lambda^* \geq 0, \quad (\text{D.8})$$

$$\lambda_i^* f_i(x^*) = 0, \quad \forall i = 1, 2, \dots, m, \quad (\text{D.9})$$

and

$$\nabla f_0(x^*) + \sum_{i=1}^m \lambda_i^* \nabla f_i(x^*) + \sum_{j=1}^r v_j^* \nabla h_j(x^*) = 0. \quad (\text{D.10})$$

The conditions (D.6) - (D.10) are called the Karush-Kuhn-Tucker (KKT) condition for optimality. Notice that the first two conditions (D.6) and (D.7) represent primal feasibility of x^* , condition (D.8) represents dual feasibility, condition (D.9) signifies the complementary slackness for the primal and dual inequality constraint pairs: $f_i(x) \leq 0$ and $\lambda_i \geq 0$, while the last condition (D.10) is equivalent to $\nabla_x L(x^*, \lambda^*, v^*) = 0$.

Appendix E

Algorithm in [84]

Treating other users' transmissions as interference, the best response of user i is given by

$$\mathbf{P}_i = \mathbf{BR}_i(\mathbf{P}_{-i}) = [BR_i(\mathbf{P}_{-i})(f_1), \dots, BR_i(\mathbf{P}_{-i})(f_K)], \quad (\text{E.1})$$

where

$$BR_i(\mathbf{P}_{-i})(f_k) = \left[\frac{1}{\beta + \lambda_i(f_k)} - \frac{M_k(f_k)}{h_{ii}(f_k)} \right]_0^{P_{\text{mask}}(f_k)}. \quad (\text{E.2})$$

Note that $[x]_a^b$ with $b > a$ denotes the Euclidean projection of x onto the interval $[a, b]$ i.e., $[x]_a^b = a$ if $x < a$, $[x]_a^b = x$ if $a \leq x \leq b$, $[x]_a^b = b$ if $x > b$.

If secondary users are to make their best-response decisions sequentially according to a fixed order, the associated algorithm is generalized in Table E.1 in the next page. In this algorithm, ε is set to a small value such as 5% in [84] to serve as the stop condition. If this condition is not satisfied after L_{max} iterations, the algorithm terminates.

Note that, the notation conventions are defined differently in [84] as compared to those used in this thesis. Specifically, in this algorithm, K means the number of subcarriers, N is the number of users, $P_i(f_k)$ is the power allocated for user i on subcarrier k , and $M_i(f_k)$ corresponds to interference plus noise i.e., μ_k^n in Chapter 5. In addition, $\lambda_i(f_k)$ adopts the derived result in (5.12), and $P_{\text{mask}}(f_k)$ uses the value given by (5.19).

TABLE E.1: Sequential price-based iterative water-filling algorithm in [84]

-
- 0: Initialize $P_i(f_k) = 0, \forall i \in \Omega_N$ and $k \in \Omega_K$; initialize iteration count $l = 0$.
- 1: Repeat iterations:
- 2: $l = l + 1$;
- 3: **for** $i = 1$ to N users **do**
- 4: **for** $k = 1$ to K channels **do**
- 5: Estimate the total interference plus noise level $M_i(f_k)$;
- 6: Compute the pricing factor $\lambda_i(f_k)$;
- 7: Estimate the channel gain $h_{ii}(f_k)$;
- 8: **end for**
- 9: $\mathbf{P}_i^{(l)} = \text{BR}_i \left(\mathbf{P}_1^{(l)}, \dots, \mathbf{P}_{i-1}^{(l)}, \mathbf{P}_{i+1}^{(l-1)}, \dots, \mathbf{P}_N^{(l-1)} \right)$;
- 10: Transmit on selected channels using $\mathbf{P}_i^{(l)}$.
- 11: **end for**
- 12: until $l > L_{\max}$ or $\left(\frac{\|\mathbf{P}_i^{(l)} - \mathbf{P}_i^{(l-1)}\|}{\|\mathbf{P}_i^{(l-1)}\|} \right) \leq \varepsilon$.
-

Appendix F

List of publications

[Journal articles]

1. Bin Da, C. C. Ko, "Dynamic resource allocation in relay-assisted OFDMA cellular system," conditionally accepted by *European Transactions on Telecommunications*.
2. Bin Da, C. C. Ko, "Dynamic spectrum sharing in OFDMA-based cognitive radio," in *IET Communications*, vol. 4, no. 17, pp. 2125 - 2132, Nov. 2010.
3. Bin Da, C. C. Ko, "Implementation of OFDMA-based cognitive radio via accessible interference temperature," in *IEICE Trans. Communications*, vol. E93-B, no. 10, pp. 2830 - 2832, Oct. 2010.
4. Bin Da, C. C. Ko, "Dynamic resource allocation in OFDMA systems with adjustable QoS," in *IEICE Trans. Communications*, vol. E92-B, no. 12, pp. 3586 - 3588, Dec. 2009.
5. Bin Da, C. C. Ko, "Resource allocation in downlink MIMO-OFDMA with proportional fairness," in *Journal of Communications*, vol. 4, no. 1, pp. 8 - 13, Feb. 2009.

[Conference proceedings]

1. Bin Da, R. Zhang, "Cooperative interference control for spectrum sharing in cellular OFDMA systems," to appear in *International Conference on Communications (ICC)* 2011, Japan.
2. Bin Da, R. Zhang, C. C. Ko, "Spectrum trading in OFDMA-based cognitive radio," in *Proc. 12th IEEE International Conference on Communication Technology (ICCT)*, China, Nov. 2010, pp. 33 - 35.
3. Bin Da, R. Zhang, C. C. Ko, "Dynamic channel switching for downlink relay-aided OFDMA system," in *Proc. 12th IEEE International Conference on Communication Technology (ICCT)*, China, Nov. 2010, pp. 36 - 39.
4. Bin Da, C. C. Ko, "Utility-based dynamic resource allocation in multi-user MIMO-OFDMA cellular systems," in *Proc. 15th Asia-Pacific Conference on Communications (APCC)*, China, Oct. 2009, pp. 113 - 117.
5. Bin Da, C. C. Ko, "Fairness-aware resource allocation in downlink OFDMA systems with partial feedback CSI," in *Proc. 15th Asia-Pacific Conference on Communications (APCC)*, China, Oct. 2009, pp. 131 - 134.
6. Bin Da, C. C. Ko, "Downlink MIMO-OFDMA resource allocation with proportional fairness," in *Proc. 14th Asia-Pacific Conference on Communications (APCC)*, Japan, Oct. 2008, pp. 1 - 5.
7. Bin Da, C. C. Ko, "Subcarrier and power allocation for downlink relay-assistant OFDMA cellular system," in *Proc. 14th Asia-Pacific Conference on Communications (APCC)*, Japan, Oct. 2008, pp. 1 - 5.

8. Bin Da, C. C. Ko, "Dynamic subcarrier sharing algorithms for uplink OFDMA resource allocation," in *Proc. 6th International Conference on Information, Communications and Signal Processing (ICICS)*, Dec. 2007, pp. 1 - 5.
9. Bin Da, C. C. Ko, "An enhanced capacity and fairness scheme for MIMO-OFDMA downlink resource allocation," in *Proc. International Symposium on Communications and Information Technologies (ISCIT)*, Oct. 2007, pp. 495 - 499.
10. Bin Da, C. C. Ko, "A new scheme with controllable capacity and fairness for OFDMA downlink resource allocation," in *Proc. IEEE 66th Vehicular Technology Conference (VTC-Fall)*, Sept. 2007, pp. 1817 - 1821.